BARRIER PROPERTIES AND MOLECULAR PHYSIOLOGY OF FISH GILL EPITHELIA AND GILL EPITHELIUM MODELS

CHUN CHIH CHEN

A DISSERTATION SUBMITTED TO
THE FACULTY OF GRADUATE STUDIES
IN PARTIAL FULFILLMENT OF THE REQUIREMENTS
FOR THE DEGREE OF
DOCTOR OF PHILOSOPHY

GRADUATE PROGRAM IN BIOLOGY
YORK UNIVERSITY
TORONTO, ONTARIO

SEPTEMBER 2020

Abstract

The fish gill epithelium interfaces directly with surrounding water and participates in numerous physiological processes. However, the barrier properties of the fish gill epithelium have been largely overlooked until recent studies have suggested that a dynamic repertoire of tight junction (TJ) associated elements control gill epithelium paracellular permeability and dictate barrier function of this tissue. Primary cultured gill epithelium models have become valuable tools to examine gill epithelium permeability, but models have been developed using few species. Furthermore, continued refinement of existing models provides enhanced insight. My thesis work focused on refining an existing primary cultured gill epithelium model derived from a freshwater (FW) bony fish (rainbow trout) by considering how epithelium TJs and permeability might be influenced by native serum as a growth supplement and heparin (an anti-coagulant used to collect extracellular fluid). A FW trout gill model was also used to examine the effect of the thyroid hormone 3,5',3'-triiodo-L-thyronine (T_3) on gill epithelium TJs and barrier function. Data indicate that (1) native serum enhances the barrier properties of the trout gill model; (2) heparin compromises epithelium integrity; and (3) T_3 may induce changes that prepare a diadromous fish for seawater (SW) entry. In addition, I examined a role for putative pore-forming claudin-10 TJ proteins in the mummichog gill and opercular epithelium and provide data supporting an integral role for Cldn-10c in Na^+ secretion across the SW fish gill. Finally, I examined the molecular physiology of the lamprey gill epithelium TJ complex through metamorphosis and I developed the first primary cultured gill epithelium model for this basal vertebrate. Peri-metamorphic observations of the lamprey gill TJ complex indicate that SW entry has a much greater impact on TJs than metamorphosis alone, and a cultured lamprey gill epithelium model, derived from FW residing larval lamprey, reveals a comparatively tight epithelium with a TJ profile that mimics the

intact gill epithelium. Together, data provide new insight into the barrier function of fish gill epithelia as well as new and improved tools to study this function.

Dedication

I cannot sufficiently describe my gratitude and appreciation towards everyone that have helped and encouraged me over the years. Most important of all, I want to thank Dr. Scott Kelly for all his support over the years. Thank you for being an amazing supervisor. Thank you and Angela for always making me feel like part of your family. I love Sophie.

I am grateful to have Dr. Andrew Donini on my thesis committee since my undergrad thesis and his continuing support over the years. I am lucky to have Dr. Jean-Paul Paluzzi as my advisor, and Dr. Carol Bucking for her help even though she is not part of my committee.

I want to give a very special thank you to Dr. Sima Jonusaite for being a great inspiration since the time she was my TA in Animal Development, and telling me to email Dr. Kelly about my sick little fish Lagiacrus. I miss you a lot Sima. Of all the lab members from this lab, there is nobody that I respect more than Dr. Helen Chasiotis who has established everything in the lab, and who happens to be amazing. It is weird I actually took the course when both Sima and Helen were TAing the course, but I did not know they were both from the same lab. I also did not know my BIOL2030 TA was from this lab until I joined the lab for like half a year…

I am extremely lucky to have Andrea Durant as one of my best friends, who has remained as my inspiration over the years. I can never forget her presentation on reptile skin when we took Dr. Tsushima's grad course together, and the times we used to subway together and cram grad course assignments. There was no Starbucks on campus at the time and we always get coffee from La Prep. I am constantly supported by my trios of BFFs Eleni Fegaras, Heyam Hayder, and Fargol Nowghani, all of whom have given me tremendous support over the years. They have been with me through my toughest times, and they are always there for me. Theanuga Chandrapalan for our zoom bubble teas and laughing at how my bicycle UberEats always delivers faster, Elia Grieco Guardian for her critical comments when I send her pictures of my failed weekly attempts at baking, and Kenny So for sending me… Nevermind.

During my journey, I am lucky to have a supportive family, and parents that let me do whatever I wish. But maybe it is now time to listen to my parents and start a YouTube channel. I have my BFF and brother by bond Robert Cheung for his continuous support, getting my weekly Coca Cola, and tolerating my extreme temper when I'm like the incredible Hulk. Joey Laffradi for helping me so much whenever I need anything.

There are a lot of people that helped me immensely. If I were to thank everyone this section will be far larger than the wine menu at the Barberian's Steak House. All of these people are important for helping me all these years, and there is no way I can thank them enough… (in no specific order) Felix Tam, Wilson Cheng, Diane Mathewsky, Chaminda Gunawardene, Jennifer Im, Sheralyn Au, Sean Mckee, Anna Zimina, Krystina Strickler, Ana Cuciureanu, Britney Picnic, Lidiya Misyura, Gil Yerushalmi, Phuong Bui, Nahid Vagharfard, Aziza Wahedi, Andrea Matei, Jacob O'brien, Julie Panakos, Janet Fleites, Dr. Wei-Li Ma, Dr. Mohammed Salem, Rosa Eskandari, Alice Dmello, David Miller, Dilraj Rai, Connie Hong, Masumi Yamamoto, Eric Chan, Lalanthi Ratnayake, the Donini lab, Paluzzi lab, Peng lab, and McDermott Lab members. Out of space…

Statement of Contribution

Chapter 1: Introduction

Contributors: Chun Chih Chen, Scott P. Kelly
Contributions: Conceptualization – C.C.C.; Figure Illustration – C.C.C.; Writing (original draft) – C.C.C.; Writing (review and editing) – C.C.C., S.P.K.

Chapter 2: The anti-coagulating agent heparin and native serum alter the barrier and junction properties of a primary cultured model fish gill epithelium

Contributors: Chun Chih Chen, Scott P. Kelly
Contributions: Conceptualization – C.C.C., S.P.K.; Methodology: C.C.C.; Validation: C.C.C.; Formal analysis: C.C.C.; Investigation: C.C.C.; Data curation: C.C.C.; Writing - original draft: C.C.C.; Writing - review & editing: C.C.C., S.P.K.; Supervision: S.P.K.; Funding acquisition: S.P.K.

Chapter 3: Thyroid hormone 3,5',3'-triiodo-L-thyronine Alters the Molecular Physiology of a Model Rainbow Trout Gill Epithelium

Contributors: Chun Chih Chen, Sheralyn Au, Scott P. Kelly
Contributions: Conceptualization – C.C.C., S.P.K.; Methodology: C.C.C.; Validation: C.C.C.; Formal analysis: C.C.C.; Investigation: C.C.C., S.A.; Data curation: C.C.C.; Writing - original draft: C.C.C.; Writing - review & editing: C.C.C., S.P.K.; Supervision: S.P.K.; Funding acquisition: S.P.K.

Chapter 4: Mummichog gill and operculum exhibit functionally consistent claudin-10 paralog profiles and Claudin-10c hypersaline response

Contributors: Chun Chih Chen, William S. Marshall**, George N. Robertson**, Regina R.F. Cozzi**, Scott P. Kelly
Contributions: Conceptualization – W.S.M., C.C.C., S.P.K.; Methodology: W.S.M., C.C.C.; Validation: W.S.M., C.C.C.; Formal analysis: W.S.M., C.C.C.; Investigation: W.S.M., C.C.C., G.N.R., R.R.F.C.; Resources: W.S.M.; Data curation: W.S.M., C.C.C.; Writing - original draft: W.S.M., C.C.C.; Writing - review & editing: W.S.M., S.P.K., C.C.C., R.R.F.C.; Supervision: W.S.M., S.P.K.; Funding acquisition: W.S.M.,S.P.K.

Chapter 5: Peri-Metamorphic Tight Junction-Associated Gene Expression Patterns in the Sea Lamprey (Petromyzon marinus) Gill

Contributors: Chun Chih Chen, Julia Sunga*, Michael P. Wilkie*, Scott P. Kelly
Contributions: Conceptualization – C.C.C., M.P.W., S.P.K.; Methodology: C.C.C., J.S.; Validation: C.C.C.; Formal analysis: C.C.C.; Investigation: C.C.C.; Resources: M.P.W.; Data curation: C.C.C.; Writing - original draft: C.C.C.; Writing - review & editing: C.C.C., S.P.K.; Supervision: S.P.K.; Funding acquisition: S.P.K., M.P.W.

Chapter 6: Development of a Primary Cultured Sea Lamprey (Petromyzon marinus) Gill Epithelium

Contributors: Chun Chih Chen, Michael P. Wilkie*, Scott P. Kelly
Contributions: Conceptualization – C.C.C., S.P.K.; Methodology: C.C.C.; Validation: C.C.C.; Formal analysis: C.C.C.; Investigation: C.C.C.; Resources: M.P.W.; Data curation: C.C.C.; Writing - original draft: C.C.C.; Writing - review & editing: C.C.C., S.P.K.; Supervision: S.P.K.; Funding acquisition: S.P.K., M.P.W.

Chapter 7: Integration and Future Directions

Contributors: Chun Chih Chen
Contributions: Conceptualization – C.C.C.; Writing (original draft) – C.C.C.; Writing (review and editing) – C.C.C.

Contributors Affiliation:
C.C.C., S.A., S.P.K.: Department of Biology, York University, Toronto, ON, Canada
M.P.W., J.S.: Department of Biology, Wilfrid Laurier University, Waterloo, ON, Canada
W.S.M., G.N.R, R.R.F.C.: Department of Biology, St. Francis Xavier University, Antigonish, NS, Canada

Table of Contents

List of Tables

List of Figures

Chapter 1 Figures

Chapter 2 Figures

Chapter 3 Figures

Chapter 4 Figures

Chapter 5 Figures

Chapter 6 Figures

List of Abbreviations

Abbreviation	Full Form
[^{3}H]PEG-400	[^{3}H]polyethylene glycol MW= 400 Da
2SW	hypersaline/2x sea water
AC	accessory cell
Actb	β-actin
AMRC	ammocoete mitochondria-rich cell
ANOVA	Analysis of variance
BCA	bicinchoninic assay
CC	chloride cell
cDNA	complementary DNA
CFTR	cystic fibrosis transmembrane conductance regulator
cgn/Cgn	cingulin
cldn/Cldn	claudin
ef-1α	elongation factor-1α
FBS	fetal bovine serum
FW	freshwater
IMRC	intercalated mitochondria-rich cell
i.u.	international unit
L-15	Leibovitz's L-15 Medium
MRC	mitochondria-rich cell
NKA	Na^+,K^+-ATPase
NKCC	Na^+,K^+,$2Cl^-$ cotransporter

List of Abbreviations (Continued)

Abbreviation	Full Form
NS	native serum
ocln/Ocln	occludin
OE	opercular epithelium
PBS	phosphate-buffered saline
PCR	polymerase chain reaction
PET	polyethylene terephthalate
PVC	pavement cells
PVDF	polyvinylidene fluoride
qPCR	Quantitative-PCR
RIPA	radioimmunoprecipitation assay
S1 – S7	metamorphosing lampreys stages 1 to 7
SDS	sodium dodecyl sulfate
SW	seawater/sea water
T_3	Triiodothyronine/3,3′,5-triiodo-L-thyronine
TEM	transmission electron micrograph
TER	transepithelial electrical resistance
TH	thyroid hormone
TJ	tight junction
TPBS	phosphate-buffered saline with 0.05% Tween 20
tric/Tric	tricellulin
ZO-1	zona-occludens 1

Chapter 1. General Introduction

1.1. Overview

Fishes are a diverse assemblage of aquatic vertebrates that consist of approximately 28,000 species which occupy a wide range of habitats (Nelson 2006). Fishes are typically divided into three separate groups that include basal jawless vertebrates (Agnatha), as well as derived (jawed) forms comprising Chondrichthyes (cartilaginous fishes) and Osteichthyes (bony fishes). As various fish species occupy almost all known aquatic habitats on the planet, their diverse lineage has resulted in unique morphological and physiological adaptations that contributes to survival strategies. Yet despite dramatic variations in the physical appearance of fishes and physiological challenges associated with diverse habitats, a requirement that all but a few fish species must fulfill is the maintenance of internal salt and water balance within a narrow range. This is especially challenging to aquatic animals as they are in direct contact with the aquatic medium, which typically presents large ionic and osmotic gradients across the entire surface of the body. Therefore, the ion/osmoregulatory epithelia of aquatic vertebrates must mediate the passive exchange of solutes and water between the intracellular fluids and the aquatic medium (Evans et al., 2005). Several key organs are important in maintaining ion/osmoregulatory homeostasis including the gill, kidney, intestine, and skin (**Figure 1-1**).

In short, freshwater (FW) fishes must maintain an internal osmolality that is considerably higher than the surrounding water (**Figure 1-1**). FW fishes constantly face the challenge of passive water influx and ion efflux across the integument and the gill, which come into direct contact with surroundings. Therefore, FW fishes must acquire ions (either from the water or food) while mitigating ion loss and at the same time eliminating excess water gained by osmosis. The latter is largely achieved by the copious production of dilute urine, while ion uptake occurs across the gill

and intestine. The organs that mitigate passive ion loss in FW fishes, are largely those that come into direct contact with water, the gill and skin. While the integument was previously considered to be a passive barrier in fishes, emerging evidence suggests that the plasticity of the fish integument allows its dynamic remodeling during osmoregulatory and environmental challenges (Dong et al., 2019; Gauberg et al., 2017). In contrast, the role of the FW fish gill in reducing passive ion loss has received more recognition, but only over the past decade has this conceptually simple property of the FW fish gill epithelium revealed itself to be intricately dynamic and complex.

The majority of fishes residing in seawater (SW) (i.e. bony fishes) face problems that are the opposite of their FW counterparts. That is, these fishes must maintain an internal osmolality that is significantly lower than the aquatic medium (**Figure 1-1**). The high ion content of SW results in passive water loss and ion-loading. In contrast to FW fishes, SW fishes drink the surrounding medium to replenish water lost passively. This is done by desalinating SW as it moves along the gut so that water follows (from gut lumen to blood) by osmosis. But the salt acquired (Na^+ and Cl^-) during this process along with salt entering the fish diffusively across exposed surfaces (i.e. across the gill and skin), must be eliminated. The gill of SW fishes secretes Na^+ and Cl^-, whereas the low volume production of concentrated urine, and intestinal precipitation of divalent cations ensures the elimination of these elements.

This review will focus on the fish gill as an osmoregulatory organ with an emphasis on the role and contribution of the gill epithelium to the maintenance of salt and water balance in fishes. In addition, because my PhD studies have focused primarily on the barrier properties of the fish gill epithelium, the introduction will provide an overview of this area as well as the model gill epithelia that have helped to broaden our understanding of the topic.

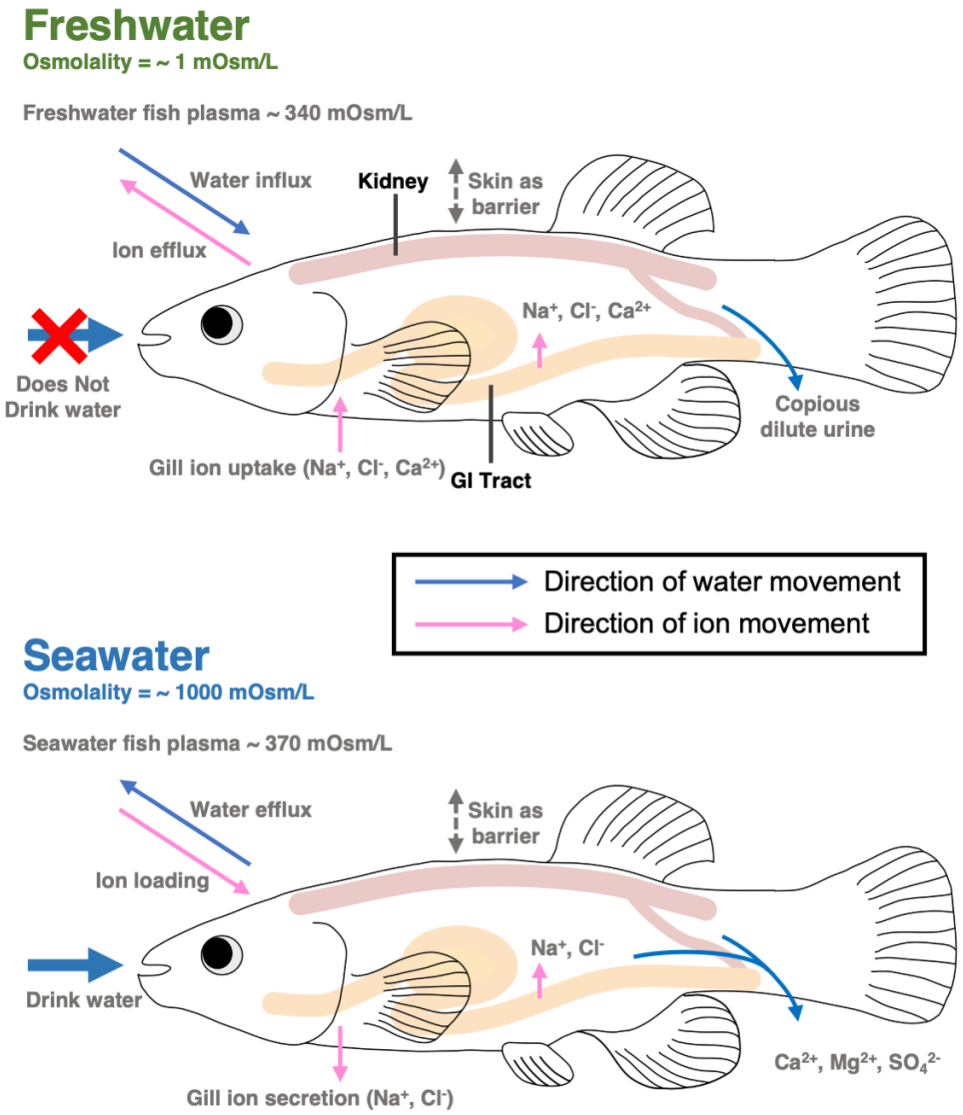

Figure 1-1. Strategies used to maintain salt and water balance in bony fish residing in (A) freshwater (FW) and (B) seawater (SW) environments. Despite the difference in the salt content of aquatic environments and resulting variations in iono-regulation strategies, all fishes maintain a similar internal fluid composition that is different than the aquatic medium.

1.2. The Gill Epithelium and Its Role in Osmoregulation

The fish gill is a complex organ that simultaneously regulates multiple key physiological functions including respiration, acid-base regulation, nitrogenous waste excretion, and salt and water balance (Evans et al., 2005). The fish gill is an architecturally complex organ with a heterogeneous epithelium that directly separates intracellular fluids from the aquatic medium. The complex architecture of the gill allows increased surface area in direct contact with the aquatic environment (Wilson and Laurent, 2002). This is especially important in the aquatic organisms as a large respiratory surface is required for gas exchange with the aquatic medium (Perry and McDonald, 1993). Therefore, the gill epithelium must be able to maintain its various important physiological functions and at the same time limit the passive exchange of solutes with the aquatic medium. The significance of the gill in piscine homeostasis and its specific role in ionic-regulation was first proposed by Homer Smith when he noted the kidneys of marine teleosts cannot produce a solution that is hypertonic to the plasma (Smith, 1930). Following Smith's observation, experiments using the perfused gill of eels later demonstrated chloride transport against a concentration gradient across the organ (Keys, 1931). These experiments became fundamental to our current understanding of gill physiology and its significance in osmoregulation.

1.2.1. General Structure of The Fish Gill Epithelium

The gills of fishes are structures located lateral to the pharynx on either side of the head. Bony fishes have four pairs of complete gill arches, or holobranches, that reside in a branchial cavity which is covered by a bony operculum. The comb like primary filaments of the gill sit on the bony gill arch, and parallel arrangements of dorsoventrally flattened secondary lamella on the primary filaments further increase overall surface area of the gill organ (Wilson and Laurent, 2002).

Respiration is achieved by positive pressure in fishes. Water is first taken in from the mouth and irrigated through the gill filaments, and by closing the mouth, water is expelled through the opercula openings. As dissolved oxygen concentration is low in aqueous medium, the expansive surface area of the gill epithelium ensures efficiency in oxygen extraction (Perry and McDonald, 1993). The gill epithelium between the various bony fish species in the various aquatic environments are similar in overall structure, but some have unique adaptations that are tailored to the specific environmental conditions, and morpho-functional changes can take place in response to changing environmental circumstances (Sollid et al., 2003; Sollid et al., 2005; Mitrovic and Perry, 2009).

The gill epithelium of fishes is a heterogenous amalgamation of epithelial cells comprising approximately 80 - 90% pavement cells (PVCs; respiratory cells). The remaining cells of the epithelium are largely made up of an admixture that include ionocytes (~ 10% of the population), mucous, neuroepithelial, and undifferentiated cells. The cellular composition of the gill epithelium in stenohaline and euryhaline fishes is dynamic. Observations of both cellular rearrangement and biochemical changes in response to changing environmental salt content are supported by a sizable literature covering all fish groups (e.g. Allen et al., 2009; Bartels et al., 2011; Bartels and Potter, 2004; Chasiotis et al., 2012b; Chen et al., 2016; McCormick and Saunders, 1987; Morash et al., 2016; Pisam et al., 1988) Moreover, reorganization of the gill epithelium cell composition can occur in during development and in response to lifestyle changes.

1.2.2. The Gill Epithelium and Solute Movement

PVCs are typically squamous to cuboidal, hexagonal epithelial cells that cover most of the gill epithelium surface. PVCs are thought to participate mainly as respiratory cells by facilitating gas exchange. However, the PVCs also serve as the main barrier to the aquatic medium and based

on morphological evidence from early studies, they were described as being linked by tight junction (TJ) complexes that are deep, tight and most likely impermeable to solutes (Sardet et al., 1979). Later examination of the electrophysiological properties of surrogate gill models composed exclusively of pavement cells confirmed this (Marshall 1985; Wood and Part, 1997). In addition, using primary cultured gill models composed of pavement cells only, it has been found that the TJs linking PVCs, and their regulation of paracellular solute movement, are responsive to numerous endocrine factors (Kelly and Wood, 2001a, 2001b; Kelly and Wood, 2002a, 2002b; Kolosov and Kelly 2020). Therefore, as PVCs make up the bulk of the gill epithelium in contact with the aquatic medium, and the endocrine system is a primary link between a changing environment and the physiological response of animals, the regulation of passive solute diffusion by PVCs contributes significantly to the overall maintenance of salt and water balance in fishes.

The fish gill ionocyte, also referred to as a chloride cell (CC) or mitochondrion-rich cell (MRC), is the main hub of transcellular solute movement across the gill epithelium (Evan et al 2005). Ionocytes are voluminous, contain numerous mitochondria as well as a convoluted tubular system and are exposed to water via an apical opening that penetrates the PVC 'carpet'. Therefore, inocytes are morphologically and functionally distinct from PVCs (Threadgold and Houston, 1964). It should also be noted that although ionocytes exhibit the same basic properties, as outlined above, various types of modification to ionocyte morphology and specific function/s have been described within and between fish species, as well as between fishes acclimated to different aquatic environments (Galvez et al., 2002). Morphological features that differ between ionocytes found in the gills of FW and SW fishes are particularly pronounced. For example, the apical surface of the SW fish gill ionocyte forms an apical crypt microenvironment with only a small opening to surrounding water, whereas the FW fish gill ionocyte presents an apical surface that is flush with

surrounding PVCs and presents a comparatively large surface area for active ion uptake (Karnaky et al., 1976). In addition, the basolateral membrane of a FW fish ionocyte is far less convoluted than that of a SW fish, with loosely distributed Na^+, K^+,ATPase (NKA) as opposed to the large amount in the SW fish gill (Karnaky et al., 1976). In the latter, differences in NKA distribution and isoforms have been proposed to be a mechanism of directional ion uptake and excretion in FW- versus SW- adapted fishes (McCormick et al., 2009; Richards et al., 2003). Finally, ionocytes of SW fishes are typically found adjacent to an accessory cell (AC), which interdigitate with the ionocyte in the apical crypt and here form shallow TJs between the cells that facilitate paracellular Na^+ secretion (Sardet et al 1979; Hootman and Philpott, 1980). The presence of ACs is rare in FW fishes, although not undescribed in some euryhaline species residing in FW (Hiroi et al., 2005; Pisam et al., 1989). However, interdigitation between the cells and the presence of shallow TJs have never been reported in the gill of a FW fish.

1.3. The Gills of Sea Lampreys and Sea Lamprey Gill Epithelium

Lampreys are considered to be living fossils as they have undergone little morphological changes in over 300 million years (Gess et al., 2006). They are jawless basal vertebrates and molecular characterization of the lamprey genome has provided insights into the evolution of more derived vertebrate forms (Osório and Rétaux, 2008; Smith et al., 2013). The gross morphology of the lamprey gill is different than that of a bony fish, but is similar between the various lamprey species (Youson and Freeman, 1976). The gill of sea lamprey consists of a pair of hemibranchs on the first and last pair of gill arches and six pairs of holobranchs in between. The arrangement and the slight curvature of the gill arches results in seven pairs of gill pouches. The gill pouches connect between the pharynx and the gill slits (branchiopores) that serve as respiratory openings from the

pharynx to the gill to the external environment. In both larval and adult lampreys, water enters through the mouth then irrigates the gill pouches and finally exits via the gill slits (Dawson, 1905). While this is a similar mechanism to water passage in teleost, the unidirectional gill irrigation becomes challenging in adult lampreys as they are often found latching onto either large rocks (during the breeding season) or in the case of parasitic species, fishes when feeding. In such circumstances, water movement in adult lampreys become a tidal flow by muscle contractions and pushes water through the branchiopores to irrigate the gill filaments (Dawson, 1905).

Lampreys are unique models for understanding the regulation of salt and water balance in vertebrates. Osmoregulation in lamprey is fundamentally similar to bony fishes as FW lamprey must compensate for diffusive ion loss and passive water gain, whereas seawater lamprey are challenged by ion loading and water loss (**Figure 1-2**). However, lamprey are within a small group of vertebrate animals with indirect development and in this regard, lamprey undergo full metamorphosis. The indirect development cycle results in significantly different physiological adaptations between the larval and adult stages of various lamprey species (Dawson 2015). The difference in larval and adult lamprey physiology is intensified by in species that exhibit a post-metamorphic migration run to the sea, which requires an ability to adapt to an environment that is dramatically different from the environment in which it lived as a larval form. While salinity tolerance in metamorphosis is also observed in diadromous bony fishes (Loretz et al., 1982; Sutterlin et al., 1977), lamprey metamorphosis is accompanied by dramatic changes in morphology that include the development of eyes, elaboration of a suctorial disc, change in body coloration, and functionalization of the fins (Potter, 1980; Potter et al., 1978; Youson, 1979). In addition, changes in lamprey feeding strategy and motility following metamorphosis results in regression of larval kidney and formation of an adult kidney, changes in circulatory capacity and metabolism,

and rearrangement of the gastrointestinal tract (Claridge and Potter, 1974; Kao et al., 2002; O'Boyle and Beamish, 1977; Silva et al., 2013).

1.3.1. Composition of the Sea Lamprey Gill Epithelium

The nomenclature used to describe and delineate the cell types that comprise the lamprey gill epithelium are similar to the canonical terms associated with the gill of bony fish species (Youson and Freeman, 1976). That is, the gill epithelium of largely comprises PVCs, ionocytes and mucous cells. But similar to bony fishes, the lamprey gill epithelium is dynamic and its cellular composition not only differs when exposed to different salinity, but select lamprey gill cells appear to be specific to each life cycle stage (Peek and Youson, 1979). Changes in the cellular composition and population of the gill epithelium are especially prominent in diadromous lamprey species that migrate between FW and SW, including the anadromous sea lamprey. To fully appreciate the gill epithelium of sea lamprey, the composition of the gill epithelium is best described in the sequence as it relates to life cycle progression.

Larval lampreys, or ammocoete, are FW stenohaline organisms and are unable to survive in an environment where the osmolality exceeds that of their own extracellular fluid (**Figure 1-3**; Reis-Santos et al., 2008; Richards and Beamish, 1981). Ammocoetes are sedentary suspension feeders that reside in the substratum of FW streams for 4 ½ to 6 years depending on species (for review see Dawson, 2015 and Mallatt, 1979). PVCs in the lamprey gill epithelium are the only epithelial cell type present during all life cycle stages (Bartels et al., 1998; Youson and Freeman, 1976). In ammocoetes, two ionocyte subtypes are observed on the gill epithelium. The first is a highly abundant mitochondria-rich cell (called the ammocoete MRC or AMRC) found on the lamella and the interlamellar regions of the gill (Morris and Pickering, 1975; Youson and Freeman, 1976). The AMRC is unique to the gill epithelium of larval lamprey and is not found in any other

life cycle stage. The second ionocyte on the ammocoete gill epithelium is an intercalated MRC (IMRC). The IMRC can be found singly or in pairs and are always present between two AMRCs in the interlamellar region (Morris and Pickering, 1975; Youson and Freeman, 1976). IMRCs regress in SW migrants but reappear in adults as they migrate back to FW during the spawning cycle of anadromous species (Bartels et al., 1998).

After the protracted larval phase, sea lamprey undergo metamorphosis during which time adult features develop (Potter et al., 1978; Youson, 2003). Intermediate stage individuals between the larval and adult phase can be described as transformers (for the first 5 weeks or so), then metamorphosing lamprey as the animals gradually completes the metamorphic process over the course of 6 months to one year. In metamorphosing lamprey, AMRCs regress, but adult ionocytes begin to surface on the gill epithelium (Bartels and Potter, 2004). The adult ionocytes, most often referred to as chloride cells (CCs) in lamprey literature, persist throughout the SW residency period of the adult and regress during FW migration in anadromous species. While these adult ionocytes are not fully exposed in post-metamorphic young adults in FW environment, they become fully exposed and form continuous rows in the interlamellar region when the lamprey acclimate to elevated salinity (Bartels et al., 1996). As a consequence, the CCs of adult lampreys are thought to contribute to the hypoosmoregulation in the SW aquatic environment.

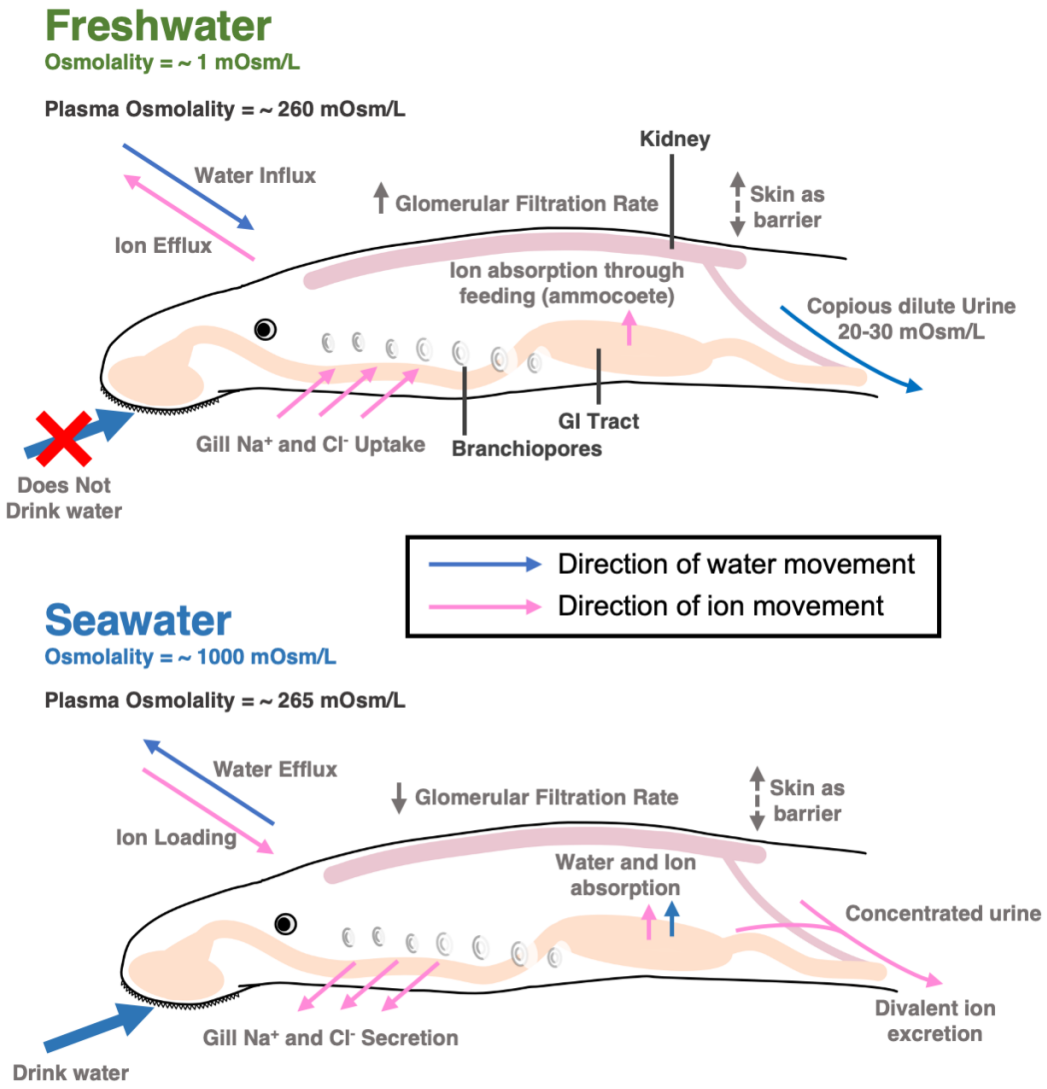

Figure 1-2. Representative diagrams for (A) FW and (B) SW adult sea lamprey (*Petromyzon marinus)* osmoregulation. Lamprey osmoregulatory strategies not only differ between lamprey species but can also vary depending on life cycle stages (Adopted and modified from Bartels and Potter, 2004).

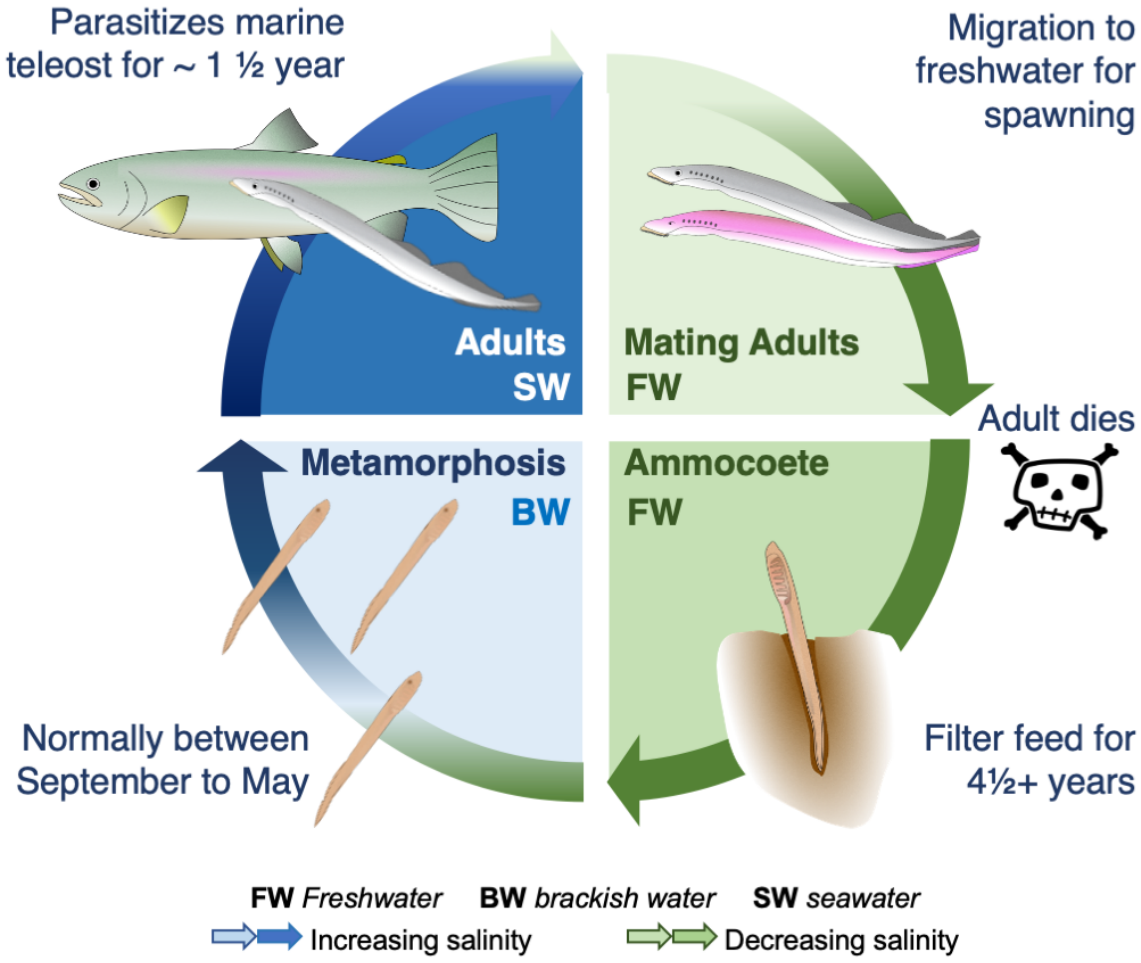

Figure 1-3. Representative diagrams for anadromous sea lamprey (*Petromyzon marinus*) life cycle stages and corresponding aquatic environment. The life cycle begins as stenohaline ammocoetes as burrowing filter feeders. Salinity tolerance increase in metamorphosing lampreys where the adults become raptorial in the marine environment. As the last stage of the life cycle, the adults migrate back to freshwater to spawn and dies.

1.4. The Surrogate Gill Model

Surrogate models of the fish gill and fish gill epithelium have contributed significantly to our current understanding of branchial ion transport physiology. Prior to the development of surrogate gill models, the architectural complexity and the cellular heterogeneity of the gill often presented limitations in the design of experiments that sought to understand the transcellular and paracellular ion-transport characteristics of the gill epithelium. Early headway in our examination of the fish gill and gill physiology were conducted using the whole organism and/or perfused gills (Bellamy and Jones, 1961; Keys, 1931). The use of perfused gill as well as excised gill explants are advantageous as experiments can be conducted in the absence of systemic factors that may impact the physiology of the organ. However, these experiments did not address cell heterogeneity and the electrophysiological characteristics of an epithelium in those days were best revealed using simple flat tissue that could be mounted in Ussing chambers. Therefore, significant advances in branchial physiology were made possible by using isolated areas of fish skin which were simple, flat and possessed the same types of cell as those found in the gill epithelium.

1.4.1. Surrogate Gill Models

Techniques to isolate, mount and study surrogate branchial epithelia in Ussing chambers were initially developed for the opercular skin derived from seawater-adapted killifish (*Fundulus heteroclitus*) and seawater-adapted longjaw mudsucker (*Gillichthys mirabilis*) (Degnan et al., 1977; Marshall, 1977). The opercular epithelium is flat section of skin lying on the underside of the operculum which possesses a cell population that closely mimics the gill, both qualitatively and quantitatively. The use of the opercular skin as a surrogate gill model led to definitive evidence for transcellular chloride secretion by SW fish gill ionocytes (Foskett and Scheffey, 1982) as well as observed differences in the barrier properties of the FW versus SW gill, as indicated by

electrophysiological endpoints (i.e. transmural resistance and/or conductance) (Ernst et al., 1980; Foskett and Scheffey, 1982; Marshall et al., 1997, 1992). Furthermore, a significant advantage of the surrogate gill model derived from the opercular skin is that it allowed both symmetrical (physiological medium on both sides of epithelia) and asymmetrical (water on apical side of epithelia and physiological media on basolateral side) experimental conditions to be conducted, and this better mimics the native transport epithelium in direct contact with the aquatic environment (Foskett et al., 1981; Foskett and Scheffey, 1982).

While Ussing chamber mounted surrogate gill models significantly accelerated an understanding of gill transport properties, a disadvantage with the system was that excised tissue was viable for comparatively short periods of time and could not be used to look at the chronic effect/s of factors that might impact gill physiology (e.g. the chronic effect/s of an endocrine factor). As a complementary approach, gill explant cultures were developed which allowed gill tissues to be maintained *ex vivo* (McCormick and Bern, 1989). Gill explant cultures allowed longer studies to be conducted, and have been reported as endocrine factor responsive (Bossus et al., 2017; Breves et al., 2014; McCormick and Bern, 1989). But explant cultures do not permit electrophysiological measurements to be made, do not address cell heterogeneity and are typically reported to begin a process of functional degradation shortly after isolation (Bossus et al., 2017).

1.4.2. Primary Cultured Gill Epithelia

Primary cell culture techniques using isolated gill cells in petri dishes was pioneered by Pärt and colleagues (1993) using cells derived from the rainbow trout (*Oncorhynchus mykiss*) gill. Primary cell culture techniques using isolated gill cells were advantageous as they overcame the morphological complexity of the native gill. Furthermore, gill ionocytes were initially found to be unable to attach to the culture substratum, and the preparation conveniently resulted in a

homogeneous culture of PVCs (Pärt et al., 1993). Despite this significant advance, it was undetermined whether the isolated gill cells develop the characteristics of polarized epithelial cells (O'Donnell et al., 2001). Furthermore, cultured cells in petri dishes were of limited use when bathed entirely in culture medium. Nevertheless, this initial success later led to the development of primary cultured rainbow trout gill PVCs on permeable cell culture inserts (Wood and Part, 1997). Techniques for a primary cultured trout epithelium incorporating both PVCs and ionocytes were soon developed as a companion methodology (Fletcher et al 2000). Further development of primary cultured gill epithelium preparations on permeable inserts have now been extended to various other teleost species including the Nile tilapia (Kelly and Wood, 2002b), green-spotted puffers (Bui and Kelly, 2011), and goldfish (Chasiotis and Kelly, 2011). Cultured gill epithelia on permeable inserts was a significant milestone as these *in vitro* models provides several experimental advantages including:

1. Primary cultured models address both issues of gill architectural complexity and gill cell heterogeneity because simple flat epithelium preparations composed of PVCs or PVCs + ionocytes can be 'grown' on permeable inserts (Fletcher et al 2000; Kelly et al., 2000; Wood and Part, 1997)
2. Primary cultured gill epithelium preparations are 'living' models that develop over time and maintain integrity for extended periods. Therefore, chronic exposure to factors that may influence the functional properties of the gill epithelium can be examined.
3. The electrophysiological properties of the epithelium models can be monitored and the passage of solutes or tracer molecules across epithelia can be examined (Kelly et al., 2000; Wood et al., 1998; Wood and Part, 1997)

4. Experiments can be conducted in both symmetrical and asymmetrical conditions, the latter allowing the researcher to mimic natural conditions where the apical surface is bathed with water (Bui and Kelly, 2015; Chasiotis et al., 2012b; Kelly and Wood, 2002b; Kelly and Wood, 2001a; Wood et al., 1998)

Measurement of electrical resistance across primary cultured gill epithelium models on permeable inserts is a non-disruptive method to measure the resistive properties of the cultured epithelium. Transepithelial epithelial resistance (TER) is the sum total of resistance (i.e. resistance generated by both the transcellular and paracellular pathway) created by passing an alternate current across the epithelium using a chopstick electrode and recorded as electrical resistance per centimeter area ($\Omega \cdot cm^2$). Total resistance measurement includes resistance from the measuring instrument, the culture medium, the permeable membrane, and the cultured epithelium. Therefore, the resistance of the cultured epithelium can be measured experimentally by controlling these factors (i.e. subtracting them as background). Gill epithelia on permeable inserts exhibit a sigmoidal increase in TER values in culture during the formation of the polarized epithelial layer (Kelly et al., 2000; Wood and Part, 1997). More importantly, increase in TER values signifies the formation of TJ assembly between the isolated gill cells (Anderson and Van Itallie, 2009; Günzel and Fromm, 2012). Cultured gill epithelia of fishes exhibit a TER that is generally higher than most mammalian derived models (Bui and Kelly, 2011; Chasiotis et al., 2010; Kelly et al., 2000; Kelly and Wood, 2002b). This is not unreasonable as the branchial epithelium is a tight barrier that limits diffusive solute passage between the aquatic medium and the internal milieu.

1.5. The TJ Complex in the Vertebrate Epithelium

The TJ is an intercellular junctional complex located circumferentially around the apical-lateral sides of epithelial and endothelial cells (Günzel and Fromm, 2012; Günzel and Yu, 2013). TJs, also described as occluding junctions, mediate the perm-selectivity properties of the vertebrate epithelium and endothelium. TJ in vertebrate epithelia was first identified in ultrathin sections by Farquhar and Palade (1963). In freeze fracture replicas, the TJ assembly can be observed as a network of anastomosing proteins connecting adjacent cells, and these largely dictate the barrier properties of the vertebrate epithelium (Tsukita and Furuse, 1999). TJ can be classified either as "tight", where the properties of the TJ proteins limits the passage of solutes, or "leaky", when there is a selective permeability across the epithelium (Zihni et al., 2016). TJ proteins are tetra-spanning transmembrane proteins with two extracellular loops, where scaffolding TJ proteins anchors the complex to the cytoskeleton (**Figure 1-4**). The extracellular loops of the TJ proteins, in contact with the extracellular loop of neighboring TJ molecules, dictates the perm-selective properties of the epithelium by solute size selectivity, hydrophobic/hydrophilic interactions, or by charge selective properties as a result of the charged residues (Anderson and Van Itallie, 2009; Van Itallie and Anderson, 2006).

1.5.1. TJ in the Fish Gill Epithelium

An essential function of the vertebrate epithelium is to maintain the compartmental organizations of body cavities and protection from the environment. In fishes, the importance of maintaining the selective permeability of epithelium is amplified when compared to terrestrial vertebrates. The aquatic environment is highly demanding on the selective barrier properties of epithelium and integument in contact with the aquatic medium. Furthermore, the gill epithelium is a thin barrier between the aquatic environment and the internal milieu. Therefore, it is unsurprising

to find a wide compendium of diverse mechanisms for the regulation of the permselective properties of the gill epithelium. The presence of TJ structures in the gills of fishes were first identified by Öberg (1967) and also later detailed by Sardet and colleagues (1979). Currently, the presence of TJ assembly has been identified in the gills of jawless fishes, in cartilaginous fishes, and in bony fishes (Gauthier et al., 2018; Wilson and Laurent, 2002). It was realized that the morphology of these TJ complexes would alter in response to changing environmental conditions. Due to the significant contributions of fish gill epithelium in the maintenance of overall piscine homeostasis, there has been considerable interests in understanding the roles of TJ proteins in fish physiology.

The molecular physiology and biochemistry of TJs in bony fishes has been examined more extensively than any other vertebrate group except for mammals (For reviews, see Chasiotis et al., 2012a; Kolosov et al., 2013), and from a molecular standpoint, the TJ complex of fishes has emerged as a tremendously dynamic structure. Changes in the molecular physiology of the fish TJ complex in almost all major organs have been reported in response to numerous variables including those that relate to development, endocrine regulation and environmental perturbation. However, the gill has been a major focal point of many studies as the gill epithelium directly interfaces with water and plays a crucial role in homeostasis of these animals. The permeability of the gill epithelium (and other osmoregulatory organs) have been directly associated with changes in mRNA and protein abundance of TJ-associated elements as a result of environmental challenges. For example, selective alterations in specific TJ protein (or transcript) abundance in ion-poor water (IPW) as well as SW have been highly beneficial in deriving an understanding of the barrier properties of the gill TJ complex, as the gill epithelium must be reorganized to compensate for changes in the salt content of surrounding water (Kelly and Wood, 2001a; Kelly and Wood, 2002a;

Bui and Kelly, 2015; Chasiotis et al., 2012b; Chen et al., 2016; Greco et al., 1996; Kolosov et al., 2017a; Kolosov and Kelly, 2016). In particular, the selective barrier properties of TJs in the SW fish salt-secreting gill epithelia has received significant research interest. In SW, TJ assemblies in the gill epithelium must limit undesirable solute passage while facilitating selective ion extrusion, and the mechanism to facilitate hypoosmoregulation has been highlighted in several studies (Bagherie-Lachidan et al., 2009; Bui and Kelly, 2014; Tipsmark et al., 2016, 2008). One specific focus is the selective passage that allows the Na^+ ions to move between the "leaky" junctions of ionocytes and ACs. Current literature supports Cldn-10 isoforms as major players in this specialized role of ion extrusion. Cldn-10 variants (specifically Cldn-10a and Cldn-10b) in the mammalian renal epithelium are models of selective ion channels (Van Itallie et al., 2006). The specific association of TJ with ionocytes was first observed in a spotted green puffer fish gill cell culture that is devoid of ionocytes, where *cldn-6*, *cldn-10d*, and *cldn-10e* were undetected by PCR (Bui and Kelly, 2011). The proposed association of Cldn-10 isoforms and gill ionocytes was further demonstrated in culture trout epithelia, where *cldn-10c* and *-10d* were absent in a model composed of PVCs only and present when the gill model contained both PVCs and ionocytes (Kolosov et al., 2014). The significance of Cldn-10 in salinity acclimation was further emphasized by Bui and Kelly (2014) who reported that Cldn-10d and -10e localized to gill ionocytes only, exhibited an increase in abundance in SW versus FW, and localized more intensely in the apical region of the SW ionocyte. Finally, the importance of Cldn-10 isoforms in hypersaline hypoosmoregulation has more recently been demonstrated in killifish, where Cldn-10c is further proposed as the important ion channel in selective Na^+ extrusion (**Figure 1-5**) (Marshall et al., 2018). In addition to the above, it is also worth noting that in a primary cultured gill epithelium model, knockdown of select genes encoding TJ proteins has been used to experimentally dissect

their contribution to the barrier properties of the tissue (Bui et al 2010; Kolosov et al., 2014, 2017b; Kolosov and Kelly, 2017).

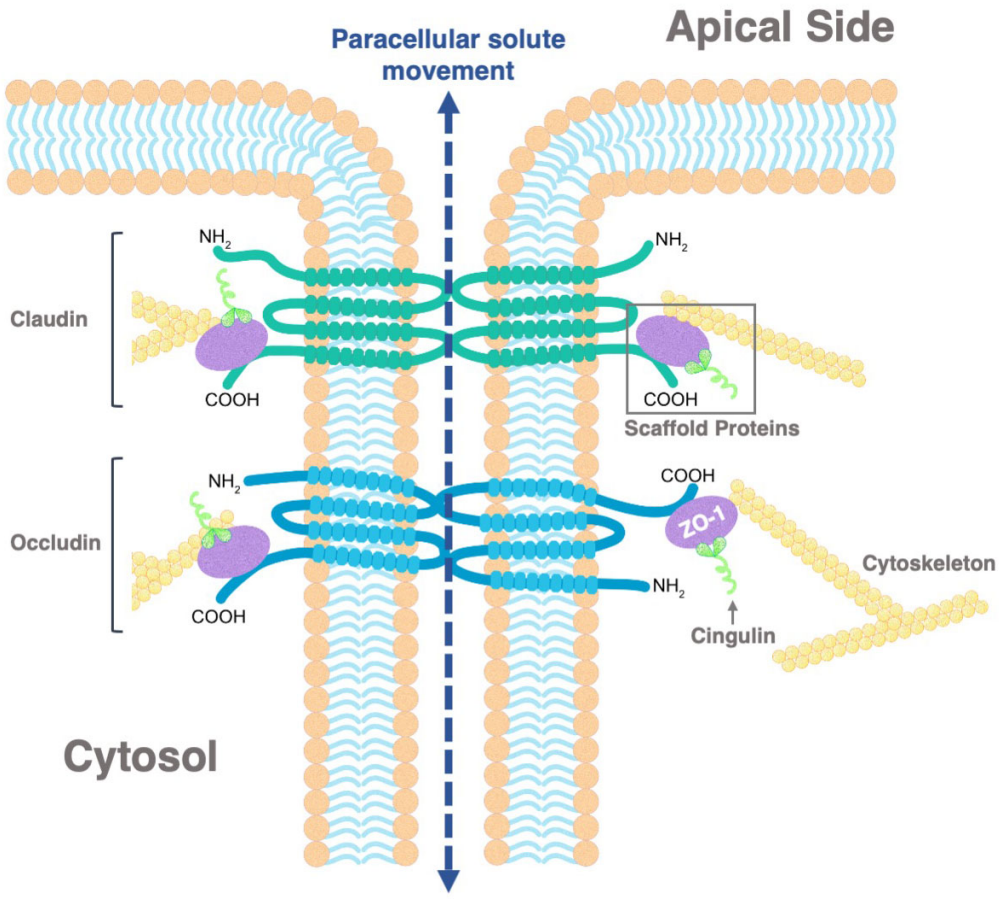

Figure 1-4. Canonical model of the vertebrate tight junction (TJ) complex. In the current view of a bicellular TJ complex, the TJ assembly is comprised of tetraspanning TJ proteins (i.e. Claudins and Occludin) localized on the apical-lateral sides of epithelial cells. The extracellular loops of the TJ contact and form the permselective properties of the complex. TJ proteins are anchored into the cytoskeleton through scaffolding TJ protein (i.e. ZO–1). Scaffolding TJ protein are also signaling molecules.

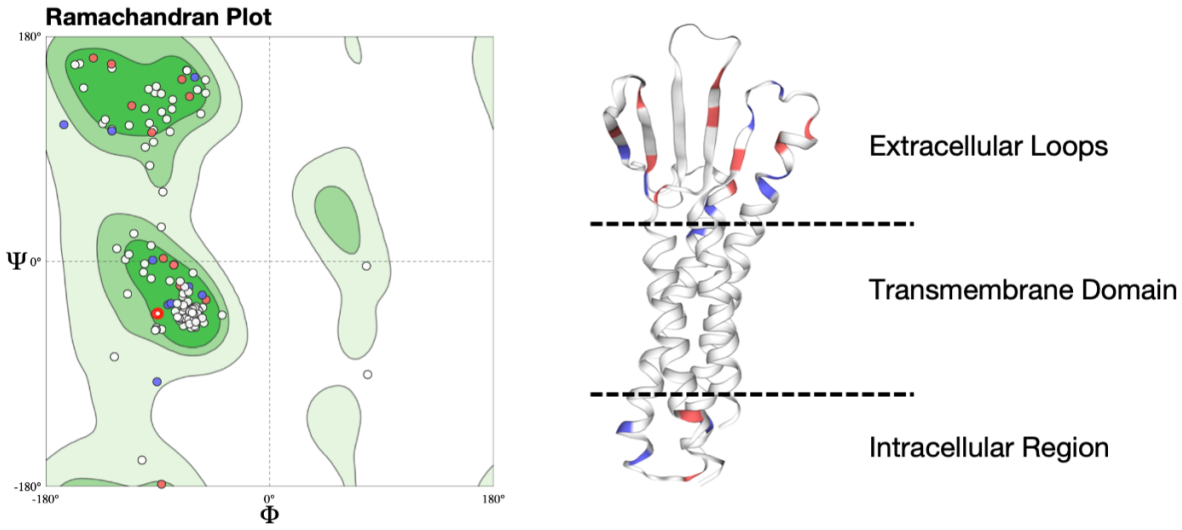

Figure 1-5. Predicted tertiary structure of killifish (*Fundulus heteroclitus*) Cldn-10c (XP_012728690). Ramachandran plot (A) and 3D model of Cldn-10c (B) shows polar extracellular loops with both positive (blue) and negative (red) residues. The hypothetical model currently suggests interactions between Cldn-10 isoforms can form the TJ pores that facilitate sodium extrusion down an electrochemical gradient into the apical crypt of SW killifish gill ionocyte.

1.6. Hypothesis and Research Objectives

Primary cultured gill epithelium preparations derived from bony fishes have been recognized as powerful tools for elucidating the barrier properties of the gill epithelium. Nevertheless, there is always scope to improve these models in order to provide insight into gill barrier properties that is as accurate as possible. In addition, there is a need to develop model gill epithelia from other fishes, particularly those that do not fall within the bony fish clade. Beyond a recognition of TJ heterogeneity as observed by electron microscope studies, little is known about the TJ complex in other major fish groups (for review see Chasiotis et al 2012). Therefore, a unifying goal of my thesis was to consider the barrier properties of the fish gill epithelium further by investigating and utilizing established gill epithelium models derived from a bony fish (the

rainbow trout) and studying the barrier properties of the lamprey gill epithelium, in part by developing the first primary cultured lamprey gill model. In this regard, I hypothesized: 1. **the expression profile of TJ-associated genes allows enhanced recognition of the barrier properties of the gill epithelium and gill epithelium models,** and 2. **a primary cultured model of the sea lamprey gill epithelium will provide a better understanding of lamprey gill epithelium barrier function.** To address the outlined goal of my studies, I had two primary objectives:

1. *To broaden the current knowledge of teleost branchial physiology by examining how endogenous factors such as native serum or endocrine factors linked to the regulation of salt and water balance in fishes can affect gill epithelium barrier function.*

2. *Consider molecular endpoints of sea lamprey gill epithelium barrier function through all defined life stages in the sea lamprey life cycle as well as develop a primary cultured model gill epithelium derived from the gills of sea lamprey.*

My first objective above will allow an enhanced understanding of the branchial physiology of the gill epithelium by utilizing an establish model to further elucidate how TJ-assembly in the fish gill epithelium respond to endogenous and exogenous factors, including utilizing an *in vivo* model to understand how TJ may facilitate hypoosmoregulation capacity in an enhanced environmental gradient. Furthermore, my second goal will provide novel insights on the roles of TJ-complex in the sea lamprey life cycle, as well as how changes in TJ-complex manifests in response to salinity acclimation. Finally, a gill epithelium model derived using larval sea lampreys will not only allow mechanistic experiments to be conducted on the cells derived from this basal vertebrate, but it will provide the first non-teleost piscine branchial epithelium model.

1.7. References

Allen, P.J., Cech, J.J., Kültz, D. (2009) Mechanisms of seawater acclimation in a primitive, anadromous fish, the green sturgeon. J Comp Physiol B Biochem Syst Environ Physiol 179: 903-920.

Anderson, James M, Van Itallie, C.M. (2009) Physiology and function of the tight junction. Cold Spring Harb. Perspect Biol 1: 1-17.

Bagherie-Lachidan, M., Wright, S.I., Kelly, S.P. (2009) Claudin-8 and -27 tight junction proteins in puffer fish *Tetraodon nigroviridis* acclimated to freshwater and seawater. J Comp Physiol B Biochem Syst Environ Physiol 179: 419-431.

Bartels, H., Fazekas, U., Youson, J.H., Potter, I.C. (2011) Changes in the cellular composition of the gill epithelium during the life cycle of a nonparasitic lamprey: Functional and evolutionary implications. Can J Zool 89: 538–545.

Bartels, H., Moldenhauer, A., Potter, I.C. (1996) Changes in the apical surface of chloride cells following acclimation of lampreys to seawater. Am J Physiol - Regul Integr Comp Physiol 270: R125-R133.

Bartels, H., Potter, I.C. (2004) Cellular composition and ultrastructure of the gill epithelium of larval and adult lampreys: Implications for osmoregulation in fresh and seawater. J Exp Biol 207: 3447-3462.

Bartels, H., Potter, I.C., Pirlich, K., Mallatt, J. (1998) Categorization of the mitochondria-rich cells in the gill epithelium of the freshwater phases in the life cycle of lampreys. Cell Tissue Res. 291: 337-349.

Bellamy, D., Jones, I.C. (1961) An apparatus for studying the gain and loss of electrolytes by the eel. Comp Biochem Physiol 3: 223-226.

Bossus, M.C., Bollinger, R.J., Reed, P.J., Tipsmark, C.K. (2017) Prolactin and cortisol regulate branchial claudin expression in Japanese medaka. Gen Comp Endocrinol 240 :77-83.

Breves, J.P., Seale, A.P., Moorman, B.P., Lerner, D.T., Moriyama, S., Hopkins, K.D., Grau, E.G. (2014) Pituitary control of branchial NCC, NKCC and Na+, K+-ATPase α-subunit gene expression in Nile tilapia, *Oreochromis niloticus*. J Comp Physiol B Biochem Syst Environ Physiol 184: 513-523.

Bui, P., Kelly, S.P. (2015) Claudins in a primary cultured puffer fish (*Tetraodon nigroviridis*) gill epithelium model alter in response to acute seawater exposure. Comp Biochem Physiol A Mol Integr Physiol 189: 91101.

Bui, P., Kelly, S.P. (2014) Claudin-6, -10d and -10e contribute to seawater acclimation in the euryhaline puffer fish *Tetraodon nigroviridis*. J Exp Biol 217: 1758–1767.

Bui, P., Kelly, S.P. (2011) Claudins in a primary cultured puffer fish (*Tetraodon nigroviridis*) gill epithelium. Methods Mol Biol 762: 179-94.

Chasiotis, H., Kelly, S.P. (2011) Effect of cortisol on permeability and tight junction protein transcript abundance in primary cultured gill epithelia from stenohaline goldfish and euryhaline trout. Gen Comp Endocrinol 172: 494-504.

Chasiotis, H., Kolosov, D., Bui, P., Kelly, S.P. (2012a) Tight junctions, tight junction proteins and paracellular permeability across the gill epithelium of fishes: a review. Respir Physiol Neurobiol 184: 269-81.

Chasiotis, H., Kolosov, D., Kelly, S.P. (2012b) Permeability properties of the teleost gill epithelium under ion-poor conditions. Am J Physiol Regul Integr Comp Physiol 302: R727-39.

Chasiotis, H., Wood, C.M., Kelly, S.P. (2010) Cortisol reduces paracellular permeability and increases occludin abundance in cultured trout gill epithelia. Mol Cell Endocrinol 323: 232-238.

Chen, C.C., Kolosov, D., Kelly, S.P. (2016) The liquorice root derivative glycyrrhetinic acid can ameliorate ionoregulatory disturbance in rainbow trout (*Oncorhynchus mykiss*) abruptly - exposed to ion-poor water. Comp Biochem Physiol A Mol Integr Physiol 199: 120-129.

Claridge, P.N., Potter, I.C. (1974) Heart Ratios at Different Stages in the Life Cycle of Lampreys. Acta Zool 55: 61–69.

Dawson, J. (1905) The Breathing and Feeding Mechanism of the Lampreys. Biol Bull 9: 91111.

Dawson HA, Quintella BR, Almeida PR, Treble AJ, Jolley JC (2015) The Ecology of Larval and Metamorphosing Lampreys. In: Lamprey Biology, Conservation and Control, Edited by Docker MF. Corvallis, Oregon: Springer Science, p. 75 - 125.

Degnan, K., Karnaky, K., Zadunaisky, J. (1977) Active chloride transport in the in vitro opercular skin of a teleost (*Fundulus heteroclitus*), a gill-like epithelium rich in chloride cells. J Physiol 271: 155-191.

Dong, Y., Blanchard, T.S., Noll, A., Vasquez, P., Schmitz, J., Kelly, S.P., Wright, P.A., Whitehead, A. (2019) Life out of water: Genomic and physiological mechanisms underlying skin phenotypic plasticity. bioRxiv 772319. https://doi.org/10.1101/772319

Ernst, S.A., Dodson, W.C., Karnaky, K.J. (1980) Structural diversity of occluding junctions in the low-resistance chloride-secreting opercular epithelium of seawater-adapted killifish (*Fundulus heteroclitus*). J Cell Biol 87: 488-497.

Evans, D.H., Piermarini, P.M., Choe, K.P. (2005) The multifunctional fish gill: dominant site of gas exchange, osmoregulation, acid-base regulation, and excretion of nitrogenous waste. Physiol Rev 85: 97-177.

Farquhar, M.G., Palade, G.E. (1963) Junctional Complexes in Various Epithelia. J. Cell Biol. 17, 375-412.

Foskett, K., Logsdon, C., Machen, T., Bern, H. (1981) Differentiation of the Chloride Extrusion Mechanism During Seawater Adaptation of a Teleost Fish, The Cichlid *Sarotherodon mossambicus*. J Exp Biol 93: 209-224.

Foskett, K., Scheffey, C. (1982) The Chloride Cell : Definitive Identification as the Salt-Secretory Cell in Teleosts. Science 215: 164-166.

Galvez, F., Reid, S.D., Hawkings, G., Goss, G.G. (2002) Isolation and characterization of mitochondria-rich cell types from the gill of freshwater rainbow trout. Am J Physiol Regul Integr Comp Physiol 282: 658-668.

Gauberg, J., Kolosov, D., Kelly, S.P. (2017) Claudin tight junction proteins in rainbow trout (*Oncorhynchus mykiss*) skin: Spatial response to elevated cortisol levels. Gen Comp Endocrinol 240: 214-226.

Gauthier, A.R.G., Whitehead, D.L., Tibbetts, I.R., Cribb, B.W., Bennett, M.B. (2018) Morphological comparison of the ampullae of Lorenzini of three sympatric benthic rays. J. Fish Biol 92: 504-514.

Gess, R.W., Coates, M.I., Rubidge, B.S. (2006) A lamprey from the Devonian period of South Africa. Nature 443: 981-984.

Greco, A.M., Fenwick, J.C., Perry, S.F. (1996) The effects of soft-water acclimation on gill structure in the rainbow trout *Oncorhynchus mykiss*. Cell Tissue Res. 285: 75-82.

Günzel, D., Fromm, M. (2012) Claudins and other tight junction proteins. Compr Physiol 2: 1819-1852.

Günzel, D., Yu, A.S.L. (2013) Claudins and the modulation of tight junction permeability. Physiol Rev 93(2): 525-569.

Hiroi, J., McCormick, S.D., Ohtani-Kaneko, R., Kaneko, T. (2005) Functional classification of mitochondrion-rich cells in euryhaline Mozambique tilapia (*Oreochromis mossambicus*) embryos, by means of triple immunofluorescence staining for Na^+,K^+– ATPase, Na^+,K^+,$2Cl^-$ cotransporter and CFTR anion channel. J Exp Biol 208: 2023-2036.

Hootman, S.R., Philpott, C.W. (1980) Accessory cells in teleost branchial epithelium. Am J Physiol Regul Integr Comp Physiol 238(3): R199-R206.

Kao, Y.H., Youson, J.H., Vick, B., Sheridan, M.A. (2002) Differences in the fatty acid composition of larvae and metamorphosing sea lampreys, *Petromyzon marinus*. Comp Biochem Physiol B Biochem Mol Biol 131: 153-169.

Kelly, S.P., Fletcher, M., Pärt, P., Wood, C.M. (2000) Procedures for the preparation and culture of "reconstructed" rainbow trout branchial epithelia. Methods Cell Sci. 22: 153-163.

Kelly, S.P., Wood, C.M. (2002a) Prolactin effects on cultured pavement cell epithelia and pavement cell plus mitochondria-rich cell epithelia from freshwater rainbow trout gills. Gen Comp Endocrinol 128: 44-56.

Kelly, S.P., Wood, C.M. (2002b) Cultured gill epithelia from freshwater tilapia (*Oreochromis niloticus*): Effect of cortisol and homologous serum supplements from stressed and unstressed fish. J Membr Biol 190: 29-42.

Kelly, S.P., Wood, C.M. (2001a) Effect of cortisol on the physiology of cultured pavement cell epithelia from freshwater trout gills. Am J Physiol Regul Integr Comp Physiol 281: 811-820.

Kelly, S.P., Wood, C.M. (2001b) The physiological effects of 3,5′,3′-triiodo-L-thyronine alone or combined with cortisol on cultured pavement cell epithelia from freshwater rainbow trout gills. Gen Comp Endocrinol 123: 280-294.

Kelly, S.P., Wood, C.M. (2001) Effect of cortisol on the physiology of cultured pavement cell epithelia from freshwater trout gills. Am J Physiol Regul Integr Comp Physiol 281: R811-R820.

Keys, A.B. (1931) Chloride and water secretion and absorption by the gills of the eel. Z Vgl Physiol 15: 364-388.

Kolosov, D., Bui, P., Chasiotis, H., Kelly, S.P. (2013) Claudins in teleost fishes. Tissue Barriers 1, e25391.

Kolosov, D., Bui, P., Donini, A., Wilkie, M.P., Kelly, S.P. (2017a) A role for tight junction-associated MARVEL proteins in larval sea lamprey (*Petromyzon marinus*) osmoregulation. J Exp Biol 220: 3657-3670.

Kolosov, D., Donini, A., Kelly, S.P. (2017b) Claudin-31 contributes to corticosteroid-induced alterations in the barrier properties of the gill epithelium. Mol Cell Endocrinol 439: 457-466.

Kolosov, D., Kelly, S.P. (2017) Claudin-8d is a cortisol-responsive barrier protein in the gill epithelium of trout. J Mol Endocrinol 59: 299-310.

Kolosov, D., Kelly, S.P. (2016) Dietary salt loading and ion-poor water exposure provide insight into the molecular physiology of the rainbow trout gill epithelium tight junction complex. J Comp Physiol B Biochem Syst Environ Physiol 186: 739-757.

Kolosov, D., Chasiotis, H., Kelly, S.P. (2014) Tight junction protein gene expression patterns and changes in transcript abundance during development of model fish gill epithelia. J Exp Biol 217: 1667-1681.

Loretz, C.A., Collie, N.L., Richman, N.H., Bern, H.A. (1982) Osmoregulatory changes accompanying smoltification in coho salmon. Aquaculture 28: 67-74.

Mallatt, J. (1979) Surface morphology and functions of pharyngeal structures in the larval lamprey Petromyzon marinus. J Morphol 162: 249-273.

Marshall, W.S. (1977) Transepithelial potential and short-circuit current across the isolated skin of *Gillichthys mirabilis* (Teleostei: Gobiidae), acclimated to 5% and 100% seawater. J Comp Physiol B 114: 157-165.

Marshall, W.S., Bryson, S.E., Wood, C.M. (1992) Calcium transport by isolated skin of rainbow trout. J Exp Biol 166: 297-316.

Marshall, W.S., Bryson, S.E., Darling, P., Written, C., Patrick, M., Wilkie, M., Wood, C.M., Buckland-Nicks, J. (1997) NaCl transport and ultrastructure of opercular epithelium from a freshwater-adapted euryhaline teleost, *Fundulus heteroclitus*. J Exp Zool 277: 23-37.

Marshall, W.S., Breves, J.P., Doohan, E.M., Tipsmark, C.K., Kelly, S.P., Robertson, G.N., Schulte, P.M. (2018) Claudin-10 isoform expression and cation selectivity change with salinity in salt-secreting epithelia of *Fundulus heteroclitus*. J Exp Biol 221: jeb168906.

Marshall, W.S., Bryson, S.E., Darling, P., Written, C., Patrick, M., Wilkie, M., Wood, C.M., Buckland-Nicks, J. (1997) NaCl transport and ultrastructure of opercular epithelium from a freshwater-adapted euryhaline teleost, *Fundulus heteroclitus*. J Exp Zool 277: 23-37.

Marshall, W.S., Bryson, S.E., Wood, C.M. (1992) Calcium transport by isolated skin of rainbow trout. J Exp Biol 166: 297-316.

McCormick, S.., Saunders, R.L. (1987) Preparatory physiological adaptations for marine life in salmonids: osmoregulation, growth and metabolism. Am Fish Soc Symp. 211-229.

McCormick, S.D., Bern, H.A. (1989) In vitro stimulation of Na^+-K^+-ATPase activity and ouabain binding by cortisol in coho salmon gill. Am J Physiol Regul Integr Comp Physiol 256(3 Pt 2):R707-15.

McCormick, S.D., Regish, A.M., Christensen, A.K. (2009) Distinct freshwater and seawater isoforms of Na^+,K^+-ATPase in gill chloride cells of Atlantic salmon. J Exp Biol 212: 3994-4001.

Mitrovic, D., Perry, S.F. (2009) The effects of thermally induced gill remodeling on ionocyte distribution and branchial chloride fluxes in goldfish (*Carassius auratus*). J Exp Biol 212: 843-852.

Morash, A.J., Mackellar, S.R.C., Tunnah, L., Barnett, D.A., Stehfest, K.M., Semmens, J.M., Currie, S. (2016) Pass the salt: Physiological consequences of ecologically relevant hyposmotic exposure in juvenile gummy sharks (*Mustelus antarcticus*) and school sharks (*Galeorhinus galeus*). Conserv Physiol 4: 1-13.

Morris, R., Pickering, A.D. (1975) Ultrastructure of the presumed ion-transporting cells in the gills of ammocoete lampreys, *Lampetra fluviatilis (L.)* and *Lampetra planeri (Bloch)*. Cell Tissue Res. 163: 327-341.

Nelson JS (2006) *Fishes of the World*. 4th ed. John Wiley and Sons, Inc. New Jersey, USA.

Öberg KE (1967) The reversibility of the respiratory inhibition in gills and the ultrastructural changes in chloride cells from the rotenone-poisoned marine teleost, *Gadus callarias L*. Exp Cell Res 45:590-602.

O'Boyle, R.N., Beamish, F.W.H. (1977) Growth and intermediary metabolism of larval and metamorphosing stages of the landlocked sea lamprey, *Petromyzon marinus L*. Environ Biol Fishes 2: 103-120.

O'Donnell, M.J., Kelly, S.P., Nurse, C.A., Wood, C.M. (2001) A maxi Cl^- channel in cultured pavement cells from the gills of the freshwater rainbow trout *Oncorhynchus mykiss*. J Exp Biol 204: 1783-1794.

Osório, J., Rétaux, S. (2008) The lamprey in evolutionary studies. Dev Genes Evol 218: 221-235.

Pärt, P., Norrgren, L., Bergström, E., Sjöberg, P. (1993) Primary Cultures of Epithelial Cells From Rainbow Trout Gills. J Exp Biol 175: 219-232.

Peek, W.D., Youson, J.H. (1979) Transformation of the interlamellar epithelium of the gills of the anadromous sea lamprey, *Petromyzon marinus L*., during metamorphosis. Can J Zool 57: 1318-1332.

Perry SF and McDonald DJ. (1993) Gas exchange. In: The Physiology of Fishes, edited by Evans DH. Boca Raton, FL: CRC, p. 251-278.

Pisam, M., Prunet, P., Boeuf, G., Jrambourg, A. (1988) Ultrastructural features of chloride cells in the gill epithelium of the atlantic salmon, *Salmo salar*, and their modifications during smoltification. Am J Anat 183: 235-244.

Pisam, M., Prunet, P., Rambourg, A. (1989) Accessory cells in the gill epithelium of the freshwater rainbow trout *Salmo gairdneri*. Am J Anat 184: 311-320.

Potter, I.C. (1980) Ecology of Larval and Metamorphosing Lampreys. Can J Fish Aquat Sci 37: 1641-1657.

Potter, I.C., Wright, G.M., Youson, J.H. (1978) Metamorphosis in the anadromous sea lamprey, *Petromyzon marinus L*. Can J Zool 56: 561-570.

Reis-Santos, P., McCormick, S.D., Wilson, J.M. (2008) Ionoregulatory changes during metamorphosis and salinity exposure of juvenile sea lamprey (*Petromyzon marinus L*.). J Exp Biol 211: 978-988.

Richards, J.E., Beamish, F.W.H. (1981) Initiation of feeding and salinity tolerance in the pacific lamprey *Lampetra tridentata*. Mar Biol 63: 73-77.

Richards, J.G., Semple, J.W., Bystriansky, J.S., Schulte, P.M. (2003) Na^+,K^+-ATPase α-isoform switching in gills of rainbow trout (*Oncorhynchus mykiss*) during salinity transfer. J Exp Bio 206: 4475-4486.

Sardet, C., Pisam, M., Maetz, J. (1979) The surface epithelium of teleostean gish gills. J Cell Biol 80: 96-117.

Silva, S., Servia, MJ, Vieira-Lanero, R., Barca, S., Cobo, F. (2013) Life cycle of the sea lamprey *Petromyzon marinus*: duration of and growth in the marine life stage. Aquat Biol 18: 59-62.

Sollid, J., De Angelis, P., Gundersen, K., Nilsson, G.E. (2003) Hypoxia induces adaptive and reversible gross morphological changes in crucian carp gills. J Exp Biol 206: 3667-3673.

Sollid, J., Weber, R.E., Nilsson, G.E. (2005) Temperature alters the respiratory surface area of crucian carp *Carassius carassius* and goldfish *Carassius auratus*. J Exp Biol 208: 1109-1116.

Smith, H.W. (1930) The absorption and excretion of water and salts by marine teleosts. Am J Physiol 93(2) 480-505.

Smith, J.J., Kuraku, S., Holt, C., et al. (2013) Sequencing of the sea lamprey (*Petromyzon marinus*) genome provides insights into vertebrate evolution. Nat Genet 45: 415-421.

Sutterlin, A.M., Macfarlane, L.R., Harmon, P. (1977) growth and salinity tolerance in hybrids within *Salmo* sp. and *Salvelinus* sp. Aquaculture 12(1): 41-52.

Threadgold, L.T., Houston, A.H. (1964) An electron microscope study of the “chloride cell” of *Salmo salar L*. Exp Cell Res 34: 1-23.

Tipsmark, C.K., Breves, J.P., Rabeneck, D.B., Trubitt, R.T., Lerner, D.T., Grau, E.G. (2016) Regulation of gill claudin paralogs by salinity, cortisol and prolactin in Mozambique tilapia (*Oreochromis mossambicus*). Comp Biochem Physiol A Mol Integr Physiol 199: 78-86.

Tipsmark, C.K., Kiilerich, P., Nilsen, T.O., Ebbesson, L.O.E., Stefansson, S.O., Madsen, S.S. (2008) Branchial expression patterns of claudin isoforms in Atlantic salmon during seawater acclimation and smoltification. Am J Physiol Regul Integr Comp Physiol 294: 1563-1574.

Tsukita, S., Furuse, M. (1999) Occludin and claudins in tight-junction strands: Leading or supporting players? Trends Cell Biol 9: 268-273.

Van Itallie, C.M., Anderson, J.M. (2006) Claudins and Epithelial Paracellular Transport. Annu Rev Physiol 68: 403-429.

Van Itallie, C.M., Rogan, S., Yu, A., Vidal, L.S., Holmes, J., Anderson, J.M. (2006) Two splice variants of claudin-10 in the kidney create paracellular pores with different ion selectivities. Am J Physiol Ren Physiol 291: 1288-1299.

Wilson, J.M., Laurent, P. (2002) Fish gill morphology: Inside out. J Exp Zool 293: 192-213.

Wood, C.M., Gilmour, K.M., Pärt, P. (1998) Passive and active transport properties of a gill model, the cultured branchial epithelium of the freshwater rainbow trout (*Oncorhynchus mykiss*). Comp Biochem Physiol A Mol Integr Physiol 119: 87-96.

Wood, C.M., Part, P. (1997) Cultured branchial epithelia from freshwater fish gills. J Exp Biol 200: 1047-1059.

Wood, C.M., Kelly, S.P., Zhou, B., Fletcher, M., O'Donnell, M., Eletti, B., Pärt, P. (2002) Cultured gill epithelia as models for the freshwater fish gill. Biochim Biophys Acta Biomembr 1566: 72-83.

Youson, J.H. (2003) The biology of metamorphosis in sea lampreys: endocrine, environmental, and physiological cues and events, and their potential application to lamprey control. J Great Lakes Res 29: 26-49.

Youson, J.H. (1979) A description of the stages in the metamorphosis of the anadromous sea lamprey , *Petromyzon marinus L*. Can J Zool 57(9): 1808-1817.

Youson, J.H., Freeman, P.A. (1976) Morphology of the gills of larval and parasitic adult sea lamprey, *Petromyzon marinus L*. J Morphol 149: 73-103.

Zihni, C., Mills, C., Matter, K., Balda, M.S. (2016) Tight junctions: From simple barriers to multifunctional molecular gates. Nat Rev Mol Cell Biol 17: 564-580.

Chapter 2. The Anti-coagulating Agent Heparin and Native Serum Alter the Barrier and Junction Properties of a Primary Cultured Model Fish Gill Epithelium

2.1. Summary

Primary cultured gill epithelium models are useful for investigating the barrier properties of fish gills. However, like many other primary cultured preparations, gill models develop in the presence of commercially available heterologous serum supplements rather than native serum. This is because heterologous serum is easy to obtain and native serum (or plasma) has historically had mixed success in primary cultured fish epithelium models. This study examined the effects of the anti-coagulating agent heparin and native serum on the barrier properties of a primary cultured trout gill model. Development of model epithelia in the presence of heparin decreased transepithelial electrical resistance (TER) and increased paracellular flux of [^{3}H]polyethylene glycol (MW 400 Da, PEG-400). In association, transcript abundance of genes encoding tight junction proteins tricellulin (Tric), zona-occludens *1* (ZO-1), cingulin (Cgn), and claudin (Cldn) -*1, -8b, -8c, -8d, -12, -23a, -27b, -28b,* and *-29a* decreased, while *cldn-30* and *-32a* mRNA abundance increased. Acutely treating the model with a high dose of heparin for 24 hours had a qualitatively similar impact on epithelium TER and paracellular [^{3}H]PEG-400 flux, but fewer TJ-associated genes exhibited changes in transcript abundance and these changes were less pronounced. In contrast, epithelia in medium supplemented with 10% rainbow trout serum (instead of 10% fetal bovine serum and prepared without an anti-coagulating agent) exhibited a marked elevation in TER and reduction in paracellular [^{3}H]PEG-400 flux. This was associated with a significant increase in transcript abundance of *ocln*, *cldn-8b*, *-8d*, *-27b* and *-28b* as well as increased protein abundance of Cldn-8d. Data suggest that using native extracellular fluid in cultured gill epithelium preparations can enhance barrier properties, but that anti-coagulating

agents used to collect extracellular fluid should be evaluated to establish if they may have deleterious effects.

2.2. Introduction

The gill of fishes presents an extensive interface that separates the internal milieu of the animal from its immediate surroundings and in this regard, the gill epithelium plays a central role in organismal physiology and homeostasis in fishes (Evans et al 2005). However, as an organ the gill exhibits profound architectural and physiological complexity and investigating its multifaceted nature can be a challenge. Primary cultured model fish gill epithelia are architecturally simplified preparations that allow the researcher to sidestep some of the difficulties associated with studying the gill epithelium and these have become useful tools for exploring the barrier properties of the fish gill epithelium (for reviews see Wood et al 2002, Bury et al 2014). Because preparations grown on permeable cell culture inserts offer a suitable representation of the passive paracellular properties of the intact gill epithelium (Wood and Pärt 1997, Kelly et al 2000), recent studies have used primary cultured model fish gill epithelia to broaden our knowledge of the tight junction (TJ) complex in fishes and the role that TJ proteins play in regulating the barrier properties of aquatic vertebrate epithelia (Chasiotis et al 2010; Kolosov and Kelly 2013; Kolosov et al 2014; Sandbichler et al 2011).

Typically, model gill epithelium preparations are cultured using a culture medium supplemented with heterologous serum derived from a mammalian source, such as fetal bovine serum (FBS) (Pärt et al 1993). This is because heterologous extracellular fluid is easy to obtain commercially, and it is a reliable product for producing realistic gill barrier models (Pärt et al 1993). In addition, the use of homologous extracellular fluid (e.g. native serum) has often met with

limited or mixed success in cultured salmonid fish tissue models. For example, native serum as a supplement in rainbow trout gill cell culture was suggested to be cytotoxic because it did not result in good cell attachment or growth (Pärt et al 1993). While these observations are in line with the deleterious effects of fish serum supplements in cultures of other trout and salmonid fish tissues (Fryer et al 1965; Collodi and Barnes 1990), they contrast with studies on other species where native fish serum has been used with success (Dickman and Renfro 1986, Kocal et al 1988, Clark et al 1987, Avella et al 1997, Wood and Kelly 2001, Chasiotis et al 2012). An advantage of utilizing serum as a cell culture medium supplement is that during blood coagulation, mitogens are released to promote tissue repair, and these mitogens seem to benefit cells in culture (Balk et al. 1983). However, Wood et al (2002) examined the use of native plasma as a supplement (or exclusive medium) for the culture of model rainbow trout gill epithelia, with mixed success. Specifically, plasma can be utilized in the trout gill culture medium with comparable results to mammalian serum but only when supplemented at a low concentration (Wood et al 2002). A high concentration of native plasma compromised the barrier properties of trout gill preparations, and when plasma was used as the exclusive medium, cultured preparations were unable to develop a meaningful transepithelial resistance (TER; Wood et al 2002). The reason/s for the apparent adverse effect of native plasma (at higher levels) on cultured gill cells remain unknown. But is worth noting that while serum is prepared in the absence of anti-coagulating chemical agents, plasma preparation requires the presence of these chemicals.

In primary cultured gill epithelium models derived from non-salmonid fishes, such as sea bass, tilapia and goldfish, native serum has been successfully utilized (Avella et al 1997, Wood and Kelly 2001, Chasiotis et al 2012). For instance, native serum supplementation was reported to benefit the morpho-functional characteristics of a model sea bass gill epithelium by contributing

to the production of cultured cells that more closely resembled those of the intact gill (Avella and Ehrenfeld 1997). Moreover, cell supplemented with native sea bass serum exhibited transport characteristics that were not found in preparations supplemented with FBS (Avella and Ehrenfeld 1997). In a model tilapia gill epithelium, the use of native serum supplements collected from fish that were either stressed or unstressed showed that circulating endocrine factors in stressed fish (cortisol in particular) would enhance the barrier properties of the model, suggesting that freshwater (FW) fish can mitigate ion loss across the gill epithelium when stress hormones such as cortisol are elevated (Kelly and Wood 2002). Finally, Chasiotis et al (2012) supplemented a primary cultured goldfish gill epithelium with FBS or native serum collected from goldfish residing in either regular FW or ion poor water (IPW). Because fish residing in IPW have a limited ability to acquire new ions (i.e. via active branchial uptake) and face a greater electrochemical gradient down which ions can be passively lost from blood to surrounding water, Chasiotis et al (2012) considered the idea that a serum supplement derived from IPW goldfish may enhance the barrier properties of a model gill epithelium even more than serum acquired from FW goldfish. This was found to be the case as preparations supplemented with native serum from IPW fish exhibiting increased TER and reduced paracellular permeability versus those supplemented with native FW fish serum. Most notably, all model goldfish preparations treated with native serum exhibited enhanced barrier properties versus models supplemented with FBS (Chasiotis et al 2012). Given the observations above, it would seem prudent to re-consider the use of native serum in primary cultured trout gill epithelium models to confirm how this supplement might influence the barrier properties of these preparations. In particular, the molecular physiology of the TJ complex should be considered in conjunction with measurements of barrier integrity because TJs play a critical role in model gill epithelium barrier formation and function (Kolosov et al 2014). Therefore,

if native serum is problematic in model salmonid fish gill epithelium culture, it can be hypothesized that the reason for this issue (and solution to it as a problem) may be found in the TJ complex. In addition, to further contemplate the idea of using plasma as an extracellular fluid supplement, it would be useful to examine the effects of anti-coagulating chemicals on gill models. Therefore, in this study the effect of the anti-coagulating agent heparin (which is commonly used to prevent the clotting of blood following its collection from fishes) and native rainbow trout serum were examined in a primary cultured model of the rainbow trout gill epithelium.

2.3. Materials and Methods

2.3.1. Experimental Animals

Stock rainbow trout (*Oncorhynchus mykiss*, 250-300 g) for primary culture were obtained from a local supplier (Humber Springs Trout Club and Hatchery, Orangeville, ON, Canada). In the laboratory, fish were held in 600 L opaque polystyrene aquaria where they were fed *ad libitum* once daily with commercial trout pellets (Martin Profishent, Elmira, ON, Canada). Tanks were supplied with flow-through, dechlorinated City of Toronto tap water (approximate composition in mM: Na^+ 0.59; Cl^- 0.92; $Ca2^+$ 0.90; K^+ 0.05; pH 7.4). Water temperature was 11 ± 1°C, and fish were held under a constant photoperiod (12h light:12h dark). Animal husbandry and experimental protocols were approved by the York University Animal Care Committee and were in line with Canadian Council on Animal Care guidelines.

2.3.2. Cell Culture Media Preparations

In accordance with Kelly et al (2000), normal complete cell culture medium comprises 6% FBS supplemented Leibovitz's L-15 Medium with 2% penicillin-streptomycin (10,000 U/mL

solution) and 0.5% gentamicin (10 mg/mL solution) (all solutions supplied by Gibco, ON, Canada). Stock heparin solution was prepared by dissolving heparin (sodium salt from porcine intestinal mucosa; Sigma-Aldrich, ON, Canada) in phosphate buffer saline (PBS, pH 7.7) to a concentration of 10 international unit (i.u.) heparin/μL PBS. Heparin solution was then divided into single-use aliquots and stored at -30°C until use. In the heparin experiment, an upper dose of 50 i.u. heparin/mL was selected based on the heparin concentration required for salmonid plasma collection (Wood et al. 2002). A lower dose of 5 i.u./mL was selected because it reflects a final heparin concentration in a prepared culture medium with 10% native plasma supplement. To add the heparin, the final PBS volume used is <0.005% of the final medium volume and this had no effect on experimental conditions. For the native serum experiments, FBS and native serum were added as supplements to complete culture medium at a volume of 10%.

2.3.3. Rainbow Trout Native Serum Preparation

Rainbow trout native serum for primary culture was obtained from fish (approximately 500-800 g) held under identical conditions as described above. Fish were rapidly net captured, and blood was immediately drawn by caudal puncture using sterile syringes (5 mL, 21G; BD Biosciences). Handling was limited to ~ 1 minute per fish and following the blood draw, fish were placed in separate holding tanks to allow for full recovery before returning them to stock aquaria. Whole blood was allowed to clot at 4°C for 1 hour prior to centrifugation (3,220 x *g*, 10 min, 4°C). The resulting serum was pooled and sterilized using 0.2 μm Acrodisc® syringe filters (Pall Life Sciences, MI, USA). Serum was divided into single use aliquots and stored in -30°C until use.

2.3.4. Primary Cultured Rainbow Trout Gill Epithelium and Physiological Measurements

Procedures for preparation and culture of a primary cultured rainbow trout gill epithelium composed of gill pavement cells was originally outlined by Wood and Pärt (1997) and described in detail by Kelly et al (2000). Briefly, epithelial cells from rainbow trout gill filaments were isolated by trypsination and seeded at a density of 13 million cells per 25 cm^2 vented cell culture flask. Culture flasks were held in an air atmosphere at 18°C and cells were bathed in 6% FBS supplemented L15 (see above). Medium was removed (with unattached material) and renewed 24 hours after first seeding and every 48 hours thereafter. At confluence, gill cells were harvested from the flasks by trypsination and seeded into permeable cell culture inserts at 0.7 million cells/culture insert (PET filters, 0.9 cm^2 growth area, 0.4 μm pore size, $1.6x10^6$ /cm^2 pore density; BD Falcon TM; BD Biosciences, Mississauga, ON, Canada) using appropriate control and treatment media under symmetrical conditions (i.e. media bathing both sides of the cell culture insert). For native serum experiments, cells were initially seeded on culture inserts with FBS. Native serum media was applied at first media change approximately 24 hours after seeding. Epithelium development was monitored daily by visually inspecting preparations and measuring transepithelial electrical resistance (TER) with chopstick electrodes (STX-2) connected to a custom-modified EVOM epithelial voltohmmeter (World Precision Instruments, Sarasota, FL). TER is expressed as ohms per centimeter squared ($\Omega \cdot cm^2$) after correcting for background resistance (i.e. TER measured across 'blank' culture inserts bathed with appropriate media). Two experiments were conducted where heparin was added to the culture medium. The first was the heparin dose experiment where varying doses of heparin (0.5, 5 and 50 i.u./mL) were added to culture media at the outset of seeding into cell culture inserts. After this, fresh heparin was added with media at each media change. The second was an acute exposure to heparin. In this experiment

a single dose of 50 i.u./mL was used, and it was added to culture medium of model gill epithelium preparations that had exhibited a plateau in TER, ~ 5-6 days after first seeding in cell culture inserts.

Paracellular permeability was determined by measuring the flux rates of [^{3}H] polyethylene glycol (PEG, molecular mass 400 Da; [^{3}H]PEG-400; PerkinElmer, Woodbridge, ON, Canada) once epithelium preparations had reached a plateau in TER. [^{3}H]PEG-400, which passes through the paracellular space between cells and not transcellularly, was added to the basolateral side of an epithelium to determine flux rate to the apical side. Calculation of PEG flux rates have previously been described by Wood et al. (1998).

2.3.5. RNA Extraction, cDNA Synthesis, and Quantitative PCR Analysis of Tight Junction (TJ) Associated Gene Transcript Abundance

Total RNA was extracted from cell culture inserts using TRIzol reagent (Life Technologies, Burlington, ON, Canada) according to the manufacturer protocol. RNA yield from each insert was determined using a spectrophotometer (MultiskanTM Spectrum, Thermos Scientific) and treated with DNase I (Amplification Grade; Life Technologies) prior to cDNA synthesis. First-strand cDNA synthesis was carried out using SuperScriptTM III Reverse Transcriptase and OligodT12-18 primers (Invitrogen Canada Inc.). Quantitative real-time PCR (qRT-PCR) was used to assess transcript abundance of genes encoding tight junction (TJ) protein in cultured trout gill epithelia. Genes examined included those encoding the TJ proteins occludin (Ocln), tricellulin (Tric), zonula occludens-1 (ZO-1), cingulin (Cgn), and claudin (Cldn)-1, -6, -7, -8b, -8c, -8d, -12, -23a, -27b, -28b, -29a, -30, -31, and -32a. Analysis was conducted in a Chromo4TM Detection System (CFB-3240, Bio-Rad Laboratories Canada Ltd.) using SYBR Green I Supermix (Bio-Rad Laboratories Canada Ltd., ON, Canada) under the following conditions: 1 cycle denaturation (90°C, 4 min)

followed by 40 cycles of denaturation (95°C, 30s), annealing (54-61°C, 30s), and extension (72°C, 30s), respectively. A final melting curve was generated from 1°C below primer annealing temperature up to 95°C. The primer sets used, specific annealing temperatures, amplicon sizes and GeneBank Accession numbers can be found in Table 2-1. Transcript abundance based on qRT-PCR results were calculated using reference genes that did not alter in response to experimental treatments in this study i.e. β-actin (actb) or elongation factor 1α (ef-1α). This was determined by statistically comparing reference gene abundance between treatments in each experiment to establish that $p > 0.05$.

2.3.6. Western Blotting

Procedure used for western blotting have been described by Chasiotis et al (2010), with slight modifications. Briefly, cultured epithelia in culture inserts for Western blotting analyses were aspirated to remove culture media and rinsed twice with ice-cold PBS. 50µL of radioimmunoprecipitation assay (RIPA) buffer was then added directly into culture inserts for collection into microcentrifuge tubes, and the cells were lysed with a sterile tuberculin syringe (1 mL, 27G; BD Biosciences). The cell lysate was centrifuged to collect supernatant (18,000 g, 4°C, 20 min,). Protein concentrations were determined using a Micro BCA Protein Assay Kit (Thermo Fisher Scientific, ON, Canada) and identical amounts of protein from each sample were loaded into a 12% SDS-PAGE gel for electrophoresis. Protein was wet-transferred onto a PVDF membrane and blocked with 5% skim milk in tris-buffered saline containing 0.1% Tween-20 (TBS-T). PVDF membrane was then incubated overnight with primary antibody against trout Claudin 8d. After incubation, the membrane was washed 3 times in TBS-T (5 min, 4°C) and proceeded with subsequent secondary antibody incubation, wash, and imaging. Chemilumiscent detection of protein was achieved using a horseradish-peroxidase conjugated secondary antibody

(Invitrogen, ON, Canada) and an ECL substrate (Thermo Scientific, ON, Canada). Image densitometry analysis was performed using Image Lab™ software (Version 6.0.0 build 26, Bio-Rad Laboratories, Inc. ON, Canada).

2.3.7. Statistical Analyses

All data are expressed as mean ± S.E.M. Statistical analyses was carried out using statistical software (Prism version 7.0d, GraphPad Software, CA, USA). Analysis of mRNA abundance was normalized to a reference gene that did not change with respect to treatment. A rank-sum test, one-way analysis of variance (ANOVA), or two-way ANOVA were performed where appropriate and followed by Holm-Šidák pairwise comparison to determine significant differences between groups ($p \leq 0.05$).

Table 2-1. Primer sets and corresponding amplicon sizes, annealing temperatures and GenBank accession numbers for genes encoding tight junction proteins (*ocln, tric,* and *cldns*), and reference genes (*actb*, *ef1α*) in rainbow trout.

Gene	Primer Sequence (5'→3')	Amplicon Size (bp)	Annealing Temp. (°C)	Accession Number
cldn-1	FOR: GAGGACCAGGAGAAGAAGG REV: AGCCCCAACCTACGAAC	182	60	BK008768
cldn-6	FOR: TGAAACCACGGGACAGATG REV: TGAAACCACGGGACAGATG	245	60	KF445436
cldn-7	FOR: CGTCCTGCTGATTGGATCTC REV: CAAACGTACTCCTTGCTGCTG	261	61	BK007965
cldn-8b	FOR: ACGACTCCCTCCTGGCTCT REV: GAGACCCATCCGATGTAGA	185	56	BK008770
cldn-8c	FOR: GCTTGATGTGCTGCTCTC REV: CCCAGAGGTCAGGAGGA	201	60	BK008771
cldn-8d	FOR: GCAGTGTAAAGTGTACGACTCTCTG REV: CACGAGGAACAGGCATCC	200	60	BK007966
cldn-12	FOR: CTTCATCATCGCCTTCATCTC REV: GAGCCAAACAGTAGCCCAGTAG	255	60	BK007967
cldn-13	FOR: AGCGGCACTCTGGACAA REV: CGGAAACCACACCTCTCC	231	59	BK008774
cldn-23a	FOR: ATCCTAAACCTCACAGCGACA REV: CGGTCTTTCCAGCACCTTAC	270	60	BK008775
cldn-27b	FOR: GCCAACATCGTAACAGGACA REV: CCAGAAGAGCACCAATGAGC	283	60	BK008776
cldn-28b	FOR: CTTTCATCGGAGCCAACATC REV: CAGACAGGGACCAGAACCAG	310	60	EU921670
cldn-29a	FOR: CTTTCATCGGCAATAACATC REV: CAGCAATGGAGAGCAGG	201	60	BK008777
cldn-30	FOR: CGGCGAGAACATAATCACAG REV: GGGATGAGACACAGGATGC	297	59	BK007968
cldn-31	FOR: TCGGCAACAACATCGTGAC REV: CGTCCAGCAGATAGGAACCAG	311	61	BK007969
cldn-32a	FOR: ATTGTGTGCTGTGCCATCC REV: AGACACCAACAGAGCGATCC	321	60	BK007970
tric	FOR: GTCACATCCCCAAACCAGTC REV: GTCCAGCTCGTCAAACTTCC	170	60	KC603902
ocln	FOR: CAGCCCAGTTCCTCCAGTAG REV: GCTCATCCAGCTCTCTGTCC	341	58	GQ476574
zo-1	FOR: AAGGAAGGTCTGGAGGAAGG REV: CAGCTTGCCGTTGTAGAGG	291	60	HQ656020
cgn	FOR: CTGGAGGAGAGGCTACACA REV: CTTCACACGCAGGGACAG	156	56	BK008767
actinβ	FOR: GGACTTTGAGCAGGAGATGG REV: GACGGAGTATTTACGCTCTGG	354	58	AF157514
ef-1α	FOR: GGCAAGTCAACCACCACAG REV: GATACCACGCTCCCTCTCAG	159	60	AF498320.1

2.4. Chapter 2 Figures

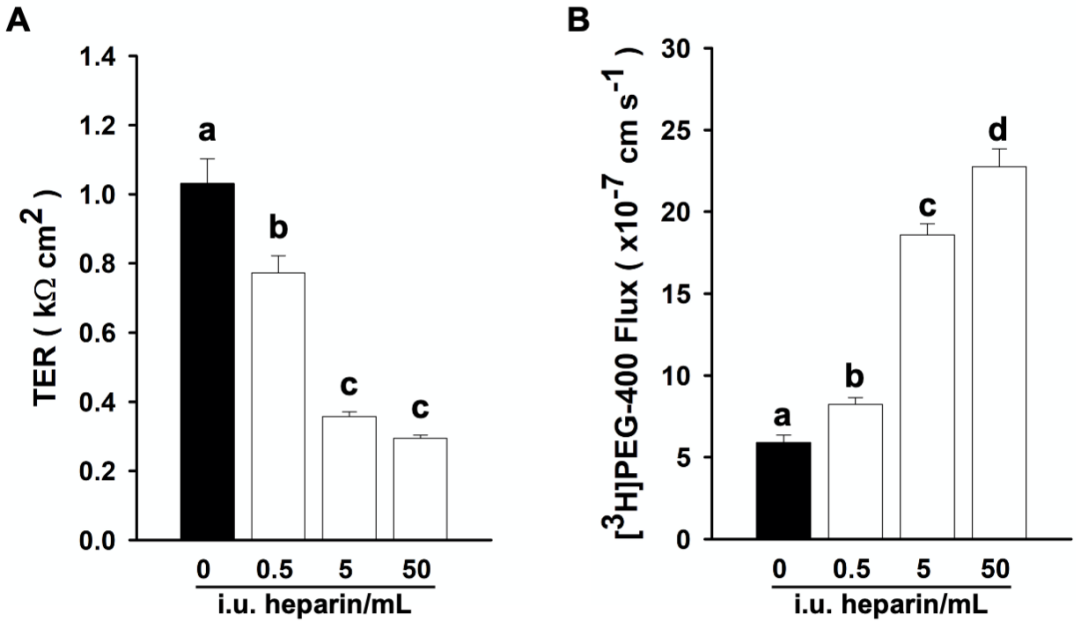

Figure 2-1. The effect of heparin (0.5, 5, and 50 i.u. heparin/mL) on (A) transepithelial-electrical resistance (TER) and (B) [^{3}H]-PEG400 paracellular biomarker flux across trout pavement cell epithelia. Different letters denote significant difference between treatment groups by one-way ANOVA ($p \leq 0.05$; n=8-10).

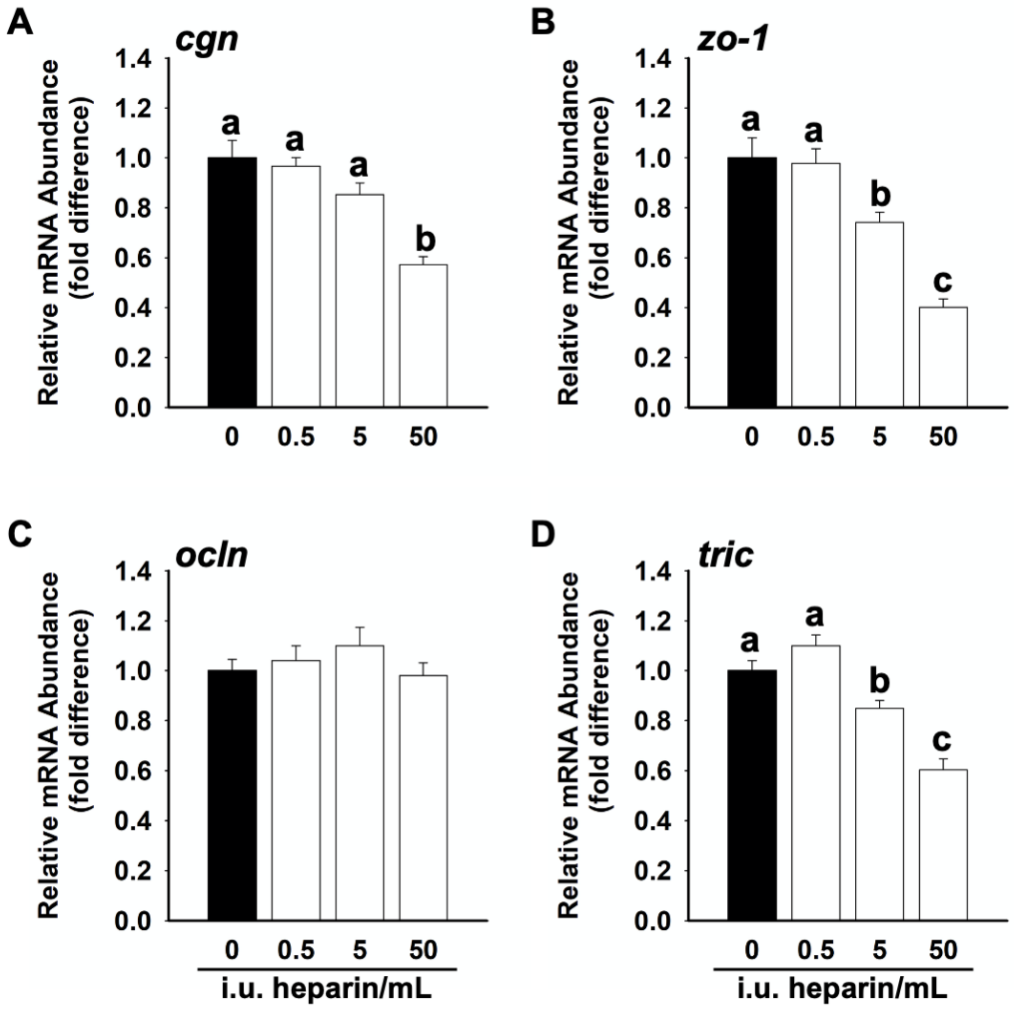

Figure 2-2. The effect of heparin on genes encoding (A) cingulin (*cgn*), (B) zona occludens-1 (*zo-1*), (C) occludin (*ocln*), and (D) tricellulin (*tric*) transcript in cultured trout pavement cell epithelia. Different letters denote significant difference between treatment groups by one-way ANOVA ($p \leq 0.05$; n=8-10).

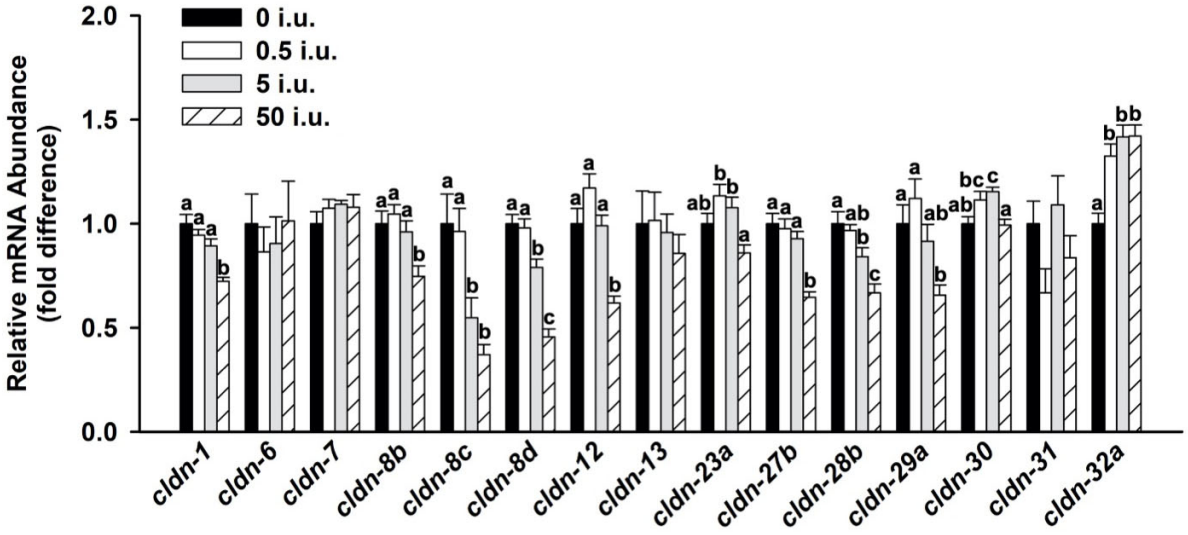

Figure 2-3. The effect of heparin on genes encoding claudins (*cldn*) family TJ proteins in cultured trout pavement cell epithelia. Different letters denote significant difference between treatment groups by one-way ANOVA ($p \leq 0.05$; n=8-10).

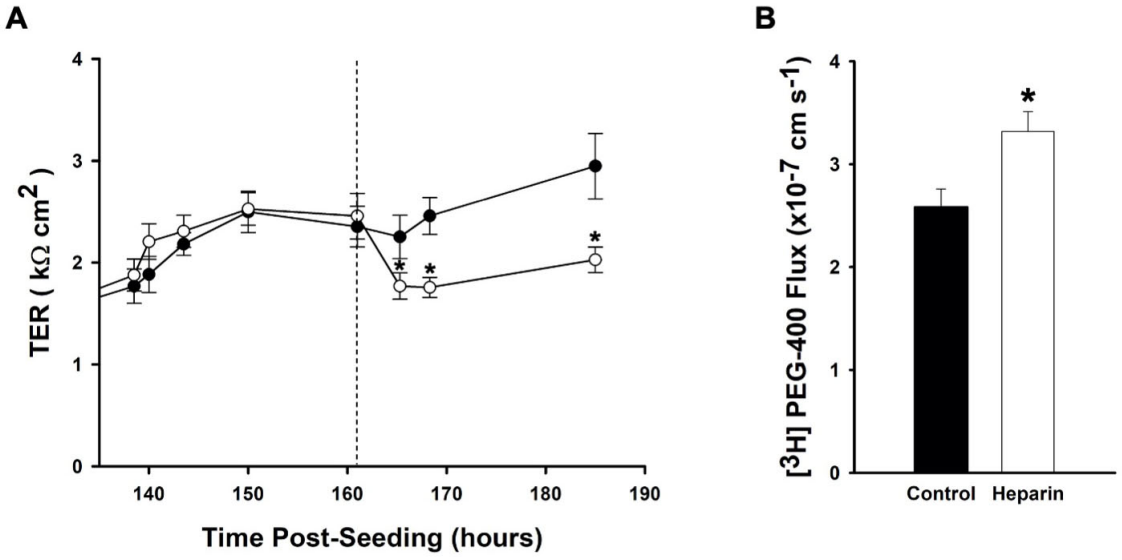

Figure 2-4. The effect of 24 hours heparin treatment on (A) TER and (B) 24 hours [^{3}H]-PEG400 flux across cultured trout pavement cell epithelia. Dotted line indicates addition of 50 i.u./mL heparin (open circles) at 161 hours post-seeding in SSI. Asterisk (*) denotes significant difference between control and heparin treatment as determined by Student's t-test ($p \leq 0.05$, n=8-10).

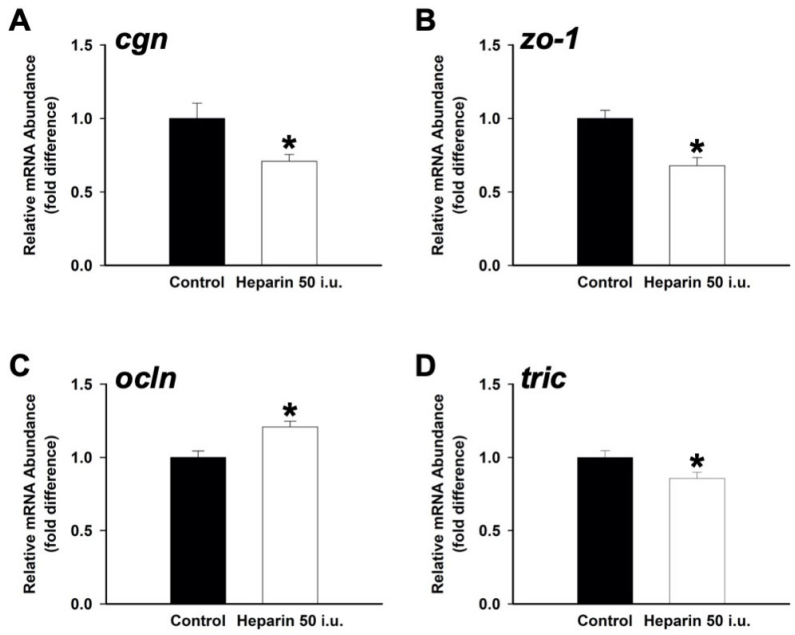

Figure 2-5. The effect of 24 hours heparin treatment on genes encoding (A) *cgn*, (B) *zo-1*, (C) *ocln*, and (D) *tric* transcript in cultured trout pavement cell epithelia. Asterisk (*) denotes significant difference between control and heparin treatment as determined by Student's t-test ($p \leq 0.05$, n=8-10).

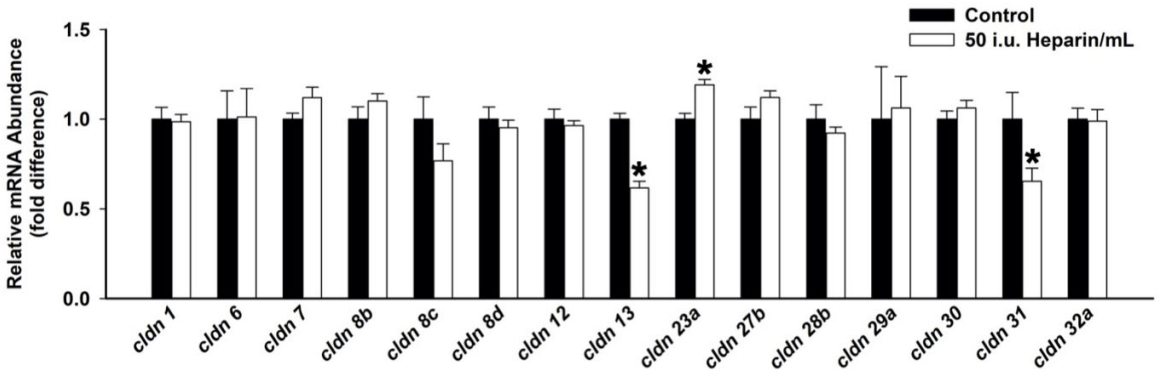

Figure 2-6. The effect of 24 hours heparin treatment on genes encoding claudins (*cldn*) family TJ proteins in cultured trout pavement cell epithelia. Asterisk (*) denotes significant difference between control and heparin treatment as determined by Student's t-test ($p \leq 0.05$, n=8-10).

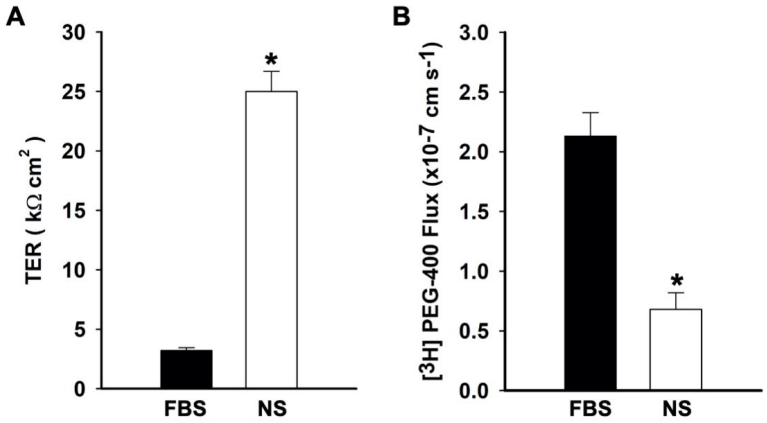

Figure 2-7. Difference in (A) TER and (B) [^{3}H]-PEG400 flux in trout pavement cell epithelia in culture inserts using media enriched with fetal bovine serum (FBS) and native serum (NS). Asterisk (*) denotes significant difference between FBS and NS as determined by Student's t-test ($p \leq 0.05$, n=7-8).

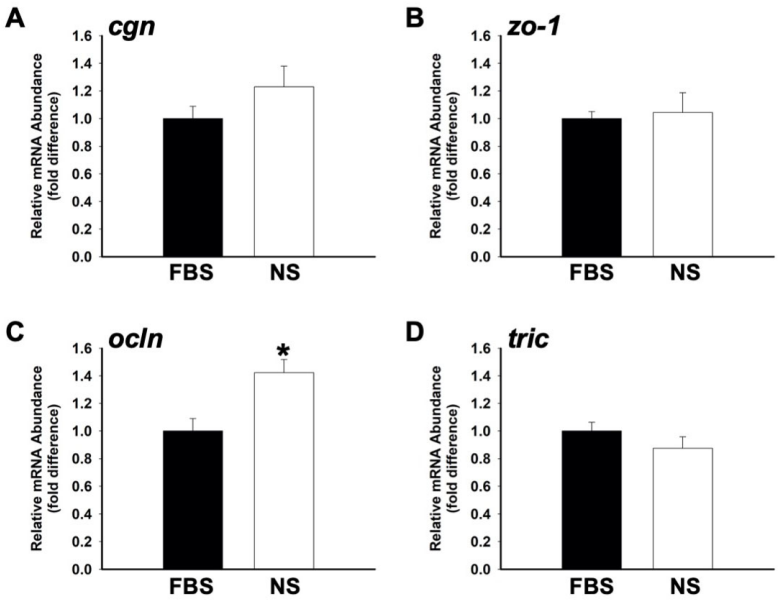

Figure 2-8. Relative transcript abundance in scaffolding TJ proteins (A) *cgn* and (B) *zo-1*, and MARVEL-domain containing TJ proteins (C) *ocln* and (D) *tric* transcript in cultured trout pavement cell epithelia in culture inserts with FBS and NS enrichment. Asterisk (*) denotes significant difference between FBS and NS as determined by Student's t-test ($p \leq 0.05$, n=7-8).

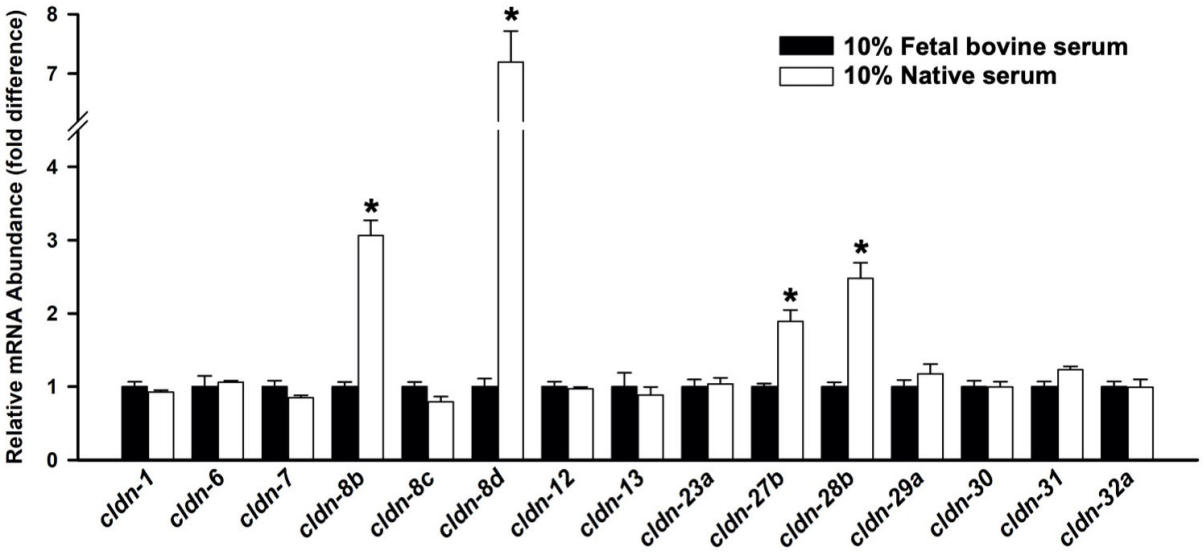

Figure 2-9. Relative transcript abundance in genes encoding claudins (*cldn*) family TJ proteins in cultured trout pavement cell epithelia in culture inserts with FBS and NS enrichment. Asterisk (*) denotes significant difference between FBS and NS as determined by Student's t-test ($p \leq 0.05$, n=7-8).

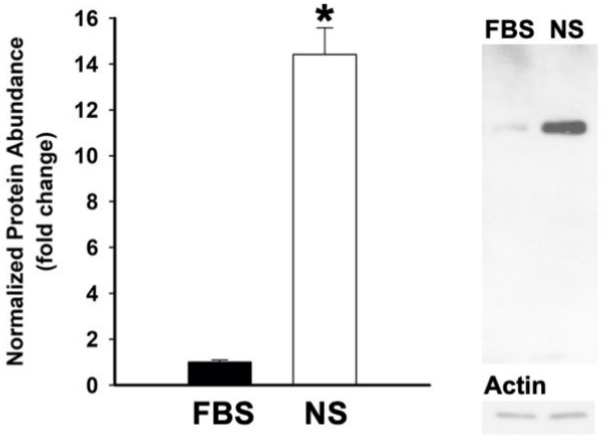

Figure 2-10. Relative CLDN-8d abundance in cultured trout pavement cell epithelia in cultured inserts with FBS and NS enrichment. Asterisk (*) denotes significant difference between FBS and NS as determined by Student's t-test ($p \leq 0.05$, n=4).

2.5. Results

2.5.1. Effects of anti-coagulating agent heparin on a primary cultured rainbow trout gill epithelia

The anti-coagulating agent heparin decreased transepithelial electrical resistance (TER) (**Figure 2-1A**) and increased [^{3}H]PEG-400 flux (**Figure 2-1B**) in the primary cultured trout gill epithelium. This effect was seen at all doses used (i.e. 0.5, 5 and 50 i.u./mL) but it was more pronounced at higher doses of heparin than lower doses. In association with changes in TER and [^{3}H]PEG-400 flux, a reduction in the transcript abundance of TJ-associated genes zonula-occludens 1 (*zo-1*), cingulin (*cgn*), tricellulin (*tric*) and claudin (*cldn*)-*1*, *-8b*, *-8c*, *-8d*, *-12*, *-27b*, *-28b*, and *-29a* occurred (**Figure 2-2A, B & D** and **Figure 2-3**). However, all transcripts that exhibited a decrease in abundance were observed in heparin treatments of 5 i.u./mL and above. Transcript abundance of the gene encoding the TJ protein occludin (Ocln) as well as the genes *cldn-6*, *-7*, *-13* and *-31* did not significantly alter in response to heparin treatment (**Figure 2-2C** and **Figure 2-3**). In addition to these trends, transcript abundance of *cldn-23a* and *-30* were greater in lower dose heparin (i.e. 0.5 and 5 i.u./mL) than high dose heparin (50 i.u./mL), and in the case of *cldn-30* this increase in the lower dose heparin treatment was significant versus control preparations (**Figure 2-3**). A final observation was that cldn-32a transcript abundance was significantly and equally elevated in all heparin doses (**Figure 2-3**).

The addition of 50 i.u./mL heparin into the cultured medium of mature epithelia that were exhibiting a plateau in TER resulted in a significant and sustained drop in TER over the 24 hour period examined (**Figure 2-4A**). This heparin-induced drop in TER was coupled with a modest but significant increase in [^{3}H]-PEG400 flux (**Figure 2-4B**). Acute treatment with 50 i.u./mL heparin for a 24 hour period was also found to decrease the transcript abundance of *cgn*, *zo-1*, and

tric, as well as *cldn -13* and *-31* (**Figure 2-5** and **Figure 2-6**). However, increased mRNA abundance of ocln and cldn-32a were also observed (**Figure 2-5** and **Figure 2-6**).

2.5.2. Effect of native serum on a primary cultured rainbow trout gill epithelia

Rainbow trout gill epithelium models bathed in a culture medium supplemented with native serum exhibited significantly higher TER (**Figure 2-5A**) and lower [^{3}H]-PEG400 flux (**Figure 2-5B**). Furthermore, the presence of native serum significantly increased transcript abundance of TJ protein genes encoding *ocln*, *cldn-8b*, *-8d*, *-27b*, and *-28b*. Meanwhile, transcript abundance of scaffolding TJ proteins *cgn* and *zo-1*, the tricellular TJ protein *tric*, and all other cldns examined in this study (i.e. *cldn-1*, *-6*, *-7*, *-8c*, *-12*, *-13*, *-23*, *-29a*, *-30*, *-31*, *-32a*) did not respond to the presence of native serum (**Figure 2-8** and **Figure 2-9**). Western blot analysis of Cldn-8d showed that a native serum-induced increase in transcript abundance of the gene encoding this TJ protein translated into increased protein abundance (**Figure 2-10**).

2.6. Discussion

2.6.1. Overview

The current study provides a first look at the direct effect of heparin on a fish epithelium *in vitro* and suggests that this anti-coagulating drug has a deleterious effect on the barrier properties of the gill epithelium at least. Because compromised gill epithelium integrity in the presence of heparin occurred in conjunction with a significant increase in the flux of a paracellular permeability marker ([^{3}H]PEG-400) and decreased mRNA abundance of numerous TJ-associated genes, data indicate that one action of heparin was to compromise the paracellular transport pathway of the gill epithelium. This occurred under chronic as well as acute conditions, although in the latter the

effect of heparin was less profound. Nevertheless, results suggest that if the anti-coagulating drug heparin were to come into contact with fish epithelial cells in culture (e.g. together with an extracellular fluid supplement which it was used to collect) or systemically, its impact on epithelium barrier function should be carefully considered. In addition to this, the use of native serum as a culture medium supplement was found to enhance the barrier properties of the primary cultured trout gill epithelium. These observations are in line with observed positive effects of native serum as a supplement in cultured gill epithelium models derived from other FW fish species (Kelly and Wood 2002; Chasiotis et al 2012b). Moreover, enhanced barrier properties in the presence of native serum occurred in association with reduced [^{3}H]PEG-400 flux and increased mRNA/protein abundance of select TJ proteins, suggesting that native serum altered the barrier function of a primary cultured trout gill epithelium model at least in part, by augmenting the paracellular transport pathway. Therefore, the hypothesis that native serum is problematic in primary cultured gill cells through its actions on the TJ complex can be rejected.

2.6.2. Effect of Heparin on Resistive Properties of Gill Epithelium

The pharmacological and medical applications of heparin have been well documented (Hirsh et al. 2001), and it is a therapeutic anti-coagulating agent (blood thinner) listed as an essential medicine by the World Health Organization (WHO, 2017). Heparin naturally occurs as a bio-compound produced by basophils and mast cells, and while other anticoagulating agents such as warfarin/Coumadin® and ethylenediaminetetraacetic acid (EDTA) also exist, heparin is commonly used for plasma preparation. Heparin's principle mode of action is through inactivation of thrombin and factor X (factor Xa) via an antithrombin-dependent mechanism (Hirsh et al. 1995). However, it is not documented whether heparin has any impact on the development of primary cultured fish cells, and as such, the use of heparin to prepare supplemental blood products for

cultured cells remains to be examined. Indeed, to the best of our knowledge, no published study has reported on the direct effects of heparin on the vertebrate tight junction complex.

An ongoing objective in the development of surrogate epithelium models for research in the physiology of fishes is to augment the authenticity of primary cultured preparations by using a bathing medium that will enhance the native properties of the tissue. Previous studies that used fresh native serum as a supplement have reported negative findings in primary cultured salmonid cells, and pre-frozen native serum and plasma have been reported as cytotoxic in several instances (Pärt et al. 1993; Wood et al 2002). In contrast, 5% fresh native trout plasma in a cultured rainbow trout gill epithelium model resulted in the development of a TER equivalent to that which developed in the presence of 5% FBS (Wood et al., 2002). This suggested that fresh native plasma may be a better extracellular supplement that native serum and FBS because plasma would facilitate the development of an epithelium with electrophysiological characteristics that mimic the gill (as occurs with FBS), but plasma would eliminate the presence of non-native proteins that may confound further proteomic study (Wood et al 2002). However, at levels higher than 5% supplementation, fresh plasma was found to have inhibitory effects on the development of model trout gill epithelium barrier properties (Wood et al 2002). Because Wood et al (2002) had prepared fresh plasma by heparinizing collected blood (with a dose of 50 i.u./mL), heparin seems likely to persist in collected plasma as it is cleared by the reticuloendothelial system and renal secretion (Garcia et al. 2012). Therefore, it could be speculated that heparin may have impacted the model trout gill epithelium when plasma was used as a supplement beyond a volume of 5%. Data from the current study support this idea, as heparin administered at doses equivalent to what would have been present in fresh plasma used by Wood et al (2002) significantly reduced the barrier properties of the primary cultured gill epithelium. Furthermore, Wood et al (2002) reported that when plasma

was added to model epithelia that had already established a plateau in TER in excess of 20 kΩ cm^2 (i.e. mature epithelia exhibiting a very high TER), there was never a substantive change in TER. Data from the current study is also consistent with this observation, in so far that the acute effect of heparin on the mature epithelium is modest compared to the effects when heparin was added to the culture medium at the outset of development. Nevertheless, in this study significant alterations were seen upon acute exposure of cultured preparations to heparin. But this seems likely to relate to the plateau TER in the current model, which is composed of gill pavement cells only and at ~ 2 kΩ cm^2, is an order of magnitude lower than the gill model used by Wood et al (2002). Cultured gill epithelia that exhibit a very high TER at plateau are much more resistant to culture condition changes than those exhibiting a lower TER (for review see Wood et al 2002). Either way, the pharmacology of heparin has mostly been focused on the delivery and absorption of heparin into the bloodstream and target tissue (Cho et al 2002; Qi et al 2004; Lamson et al 2020), and to the best of our knowledge, these first time observations that the direct effect of heparin may compromise vertebrate epithelium barrier properties indicate that this effect should be considered broadly.

2.6.3. Effects of Heparin on TJ Protein mRNA Abundance in Trout Epithelium

In association with the negative impact of heparin on model gill epithelium TER and [^{3}H]PEG-400 flux, a number of changes occurred in the mRNA abundance of TJ-associated genes. These changes suggest a pernicious effect of heparin on the development of the vertebrate epithelium TJ complex. More specifically, a decrease in the transcript abundance of several TJ-associated genes that have previously been documented as (or suggested to be) barrier-forming TJ proteins in fishes occurred. These included *tric*, *cldn-8d*, *-12*, *-23a*, *-28b*, and *-30* (Chasiotis and Kelly, 2011; Kelly and Chasiotis, 2011; Kolosov and Kelly 2013, 2017, 2018). In contrast, *cldn-*

32a transcript abundance increased at all doses of heparin tested, but transcript encoding this TJ protein has been reported to decrease as TER develops in primary cultured trout gill epithelia (Kolosov et al 2014). Therefore, these results are also consistent with a heparin-induced decrease in TER in the current study. Taken together, heparin-induced changes seen in the barrier properties of the cultured trout gill model seem likely to be driven by a compromised TJ complex.

The decrease in resistive properties during acute heparin treatment elicited a transcriptional response in TJ complex scaffolding proteins as well as a comparatively small number of transmembrane TJ protein genes. The changes observed in the TJ complex scaffolding/cytosolic components were a reduction in abundance (which also occurred under chronic treatment conditions) and presumably this would see a reduced ability for transmembrane TJ proteins to properly exhibit their function/s. Transcriptional changes in *ocln* and *tric* may be a potential compensatory mechanism for the loss of barrier properties in the acute treatment, as has been observed in cases where loss of function conditions have been experimentally induced for select TJ-associated genes in a primary cultured gill epithelium model (Kolosov and Kelly 2017; Kolosov et al 2017). However, as was observed in the chronic heparin response, the effect of heparin is potent and compensatory mechanisms in the epithelium do not overcome the pharmacological actions of the drug. Interestingly, *cldn 23a* transcript consistently elevated in response to acute heparin exposure, suggesting there may potentially be a direct effect in signaling mechanism that alters Cldn-23a in response to heparin.

2.6.4. Effect of Native Serum on a Primary Cultured Trout Epithelium

The use of native serum as a supplement in the primary cultured trout epithelium model resulted in the development of robust resistive properties characterized by high TER and low flux rates of a paracellular permeability marker. Increased TER and reduced PEG permeability in the

presence of native serum are consistent with previously documented observations using gill epithelium models derived from Nile tilapia and goldfish (Kelly and Wood 2002; Chasiotis et al. 2011). In contrast, Avella and Ehrenfled (1997) reported a reduction in the TER of a primary cultured sea bass gill epithelium when native serum was used as a supplement, despite seeing enhanced morpho-functional characteristics (i.e. cell morphology similar to the intact gill, increased rate of transcellular Cl^- secretion). But it should be noted that model tilapia and goldfish gill epithelia were derived from fish held in FW, as was the native serum used to culture cells. By comparison, model sea bass gill preparations and sea bass serum were derived from fish held in SW. In this regard, it is broadly accepted that in order to mitigate passive ion loss to surrounding water, the FW fish gill epithelium is "tight" compared to the "leakier" SW gill (Evans et al 2005), so these differences in response to native serum may reflect the conditions from which cells and serum were sourced. Irrespectively, the important take home message is that in all cases, native serum was successfully used to produce a primary cultured gill model with enhanced properties. In the case of rainbow trout, this contrasts with previous reports that native serum can be cytotoxic to cultured gill cells (Pärt et al 1993; Wood et al 2002). Moreover, native serum resulted in elevated TER, whereas fresh plasma (at 5% supplementation) produced an epithelium with resistive properties equivalent to FBS. Therefore, data from the current study suggest that native serum can be considered a suitable alternative to mammalian serum in the culture of rainbow trout gill epithelium models and more generally, native serum should be considered an option to explore in the primary culture of salmonid fish epithelial cells.

A possible explanation for the discrepancies of native serum use between this and previous studies using rainbow trout gill cells may be the timing of serum supplement addition to the culture medium. More specifically, in the current study, cultured trout gill cells are first seeded into 25

cm^2 cell culture flasks in the presence of L-15 medium supplemented with FBS. After the cells become confluent, they are trypsinated and re-seeded into cell culture inserts using, again, L-15 medium supplemented with FBS. It is then 24 h after this seeding that non-adherent material is washed out and FBS supplemented L-15 is replaced with native serum supplemented L-15 medium. Therefore, cultured gill models are exposed to native serum as a supplement for a 5-6 day period, but they attach to commercial cell culture plasticware in the presence of FBS. This approach was also taken when native serum was successfully used with cultured gill models derived from tilapia (Kelly and Wood 2002) and goldfish (Chasiotis et al 2012). So, the 'cytotoxic' effect of native serum may relate to the inability of freshly isolated fish cells to attach (or attach well) to commercial cell culture plasticware in the absence of FBS. Why this might occur will require further study, but it could be speculated that commercial plasticware is designed to enhance/promote the attachment of mammalian cells and this works optimally with serum derived from a mammalian source.

2.6.5. Effects of Native Serum on TJ Protein mRNA Abundance in Trout Epithelium

The presence of native serum as a supplement significantly increased *ocln*, *cldn-8b*, *-8d*, *-27b*, and *-28b* transcript abundance. Using a knockdown (KD) approach, Ocln has been established as a barrier-forming TJ protein in the gill epithelium of goldfish (Chasiotis et al 2012) and rainbow trout (Kolosov and Kelly, personal communication), which means that elevated *ocln* mRNA abundance may contribute to the enhanced TER and reduced [^{3}H]PEG-400 permeability observed in the presence of native serum. However, changes in *ocln* mRNA were modest at best and certainly much lower than those observed for *cldn-8d*, which exhibited an elevation in transcript abundance that far exceeded all other observed changes in transcript abundance of TJ-associated

genes. Elevated *cldn-8d* transcript abundance translated into increased Cldn-8d protein abundance, as measured using a custom synthesized rainbow trout Cldn-8d antibody. Using a KD approach, Cldn-8d has also recently been established as a barrier-forming TJ protein in the gill epithelium of fishes (Kolosov and Kelly 2017), so it seems likely that Cldn-8d is contributing significantly to the enhanced barrier properties of the cultured gill model when native serum is being used as a supplement. Much less is known about *cldn-8b, -27b* and *-28*, but they have all indirectly been associated with physiological events that either require a gill epithelium tightening response or have been shown to increase in abundance in association with induced tightening in a surrogate gill model (Chaiotis and Kelly 2011; Kelly and Chasiotis 2011; Sandbichler et al. 2011; Chen et al. 2016; Kolosov and Kelly 2016). Therefore, it seems likely that changes in the abundance of these TJ-associated genes will reflect a contribution to the development of enhanced model barrier function in association with native serum. But the important question to explore next is why these TJ proteins, and in particular Cldn-8d, respond to native serum while others do not.

2.7. Conclusions and Perspectives

Despite previous research by Pärt and colleagues (1993) having a limited success with NS with primary cultured trout gill cells, their study has become a foundation of cultured teleost gill epithelium model. Moreover, NS supplement allows the isolated gill cells to develop in a medium more akin to the native bathing medium. We also demonstrated that the presence of the anti-coagulating agent heparin can lead to a decrease in the resistive properties of a cultured branchial epithelia model. Moreover, this study identifies the specific TJ proteins affected by heparin and NS in cultured trout gill. In the current perspective, it will be prudent to identify the homologous growth factors and compounds present in the NS, to potentially elucidate mechanisms for the

control of teleost salt and water balance. This study demonstrated the complexity and nuance of the trout primary culture system that have yet to be fully explored.

2.8. References

Avella, M., Berhaut. J., Payan, P. (1994) Primary culture of gill epithelial cells from the sea bass *Dicentrarchus labrax*. In Vitro Cell Dev B 30A: 41-49.

Balk, S.D., Levine, S.P., Young, L.L., LaFleur, M.M., and Raymond, N.M. (1981) Mitogenic factors present in serum but not in plasma. Proc Natl Acad Sci 78(9): 5656-5660.

Barton, B.A., Peter, R.E., and Paulencu, C.R. (1980) Plasma cortisol levels of fingerling rainbow trout (*Salmo gairdneri*) at rest, and subjected to handling, confinement, transport and stocking. Can J Fish Aquat Sci. 37:805-811.

Bazzoni, G., Martínez-Estrada, O.M., Orsenigo, F., Cordenonsi, M., Citi, S., and Dejana, E. (2000) Interaction of junctional adhesion molecule with the tight junction components ZO-1, cingulin, and occluding. J Biol Chem 275(27) 20520-20526.

Bjornsson, T.D., and Levy, G. (1979) Pharmacokinetics of heparin. II. Studies of time dependence in rats. J Pharmacol Exp Ther 210: 243-246.

Bjornsson, T.D., Wolfram, K.M., and Kitchell, B.B. (1982) Heparin kinetics determined by three assay methods. Clin Pharmacol Ther 31: 104-113.

Bui P and Kelly SP (2015) Claudins in a primary cultured puffer fish (*Tetraodon nigroviridis*) gill epithelium model alter in response to acute seawater exposure. Comp Biochem Phys B 189: 91-101.

Bury NR, Schnell S, Hogstrand C (2014) Gill cell culture systems as models for aquatic environmental monitoring. J Exp Biol 217: 639–650.

Chasiotis, H., Effendi, J.C., Kelly, S.P. (2009) Occludin expression in goldfish held in ion-poor water. J Comp Physiol B 179: 145–154.

Chasiotis, H., Wood, C.M., Kelly, S.P. (2010) Cortisol reduces paracellular permeability and increases occludin abundance in cultured trout gill epithelia. Mol Cell Endocrinol 323: 232–238.

Chasiotis, H., Kolosov, D., Bui, P., Kelly, S.P., (2012a). Tight junctions, tight junction proteins and paracellular permeability across the gill epithelium of fishes: a review. Resp Physiol Neurobiol 184: 269–281.

Chasiotis, H., Kolosov, D., and Kelly, S.P. (2012b) Permeability properties of the teleost gill epithelium under ion-poor conditions. Am J Physiol Regul Integr Comp Physiol 302: R727–R739.

Cho, S.Y., Kim, J.S., Li, H., Shim, C., Linhardt, R.J., and Kim, Y.S. (2002) Enhancement of paracellular transport of heparin disaccharide across Caco-2 cell monolayers. Arch Pharm Res 25(1): 86-92.

Cordenonsi, M., D'Atri, F., Hammar, E., Parry, D.A.D., Kendrick-Jones, J., Shore, D., and Citi, S. (1999) Cingulin contains globular and coiled-coil domains and interacts with ZO-1, ZO-2, ZO-3, and myosin. J Cell Biol 147:1569-1582.

Evans, D.H., Piermarini, M.P., and Choe, K.P. (2005) The multifunctional fish gill: dominant site of gas exchange, osmoregulation, acid-base regulation, and excretion of nitrogenous wast. Physiol Rev 85: 97–177.

Garcia, D.A., Baglin, T.P., Weitz, J.I. (2012) Antithrombotic Therapy and Prevention of Thrombosis, 9th ed: American College of Chest Physicians Evidence-Based Clinical Practice Guidelines. CHEST 141(2) e24S-e43S.

Gauberg, J., Kolosov, D., Kelly, S.P. (2017) Claudin tight junction proteins in rainbow trout (Oncorhynchus mykiss) skin: Spatial response to elevated cortisol levels. Gen Comp Physiol 240: 214–226.

González-Mariscal, L., Betanzos, A., Nava, P., Jaramillo, B.E., (2003) Tight junction proteins. Prog Biophys Mol Bio 81, 1–44.

Hayman, E.G., Pierschbacher, M.D., Suzuki, S., et al. (1985) Vitronectin - A major cell attachment-promoting protein in fetal bovine serum. Exp Cell Res 160(2): 245-258.

Hirsh, J., Raschke, R., Warkentin, T.E., et al. (1995) Heparin - Mechanism ff Action, Pharmacokinetics, Dosing Considerations, Monitoring, Efficacy, and Safety. CHEST 108(4): S258-S275.

Hirsh, J., Anand, S.S., Halperin, J.L., et al. (2001) Mechanism of Action and Pharmacology of Unfractionated Heparin. Arterioscler Thromb Vasc Biol. 21: 1094-1096.

Hrubec, T.C., and Smith, S.A. (1999) Differences between plasma and serum samples for the evaluation of blood chemistry values in rainbow trout, channel catfish, hybrid tilapias, and hybrid striped bass. J Aquat Anim Health 11: 116–122.

Kelly, S.P., Fletcher, M., and Wood, C.M. (2000) Procedures for the preparation and culture of 'reconstructed' rainbow trout branchial epithelia. Methods in Cell Science 22: 153–163.

Kelly, S.P., and Wood, C.M. (2002) Cultured gill epithelia from freshwater tilapia (Oreochromis niloticus): Effect of cortisol and homologous serum supplements from stressed and unstressed fish. J Membrane Biol 190: 29-42.

Kelly, S.P., and Chasiotis, H. (2011) Glucocorticoid and mineralocorticoid receptors regulate paracellular permeability in a primary cultured gill epithelium. J Exp Biol 214: 2308-2318.

Kocal, T., Quinn, B.A., Smith, I.R., Ferguson, H.W., and Haye, M.A. (1988) Use of trout serum to prepare primary attached monolayer cultures of hepatocytes from rainbow trout (Salmo gairdneri). In Vitro Cell Dev. B 24(4): 304-308.

Kolosov, D., and Kelly, S.P. (2013) A role for tricellulin in the regulation of gill epithelium permeability. Am. J. Physiol. Regul. Integr. Comp. Physiol. 304: R1139-R1148.

Kolosov, D. and Kelly, S.P. (2017) Claudin-8d is a cortisol-responsive barrier protein in the gill epithelium of trout. J. Mol. Endocrinol. 59, 101-114.

Kolosov, D. and Kelly, S.P. (2018) Tricellular tight junction-associated angulins in the gill epithelium of rainbow trout. Am. J. Physiol. Regul. Integr. Comp. Physiol. 315: R312-R322.

Kolosov, D., Bui, P., Chasiotis, H., Kelly, S.P., (2013) Claudins in teleost fishes. Tissue Barriers 1 (3), e25391.

Kolosov, D., Chasiotis, H., and Kelly, S.P. (2014) Tight junction protein gene expression patterns and changes in transcript abundance during development of model fish gill epithelia. J Exp Biol 217: 1667-1681.

Kolosov, D., Donini, A. and Kelly, S.P. (2017) Claudin-31 contributes to corticosteroid-induced alterations in the barrier properties of the gill epithelium. Mol. Cell. Endocrinol. 439: 457-466.

Lamson, N.G., Berger, A., Fein, K.C. and Whitehead, K.A. (2020) Anionic nanoparticles enable the oral delivery of proteins by enhancing intestinal permeability. Nat Biomed Eng 4: 84–96.

Pärt, P., Norrgren, L., Bergström, E., and Sjöberg, P. (1993) Primary cultures of epithelial cells from rainbow trout gills. J Exp Biol 175: 219–232.

Sandbichler, A.M., Egg, M., Schwerte, T., and Pelster, B. (2011) Claudin 28b and F-actin are involved in rainbow trout gill pavement cell tight junction remodeling under osmotic stress. J Exp Biol 214: 1473-1487.

Wood, C.M., and Pärt, P. (1997) Cultured branchial epithelia from freshwater fish gills. J Exp Biol 200: 1047-1059.

Wood, C.M., Gilmour, K.M., and Part, P. (1998) Passive and active transport properties of a gill model, the cultured branchial epithelium of the freshwater rainbow trout (*Oncorhynchus mykiss*). Comp Biochem Physiol A 119: 87–96.

Wood, C.M., Eletti, B., and Pärt, P. (2002) New methods for the primary culture of gill epithelia from freshwater rainbow trout. Fish Physiol Biochem. 26: 329–344.

Zhang, H., Mi, J., Huo, Y., Huang, X., Xing, J., Yamamoto, A., and Gao, Y. (2014) Absorption enhancing effects of chitosan oligomers on the intestinal absorption of low molecular weight heparin in rats. Int J Pharm. 466(1-2): 156-162.

Zheng, X., Baker, H., Hancock, W.S., et al. (2006) Proteomic Analysis for the Assessment of Different Lots of Fetal Bovine Serum as a Raw Material for Cell Culture. Part IV. Application of Proteomics to the Manufacture of Biological Drugs. Biotechnol Prog (22) 1294−1300.

Chapter 3. Thyroid hormone 3,5',3'-triiodo-L-thyronine Alters the Molecular Physiology of a Model Rainbow Trout Gill Epithelium

3.1. Summary

The thyroid hormone (TH) 3,5',3'-triiodo-L-thyronine (T_3) is the principle active TH in teleost fishes. In this study, the effect of T_3 on the barrier properties and molecular physiology of the tight junction (TJ) complex was examined using a primary cultured rainbow trout gill model. The model epithelium was composed of gill pavement cells and ionocytes, and the presence of T_3 (10 and 100 ng/mL) in culture medium over a ~ 6 day period resulted in a decrease in transepithelial resistance (TER) of these preparations but no significant alteration in the paracellular flux rate of polyethylene glycol (MW 400 Da, PEG-400). In response to T_3 treatment, an elevation of Na^+/K^+-ATPase α1b (NKA- α1b) transcript was observed at 10 ng/mL but not at higher 100 ng/mL dose. In addition, decreased transcript abundance of genes encoding claudin (Cldn) family tight junction (TJ)-associated genes *cldn-7*, *-8d*, *-27*, and *-28b* occurred as did an increase in transcript abundance of *cldn-10c* at 10 ng/mL. However, a number of genes of interest did not exhibit altered mRNA abundance in response to T_3 treatment in the gill epithelium model, including *nka-α1a*, TJ-scaffolding proteins *cgn* and *zo-1*, MARVEL-domain proteins *ocln* and *tric*, and *cldn-8b*, *-12*, *-23a*, *-31*, and *-32a*. Nevertheless, a modest reduction in mRNA abundance of *cldn-8d* translated into significant reduction in Cldn-8d protein abundance, whereas Tric was unaltered in mRNA and protein abundance. Data suggest that T_3 influences the electrophysiology of the gill epithelium and the molecular physiology of TJ complex, but that the relationship between barrier function and TJ-associated proteins in response to TH treatment is not straightforward.

3.2. Introduction

Thyroid hormones (THs) are involved in the regulation of physiological functions including growth, metabolism, and metamorphosis (Power et al., 2001). As a feature of chordate groups, TH producing glands and follicles, and peripheral mechanisms of TH action have been widely investigated (reviewed by Muller 2014 and Laudet 2011). The basic histological unit of all vertebrate thyroid gland is the follicle, a hollow compartment that consists of a layer of epithelial cells enclosing a fluid filled compartment (Norris and Carr 2013). In teleost fishes, the thyroid follicles are scattered singly or in small groups under the loose connective tissues in the pharyngeal region. In some fishes, however, the thyroid follicles are also found dispersed outside the typical pharyngeal regions (Qureshi and Sultan 1976; Geven et al 2007). Thyroid hormone is natively synthesized as thyroxine (T_4) by thyroid follicles. De-iodination of T_4 by deiodinases covalently removes a peripheral iodine producing 3,5',3'-triiodo-L-thyronine, or triiodothyronine (T_3; reviewed by Darras and Van Herck, 2012). While T_4 and T_3 are both biologically active molecules, T_3 is considered as the main bioactive form of TH in vertebrates. Furthermore, the type III iodothyronine deiodinase (D3), the main factor in the degradation of T_3 has been identified in the brain and gill of Nile tilapia (*Oreochromis niloticus*, which suggests a potential mechanism for localised regulation of TH (Sanders et al. 1999).

In amphibians and fishes, TH has been studied extensively for its roles in the initiation of metamorphosis. An outstanding example of THs in teleost metamorphosis is the Japanese flounder, where during the process of metamorphosis, the animal shifts from a bilateral symmetry to asymmetry with extensive remodeling of tissues and organs (Miwa et al. 1988). This metamorphosis in the Japanese flounder is triggered by a surge in TH levels (Miwa et al. 1988; Tagawa et al. 1990). In a more subtle manner, salmonid smoltification and increased salinity

tolerance coincides with the seasonal changes of increased photoperiod between April and May, as well as correlates to elevated circulating TH levels (McCormick et al. 1987). While salmonid smoltification is less dramatic than the morphological changes Japanese flounder undergo, changes in physiological TH levels in smoltification is critical to salmonids in the physiological changes involved as the animals begin to migrate to a new aquatic environment with increased salinity (McCormick et al. 2007).

The teleost gill is a multifunctional organ that is simultaneously involved in various functions which contribute to the maintenance of piscine homeostasis (reviewed by Evan et al. 2005). One of these functions is the contribution of the gill epithelium to the maintenance of overall salt and water balance (reviewed by Evan et al. 2005). In this regard, the morphology and function of the gill is directly controlled by systemic hormonal factors (Laurent and Perry 1990; Wong and Chan 2001). These hormones include cortisol, prolactin, growth hormones, and in the current context, TH. Previous findings suggest that THs play a strong supportive role in teleost fish osmoregulation (McCormick 2001). In several studies, changes in TH levels have not only been linked to metamorphosis in salmonids, but also elevated gill activity of the ion transport enzyme Na^+-K^+-ATPases (NKA; Virtanen and Soivio 1985; McCormick et al. 2013). In order to dissect the mechanisms of TH on gill cells, a primary cultured trout gill epithelium model (composed of pavement cells on permeable cell culture inserts) was previously utilised to examine the effects of T_3 on the barrier and transport properties of the branchial epithelium, as well as the direct effect of T_3 on NKA activity in these cells (Kelly and Wood 2001). The study reported a decrease in electrophysiological resistance that was coupled with increased paracellular permeability at a particularly high T_3 concentration. Moreover, the addition of cortisol potentiated the effect of T_3 on NKA activity of gill pavement cells (Kelly and Wood 2001). The presence of T_3 in gill culture

resulted in an amplification in the net flux of both sodium and chloride ions (i.e. ion loss from basolateral medium to apical water) across the cultured epithelium (Kelly and Wood 2001). An extended observation by Kelly and Wood (2001) was that TH may influence the barrier properties of the gill model by modulating transcellular and paracellular components of membrane transport independently, depending on TH level in the system. For example, in the presence of a physiologically relevant concentration of 10 ng/mL T_3, TER was reduced but not the flux rate of a paracellular marker. Instead, T_3 at this dose stimulated gill cell NKA activity. In contrast, a dose of 100 ng/mL T_3 reduced TER, increased paracellular marker flux and elicited only modest changes in NKA activity (Kelly and Wood 2001). But the potential influence of TH on the gill epithelium tight junction (TJ) complex was not addressed in early studies. In light of this, and because the influence of endocrine factors on the TJ complex is now being increasingly recognized as critical in establishing the resistive properties of the branchial epithelium (e.g. Bui et al. 2010; Chasiotis et al. 2010; Chasiotis and Kelly 2011; Kelly and Chasiotis 2011; Chasiotis et al. 2012; Kolosov and Kelly 2013, 2017, 2019, 2020; Kolosov et al 2017), the effect of TH on gill epithelium barrier properties and the gill TJ complex warrants further investigation.

The objective of this study was to use a cultured trout gill epithelium model to consider the relationship between TH and gill epithelium barrier properties as they relate to the gill TJ complex. A rainbow trout gill model composed of pavement cells and ionocytes was used to examine the direct effects of TH on endpoints of epithelium permeability as well as the molecular physiology of the TJ. It can be hypothesized that TH-induced changes in the barrier properties of the model gill epithelium will be coupled with alterations in TJ-associated gene transcript or protein abundance when measured differences in paracellular pathway permeability occur. When these do not occur, changes in TER will reflect alterations in the transcellular pathway.

3.3. Materials and Methods

3.3.1. Experimental Animals

Rainbow trout (*Oncorhynchus mykiss*, approximately 250 g) for gill cell primary culture were obtained from a local hatchery (Humber Springs Trout Club and Hatchery, Orangeville, ON, Canada) and reared in 600 L opaque polystyrene aquaria. Fish were fed *ad libitum* once daily with commercial trout pellets (Martin Profishent, Elmira, ON, Canada). Tanks were supplied with aerated flow-through, dechlorinated City of Toronto tap water (approximate composition in μM: Na^+ 590; Cl^- 920; Ca^{2+} 900; K^+ 50; pH 7.4) and maintained at 11 ± 1°C. Fish were held under a constant photoperiod (12 light:12 dark). All animal husbandry and experimental protocols follow the York University Animal Care Committee and the Canadian Council on Animal Care guidelines.

3.3.2. Cell Culture Media Preparations

A stock thyroid hormone solution was prepared by dissolving 3,3′,5-Triiodo-L-thyronine sodium salt (T_3; Sigma-Alderich, ON, Canada) in phosphate buffered saline (PBS, pH 7.7) to a final concentration of 0.5 mg/mL. A few drops of 5 M NaOH solution was required to dissolve T_3. The stock solution was stored in -30°C as single-use aliquots. Complete medium for tissue culture was prepared using Leibovitz's L-15 tissue culture medium supplemented with a final concentration of 6% fetal bovine serum, 200 unit/mL penicillin-streptomycin, and 0.05 mg/mL gentamicin solutions (all items supplied by Gibco™ Cell Culture, ON, Canada). T_3 media was prepared using appropriate volumes of PBS (0 ng/mL) or stock T_3 solutions to make up a control, 10, and 100 ng T_3/mL culture media. The final solvent volume added to culture media represents <0.001% of the final medium volume and had no effect on final media pH.

3.3.3. Primary Cultured Rainbow Trout Gill Epithelia and Physiological Measurements

Procedures for preparation of double seeded inserts from rainbow trout gill was described previously by (Kelly et al., 2000)). Briefly, branchial epithelial cells from rainbow trout gill filaments were isolated by trypsination and seeded 3 million cells/culture insert (PET filters, 0.9 cm^2 growth area, 0.4 μm pore size, $1.6x10^6$ /cm^2 pore density; BD Falcon TM; BD Biosciences, Mississauga, ON, Canada) containing 1 mL complete medium on both apical and basolateral compartments. Cultures were then held in an air atmosphere at 18°C. Fresh culture medium was applied (1.5 mL apical/2.0mL basolateral) after 24 hours followed by a second round of trypsination and seeding at 2 million cells/culture insert, with media volumes adjusted to 1.5 mL and 2.0 mL apical and basolateral media respectively. Control and treatment media were applied to culture inserts on day 3 and the media was refreshed every 48 hours. Transepithelial electrical resistance (TER) measurements were obtained using STX-2 chopstick electrodes connected to a custom-modified EVOM epithelial voltohmmeter (World Precision Instruments, Sarasota, FL), and expressed as ohms per centimeter squared ($\Omega \cdot cm^2$) after correcting for background resistance. Epithelia development was followed by TER until a plateau was measured (~6 days after seeding into culture inserts). Paracellular permeability was measured using a bio-marker (polyethylene glycol, molecular mass 400 Da; [^{3}H]PEG-400; American Radiolabeled Chemicals, Inc., Saint Louis, MO, USA) once the epithelia had reached a plateau in TER. [^{3}H]PEG-400 was added to the basolateral side of culture inserts (0.5 μCi/mL) for 12 hours, and its migration rate to the apical side was measured using methods and calculations previously described (Wood et al. 1998).

3.3.4. Total RNA Isolation, cDNA Synthesis, and Quantitative PCR Analysis

Trout epithelia for real-time PCR analyses were harvested by addition of 1.0 mL TRIzol reagent (Life Technologies, Burlington, ON, Canada) into culture inserts. Total RNA was then

isolated following the manufacturer's protocol. RNA yield from each insert was determined using a spectrophotometer (Multiskan^{TM} Spectrum, Thermos Scientific) and treated with DNase I (Amplification Grade; Life Technologies) prior to cDNA synthesis. First-strand cDNA synthesis was carried out using SuperScript^{TM} III Reverse Transcriptase and Oligo(dT)$_{12-18}$ primers (Invitrogen Canada Inc.) Quantitative real-time PCR (qRT-PCR) was conducted to assess transcript abundance of genes encoding Na^+-K^+-ATPase (NKA) isoforms and tight junction (TJ)-associated genes in cultured trout gill epithelia. Genes examined include Na^+-K^+-ATPase isoforms α-1a (*nka α-1a*) and α-1b (*nks α-1b*), occludin (*ocln*), tricellulin (*tric*), zonula occludens-1 (*zo-1*), cingulin (*cgn*), and claudin (*cldn*) family members including *cldn-7*, *-8b*, *-8d*, *-10c*, *-12*, *-23a*, *-27b*, *-28b*, *-31*, and *-32a*. qRT-PCR experiments were conducted in a Chromo4^{TM} Detection System (CFB-3240, Bio-Rad Laboratories Canada Ltd.) using SYBR Green I Supermix (Bio-Rad Laboratories Canada Ltd., ON, Canada) under the following conditions: 1 cycle denaturation (90°C, 4 min) followed by 40 cycles of denaturation (95°C, 30s), annealing (54-61°C, 30s), and extension (72°C, 30s), respectively. A final melting curve was generated from 1°C below primer annealing temperature at °C intervals up to 95°C. The gene selected as a reference for qRT-PCR analysis was β-actin (*actb*) as it did not significantly alter in response to the T_3 treatments. The primer sets used, specific annealing temperatures, amplicon sizes and GeneBank Accession numbers of all genes examined in this study are detailed in **Table 3-1**.

3.3.5. Western Blotting

Protein from cultured trout epithelium preparations on permeable inserts was isolated for Western blotting as previously described by Chasiotis et al (2010). Briefly, cultured inserts were first rinsed with ice-cold PBS twice prior to the addition of a lysis buffer (0.01 M Tris–HCl, pH=7.5, 1 mM EDTA, 0.1 mM NaCl, 1mM PMSF) with 1:200 protease inhibitor cocktail (Sigma-Aldrich

Canada Ltd.). The cells were homogenized by mechanical agitation with a syringe (BD PrecisionGlide, 3 mL, 20 G) and cell lysate was incubated on ice (30 min) and centrifuged (4°C, 17,949 x *g*, 20 min) and supernatant collection. Protein concentrations were then determined using a Bradford assay (Sigma Aldrich) and samples were stored in single use aliquots in -30 °C. Identical amounts of protein samples (5 µg) were loaded into a SDS-PAGE gel for electrophoresis separation and subsquent blotting onto an Immobilon®-P PVDF membrane (Millipore Sigma). Detection of Cldn-8d and Tric proteins abundance was then conducted using verified custom-synthesized antibody against trout Cldn-8d and Tric (Kolosov and Kelly 2017; Kolosov and Kelly 2018). Subsequent image densitometry analysis was performed using Bio-Rad Image Lab™ software (Version 6.0.0 build 26; Bio-Rad Laboratories, Inc.) Target protein abundance was normalized to total protein stain using Coomassie brilliant blue staining.

3.3.6. Statistical Analyses

All data are expressed as mean values ± S.E.M. Statistical analyses were carried out using a statistical software (Prism 7, version 7.0d, GraphPad Software, USA). For transcript abundance measurement, gene of interest mRNA abundance was normalized using the reference gene (β-actin) that did not change with respect to treatment ($p \geq 0.90$). One-way analysis of variance (ANOVA) followed by Holm-Šídák pairwise comparison or Student's t-test were performed where appropriate to determine significant differences between groups ($p \leq 0.05$).

Table 3-1. Primer sets, amplicon size, PCR annealing temperature, and gene accession numbers for rainbow trout tight junction proteins and β-actin.

Gene	Primer sequence (5'➞3')	Amplicon size (bp)	Annealing temperature (°C)	Accession number
actb	For: GGACTTTGAGCAGGAGATGG Rev: GACGGAGTATTTACGCTCTGG	354	58	AF157514
nka α-1a	For: AGAAAGCCAAGGAGAAGATG Rev: AGCCCGAACCGAGGATAGAC	133	56	NM_001124461.1
nka α-1b	For: AGCAAGGGAGAAGAAGGACA Rev: GAGGAGGGGTCAGGGTG	176	59	NM_001124460.1
cgn	For: CTGGAGGAGAGGCTACACAG Rev: CTTCACACGCAGGGACAG	156	56	BK008767
zo-1	For: AAGGAAGGTCTGGAGGAAGG Rev: CAGCTTGCCGTTGTAGAGG	291	60	HQ656020
ocln	For: CAGCCCAGTTCCTCCAGTAG Rev: GCTCATCCAGCTCTCTGTCC	341	58	GQ476574
tric	For: GTCACATCCCCAAACCAGTC Rev: GTCCAGCTCGTCAAACTTCC	170	60	KC603902
cldn-7	For: CGTCCTGCTGATTGGATCTC Rev: CAAACGTACTCCTTGCTGCTG	261	61	BK007965
cldn-8b	For: ACGACTCCCTCCTGGCTCT Rev: GAGACCCATCCGATGTAGA	185	56	BK008770
cldn-8d	For: GCAGTGTAAAGTGTACGACTCTCTG Rev: CACGAGGAACAGGCATCC	200	60	BK007966
cldn-10c	For: CCTGGTCTGCTCTACAATGC Rev: CCCGAAGAATCCCAAAATAA	223	58	BK008772
cldn-12	For: CTTCATCATCGCCTTCATCTC Rev: GAGCCAAACAGTAGCCCAGTAG	255	60	BK007967
cldn-23a	For: ATCCTAAACCTCACAGCGACA Rev: CGGTCTTTCCAGCACCTTAC	270	60	BK008775
cldn-27b	For: GCCAACATCGTAACAGGACA Rev: CCAGAAGAGCACCAATGAGC	283	60	BK008776
cldn-28b	For: CTTTCATCGGAGCCAACATC Rev: CAGACAGGGACCAGAACCAG	310	60	EU921670
cldn-31	For: TCGGCAACAACATCGTGAC Rev: CGTCCAGCAGATAGGAACCAG	311	61	BK007969
cldn-32a	For: ATTGTGTGCTGTGCCATCC Rev: AGACACCAACAGAGCGATCC	321	60	BK007970

3.4. Chapter 3 Figures

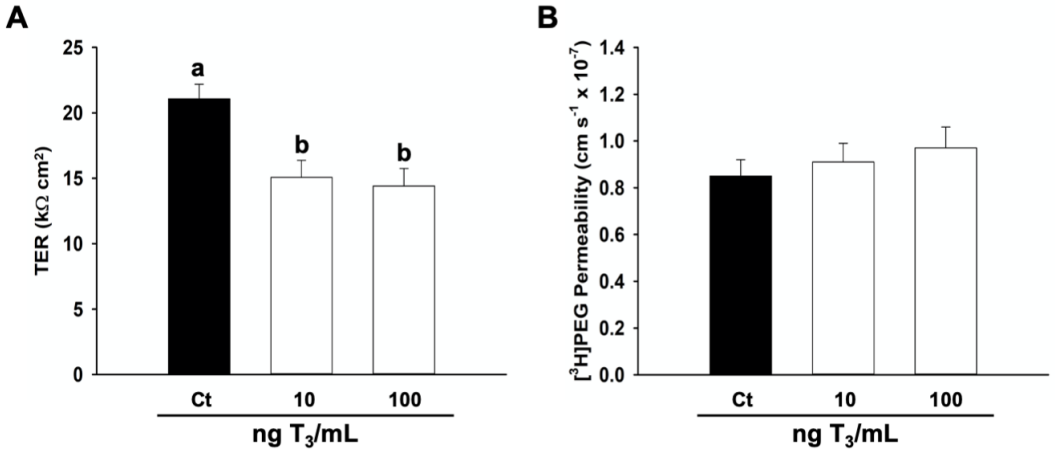

Figure 3-1. Effect of thyroid hormone T_3 (0, 10, and 100 ng/mL) on (A) transepithelial electrical resistance and (B) [^{3}H]PEG-400 flux on cultured trout gill epithelia. Data are expressed as mean values ± SEM (n=7-8). Significant differences between treatment groups by one-way ANOVA is denoted by different letters ($p<0.05$, n=8-10).

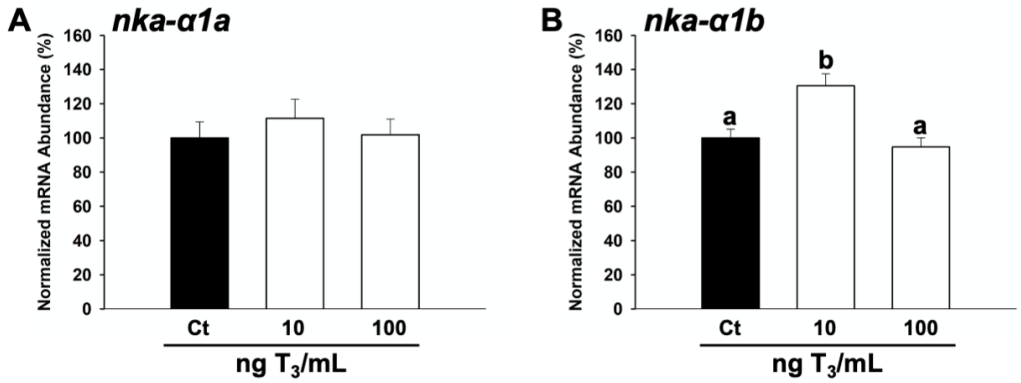

Figure 3-2. Effects of thyroid hormone T_3 (0, 10, and 100 ng/mL) on mRNA abundance of Na^+-K^+-ATPase α-subunit isoforms (A) *nka-α1a* and (B) *nka-α1b* in cultured trout gill epithelia. Data are expressed as mean values ± SEM (n=7-8). Significant differences between treatment groups by one-way ANOVA is denoted by different letters ($p<0.05$, n=8-10).

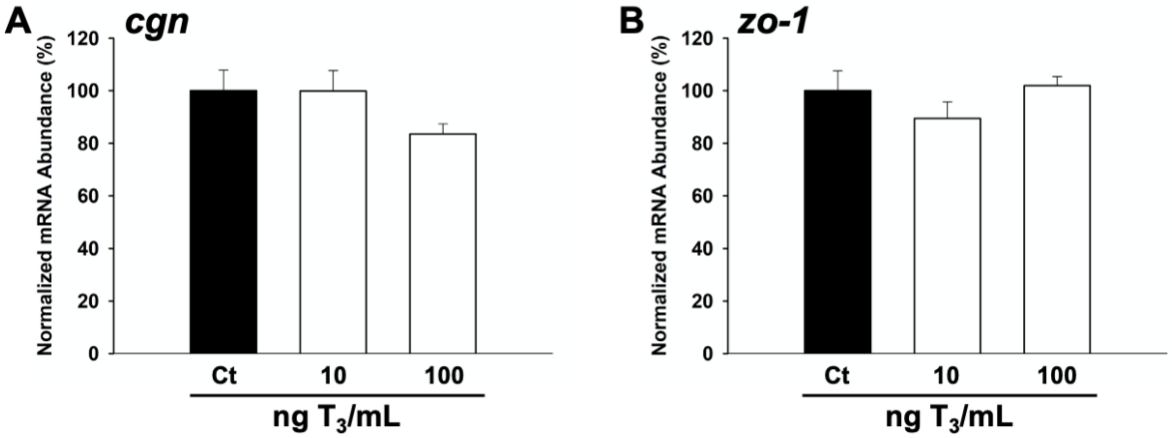

Figure 3-3. Effects of thyroid hormone T_3 (0, 10, and 100 ng/mL) on mRNA transcripts of TJ-associated scaffolding proteins (A) cingulin (*cgn*) (B) zona occludens-1 (*zo-1*) in cultured trout gill epithelia. Data are expressed as mean values ± SEM (n=7-8). Significant differences between treatment groups by one-way ANOVA is denoted by different letters ($p<0.05$, n=8-10).

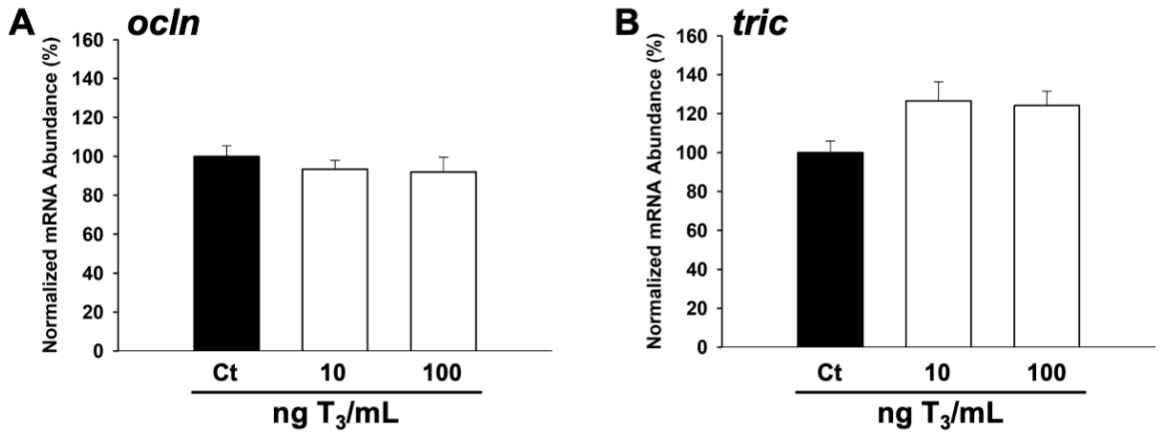

Figure 3-4. Effects of thyroid hormone T_3 (0, 10, and 100 ng/mL) on mRNA transcripts of MARVEL-domain TJ proteins (A) occludin (*ocln*) and (B) tricellulin (*tric*) in cultured trout gill epithelia. Data are expressed as mean values ± SEM (n=7-8). Significant differences between treatment groups by one-way ANOVA is denoted by different letters ($p<0.05$, n=8-10).

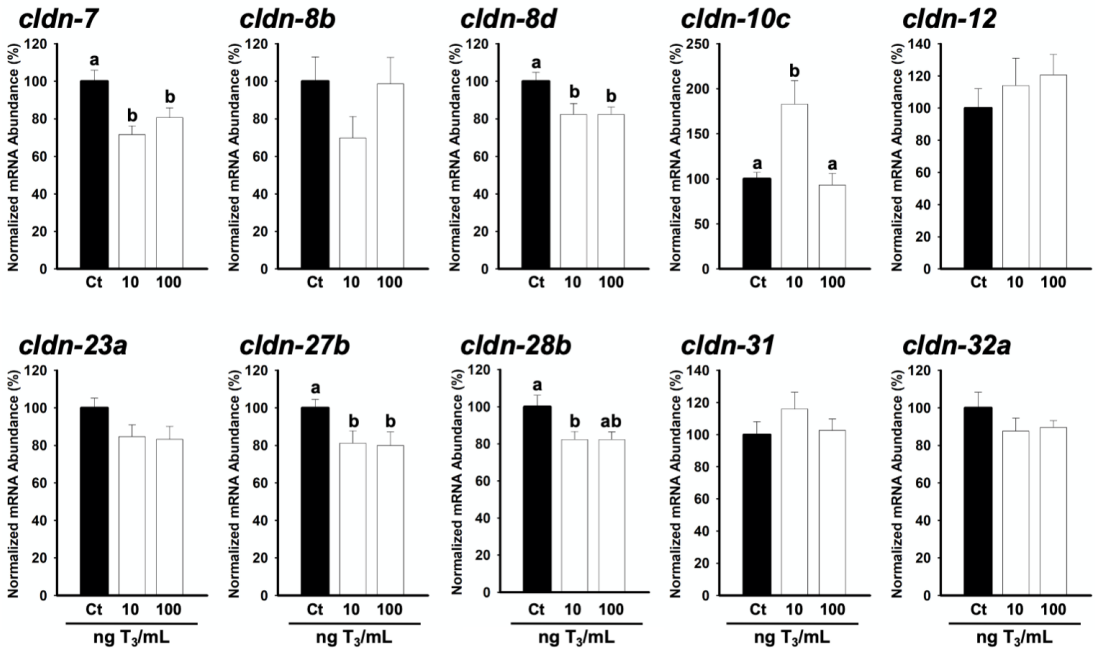

Figure 3-5. Effects of thyroid hormone T_3 (0, 10, and 100 ng/mL) on mRNA transcripts of claudin (*cldn*) family TJ proteins in cultured trout gill epithelia. Data are expressed as mean values ± SEM (n=7-8). Significant differences between treatment groups by one-way ANOVA is denoted by different letters ($p<0.05$, n=8-10).

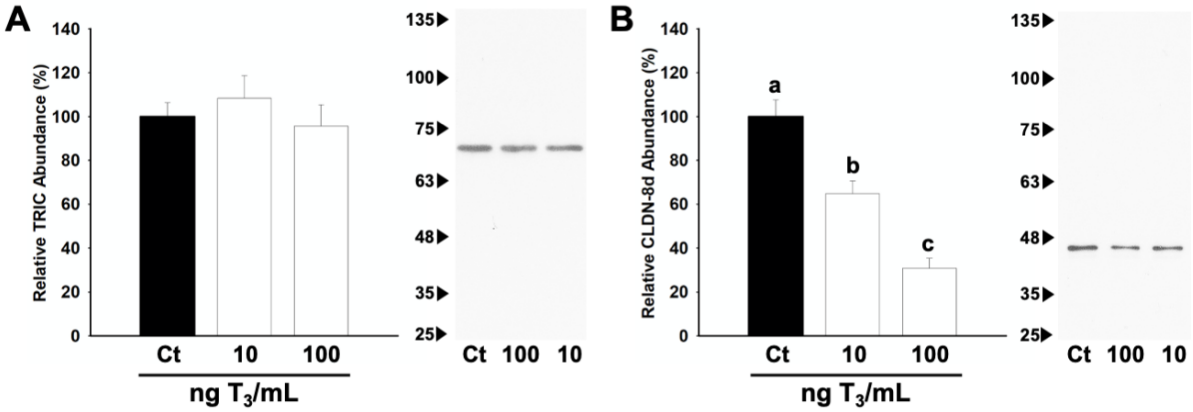

Figure 3-6. Relative protein abundance of trout (A) TRIC and (B) CLDN-8d in cultured trout gill epithelia in response to T_3 treatments. Data are expressed as mean ± SEM (n=5-6). Significant differences between treatment groups by one-way ANOVA is denoted by different letters ($p<0.05$, n=4-5).

3.5. Results

The thyroid hormone T_3 decreased TER of the cultured gill model equally at both doses used, but did not alter flux of the paracellar marker [^{3}H]PEG-400 (**Figure 3-1**). T_3 treatment significantly increased mRNA abundance of Na^+-K^+-ATPase (NKA) α1b isoform at 10 ng/mL but no significant effect was observed at 100 ng/mL (**Figure 3-2**). Transcript abundance of NKA-α1a did not alter in response to T_3 treatment.

Transcript abundance of genes encoding TJ proteins were examined in response to T_3 treatment of the cultured epithelium. Transcript abundance of scaffolding TJ proteins *cgn* and *zo-1* was not significantly altered in response to either of the T_3 doses used (**Figure 3-3**). Furthermore, transcript abundance of MARVEL domain-containing proteins including *ocln* and *tric* also did not respond to T_3 treatment (**Figure 3-4**). However, changes were observed in transcript abundance of select *cldn* family TJ proteins (**Figure 3-5**). More specifically, transcript abundance of *cldn-7*, *-8d*, and *-27b* significantly decreased in response to the addition of both 10 and 100 ng/mL T_3 in culture media. In contrast, transcript abundance of *cldn-10c* was elevated, but only at a dose of 10 ng/mL T_3. Finally, *cldn-28b* transcript abundance decreased significantly at 10 ng/mL but not with the higher 100 ng/mL T_3 addition. Transcript abundance of *cldn-8b*, *-12*, *-23*, *-31*, and *-32a* did not respond to T_3 treatments. Western blotting using custom-synthesized antibodies against trout Tric and Cldn-8d showed a decrease in Cldn-8d abundance in response to T_3 and no change in Tric abundance (**Figure 3-6**).

3.6. Discussion

3.6.1. Overview

The effect of T_3 on gill epithelium barrier properties and the molecular physiology of the gill epithelium TJ complex was examined using a model gill epithelium preparation composed of both branchial pavement cells and ionocytes. The presence of T_3 significantly decreased TER of the preparation and, at a low dose of 10 ng/mL, did not alter the flux rate of the paracellular permeability marker [^{3}H]PEG-400. These observations are consistent with previous studies on the direct effect of T_3 on the gill pavement cell epithelium (Kelly and Wood 2001a). However, at a higher dose of 100 ng/mL T_3, Kelly and Wood (2001a) described a significant decrease in TER and increase in paracellular permeability. In this study, a reduction in TER was also observed in response to a 100 ng/mL T_3 treatment regime, but a change in paracellular permeability was not detected. Therefore, altered gill epithelium barrier properties occurred upon exposure to T_3 irrespective of dose, as previously reported, but in the current study this did not occur in association with a measured change in paracellular permeability. Nevertheless, significant alterations in TJ-associated gene mRNA and protein abundance did occur at both doses of T_3 examined in this study, which suggests that TH can influence the molecular physiology of the gill TJ complex and this may play an important role in gill function when TH levels naturally elevate or diminish. However, the hypothesis that TH-induced changes in the barrier properties of the model gill epithelium will be coupled with alterations in TJ-associated gene transcript or protein abundance when measured differences in paracellular pathway permeability occur cannot be accepted. This is because no difference in [^{3}H]PEG-400 permeability was detected between control and treatment groups in this study.

3.6.2. The effect of T_3 on Model Trout Gill Epithelium Barrier Properties

The direct effect of TH on the transport properties of primary cultured fish gill cells/epithelia has previously been considered in two studies (Kelly and Wood 2001a; Tse et al. 2007). However, of these two, only Kelly and Wood (2001a) have reported on the effects of TH on barrier properties of a cultured gill epithelium. While the current study produced results that were largely consistent with Kelly and Wood (2001a), a notable difference was that the highest T_3 concentration (100 ng/mL) in the current work did not cause an alteration in [^{3}H]PEG permeability, as reported by Kelly and Wood (2001b). In previous studies by Wood and Kelly (2001a) as well as Tse et al (2007), primary cultured gill pavement cells were used exclusively, while the current study used a model epithelium composed of gill pavement cells and ionocytes. In the intact gill, pavement cells make up the bulk of the epithelium while ionocytes represent around 10% of the overall cell population. Therefore, it is pavement cells that present most of the barrier between the surroundings of a fish and its blood. In primary culture, a model trout gill epithelium composed exclusively of pavement cells typically exhibits a lower TER (upon maturation) than models composed of both pavement cells and ionocytes (for review see Wood et al 2002). Models that exhibit a lower starting TER also tend to exhibit greater alterations in TER and paracellular permeability marker molecules upon experimental manipulation (i.e. they appear to be more sensitive to experimental variables such as hormone treatment). In contrast, models composed of both pavement cells and ionocytes that achieve a high TER plateau upon maturation tend to be less sensitive to experimental manipulation with endocrine factors. Therefore, although both models can exhibit a qualitatively consistent response to endocrine factors (see Kelly and Wood 2001a; Wood et al 2002), using a model composed of both pavement cells and ioncoytes, with a high TER at maturity, may have resulted in some nuances of T_3-induced alterations being lost. Another

variable to consider is that Kelly and Wood (2001) used PEG with a MW of 4000 Da (i.e. [^{3}H]PEG-4000) rather than PEG-400 to measure paracellular permeability. PEG-400 moves across the epithelium (through the paracellular pathway) faster than PEG-4000 as a consequence of its smaller size, and this could have had an impact on the results. A final possibility is that because peripheral regulation of THs have been identified in the gills of teleost (Sanders 1999; Arjona 2011), the inclusion of ionocytes may contribute to a muted response through T_3 clearance under elevated conditions. In all cases further study will be required, but the fact that TH can impact gill epithelium barrier properties as determined by TER is a consistent response across studies.

3.6.3. Effects of T_3 on NKA Isoforms in a Model Trout Gill Epithelium

The effects of TH on gill NKA activity has been contradictory in previous studies (for example Dangé 1986; Madsen and Korsgaard 1989; Subash 2000). NKA is a membrane bound enzyme that provides the driving force in teleost osmoregulatory epithelia (Zadunaisky 1984). Therefore, NKA is a key enzyme in osmoregulation, and NKA isoforms and their switching have been revealed to play a crucial role in salinity acclimation of salmonids (Richards et al. 2003; McCormick et al., 2009). In the current culture preparation, a significant increase in *nka-α1b* abundance was observed under physiologically relevant T_3 concentration. The current model of freshwater teleost osmoregulation suggests NKA-α1a is important for the movement of Na^+ into the extracellular fluid by freshwater gill ionocyte. In contrast, NKA-α1b isoform is critical for removing intracellular Na^+ following the activity of gill Na^+,K^+,2Cl^- cotransporter (Richards et al. 2003; Pelis et al. 2011). Significant increase in *nka-α1b* in FW derived trout epithelium may suggest that this isoform is sensitive to T_3 and this could act as a preparatory mechanism that allows salmonids to acclimate to increase salinity gradients that often coincide with alterations in

TH and NKA isoform levels during smoltification (McCormick 1987; Jones et al. 2002; McCormick 2007).

In vivo studies on the effects of TH and gill NKA activity have been examined using direct TH injections (i.e. Dangé 1986; Madsen 1990). However, previous studies demonstrated mix findings on the effects of TH and gill NKA activity. TH may require a highly coordinated and synergetic effects with other osmoregulatory hormones. Despite being a passive barrier, cultured pavement cell epithelium was observed to increase NKA activity by T_3 that is further potentiated in the presence of cortisol (Kelly and Wood 2001a). In a pavement cell culture derived from the Japanese eel, presence of T_3 in culture media did not alter the ratio between NKA-α1a and NKA-α1b abundance (Tse et al 2007). The result was not unexpected as PVCs are not known to participate in active ion transport of the gill epithelium. Therefore, while TH may not directly activate the transcellular ion movements in the gill epithelium, TH may determine the directionality of ion transport in ionocytes.

3.6.4. Effects of T_3 on the Molecular Physiology of the Model Trout Gill TJ

The TJ complex has become a focal point in understanding how the barrier properties of the gill epithelium contribute to the overall salt and water balance in teleost fishes (reviewed by Chasiotis et al. 2012; Kolosov et al. 2013). In primary cultured gill epithelium models, TJs have been demonstrated to be dynamic assemblies that modulate in response to endocrine and environmental factors. Cortisol is an outstanding example of direct endocrine regulation of gill barrier properties via alterations in the TJ assembly (Chasiotis et al 2010; Chasiotis and Kelly 2011b; Chasiotis and Kelly 2012; Kolosov and Kelly 2013, 2017, 2018). In the current study, T_3 significantly altered select TJ protein mRNA transcript abundance without any measurable change in the paracellular barrier properties. Current data suggest T_3 does not alter the TJ scaffold

components (i.e. ZO-1 and Cgn) that provide the overall structure of the TJ assembly (Fanning and Anderson 2009; Odenwald et al 2018). Furthermore, the presence of T_3 did not alter the transcript abundance of MARVEL-domain containing TJ proteins including Ocln and Tric, which have been previously demonstrated to be cortisol responsive (Chasiotis and Kelly 2010; Kolosov and Kelly 2013). In contrast, the effect of T_3 on culture gill epithelium largely manifest as changes in gill *cldn* mRNA transcript abundance.

Claudins are a family of TJ proteins that exhibit organ-specific and within-tissue expression patterns in association with distinctive barrier functions (Angelow et al 2008; Kolosov et al 2013). Cldn family TJ proteins can provide either barrier or pore function in both epithelia and endothelia (Günzel and Yu 2013). The presence of T_3 significantly alters transcript abundance of select claudins including *cldn -7*, *-8d*, *-10c*, *-27b*, and *-28b*. All but one of these genes (i.e. *cldn-10c*) exhibited a decrease in mRNA abundance in response to T_3 treatment. Additionally, protein abundance of Cldn-8d was significantly lowered in response to TH treatment. In trout, *cldn-7, -8d, -27b* and *-28b* all exhibit comparatively restricted expression profiles and the organ in which they are most abundant is the gill (Kolosov et al 2014). In addition, these *cldn* genes have all been associated with barrier function (or formation) in the gill epithelium of fishes. For example, KD studies have shown that Cldn-8d is a barrier protein in the fish gill epithelium (Kolosov and Kelly 2017), while *cldn-27b* and *-28b* both exhibit an increase in abundance in association with the development or elevation of cultured gill epithelium resistive properties (Kelly and Chasiotis 2011; Kolosov and Kelly 2017; Kolosov et al 2014). Additionally, Sandbichler et al (2011) reported a reduction in Cldn-28b in association with increase gill epithelium permeability. Furthermore, *cldn-7* has been reported to exhibit an increase in transcript abundance in association with the development of gill epithelial cell confluence, after which it remains constitutively high (Kolosov

et al 2014). In light of this, there would appear to be compelling evidence to suggest that one target of T_3 in the gill may be the TJ complex and more specifically, TJ proteins that play an important role in maintaining epithelium barrier properties.

An important question however, is what could a reduction in gill epithelium permeability (or the abundance of these TJ proteins) achieve? Two T_3-induced changes in the current study provide some evidence to suggest a function association with the role and properties of the gill epithelium upon acclimation of fish to a marine setting. More specifically, when a FW fish acclimates to seawater, the gill epithelium becomes 'leakier' to facilitate the paracellular secretion of Na^+ through selectively permeable, shallow TJs that reside between gill ionocytes (Evans et al 2005). Elevated NKA activity plays an important role in this process by indirectly assisting in the transcellular secretion of Cl^- into ionocyte apical crypts. This establishes the electrochemical gradient down which Na^+ moves, and thus excess Na^+ and Cl^- are secreted from the fish across the gill. In light of this, the first piece of evidence to suggest that T_3 may be helping to reorganize the gill in preparation for sea water entry is an observed increase in the abundance of *nka-α1b* in the cultured gill model as suggested above. However, the second piece of evidence is the observed T_3-induced increase in *cldn-10c* abundance. More specifically, there is mounting evidence that Cldn-10 isoforms play a key role in the formation of the paracellular channels that facilitate Na^+ extrusion across the gill epithelium of a marine fish (Tipsmark et al 2008; Bui et al 2010; Bui and Kelly 2014; Marshall et al. 2018). These TJ proteins are typically expressed almost exclusively in the gill of fishes, where they are characteristically found only in gill epithelium ionocytes (Bui et al 2010; Bui and Kelly 2014). Furthermore, in association with acclimation to a hyperosmotic environment, the abundance of gill Cldn-10 proteins increases (Tipsmark et al 2008; Bui et al 2010; Bui and Kelly 2014; Marshall et al. 2018). Therefore, in order to acclimate to seawater the gill

epithelium of a fish (amongst other things) has to exhibit a cell-specific increase in Cldn-10 abundance. In the cultured trout gill epithelium, T_3 elevates the mRNA abundance of *cldn-10c* which is consistent with the above. Furthermore, *cldn-10c* is found exclusively in model gill ionocytes (i.e. this gene is not present in trout gill pavement cells) (Kolosov et al 2014). So the response seen following T_3 treatment is generated by the model gill ionocytes only. It would also be interesting to consider the possibility that reduced *cldn-28b* may be functionally linked to elevated *cldn-10c*, because although *cldn-28b* is not present exclusively in ionocytes (i.e. it can be found in pavement cells), it may be enriched in gill ionocytes because it exhibit significantly greater abundance in model gill epithelia that possess these cells (Kolozov et al 2014). Therefore, a *cldn-28b*-induced reduction in the barrier function of junctions that link ionocytes to adjacent cells may help to facilitate the construction of a selectively permeable paracellular pathway controlled by Cldn-10c. However, what is clear is that although the molecular physiology of the gill may be altered in preparation for a seawater setting, the functional properties of the gill, at least from a paracellular point of view, appear to remain intact. But this is not unusual as salmonid fish preparation for seawater entry takes place in FW. So, mechanisms cannot be functional until the fish migrate to a marine setting.

3.7. Conclusions and Perspectives

The current study examined the effects of T_3 on a primary cultured model trout gill epithelium composed of pavement cells and ionocytes. Despite changes in the electrical resistance and TJ associated proteins, T_3 did not alter the overall barrier properties of the culture epithelium. The current results suggest that the decrease in electrical resistance is tied to transcellular ion transport, and potential compensatory mechanisms may exist in response to the decrease in the TJ components observed. Significant changes in transcript abundance of *nka-α1b* and *cldn-10c* were

also observed in response to T_3 treatment, but it is currently not clear whether this alters the direction of ion transport characteristics in the gill epithelium. The current culture model using cells derived from FW fishes have been demonstrated to have limited ion transport properties, therefore a new model that stimulates active ion transport using FW derived fishes may be required to elucidate the significance of TH in teleost osmoregulation.

3.8. References

Angelow, S., Ahlstrom, R., Yu, A.S.L. (2008) Biology of claudins. Am J Physiol - Ren Physiol 295(4): F867-F876.

Arjona, F.J., Vargas-Chacoff, L., Martin de Rio, M.P., et al. (2011) Effects of cortisol and thyroid hormone on peripheral outer ring deiodination and osmoregulatory parameters in the Senegalese sole (*Solea senegalensis*). J Endocrinol 208: 323-330.

Bui, P., Bagherie-Lachidan, M., Kelly, S.P. (2010) Cortisol differentially alters claudin isoforms in cultured puffer fish gill epithelia. Mol Cell Endocrinol 317: 120-126.

Chasiotis, H., Wood, C.M., Kelly, S.P. (2010) Cortisol reduces paracellular permeability and increases occludin abundance in cultured trout gill epithelia. Mol Cell Endocrinol 323: 232-238.

Chasiotis, H., and Kelly, S.P. (2011a) Permeability properties and occludin expression in a primary cultured model gill epithelium from the stenohaline freshwater goldfish. J Comp Physiol - B 181: 487-500.

Chasiotis, H. and Kelly, S.P. (2011b) Effect of cortisol on permeability and tight junction protein transcript abundance in primary cultured gill epithelia from stenohaline goldfish and euryhaline trout. Gen Comp Endocr 172: 494-504.

Chasiotis, H., and Kelly, S.P. (2012) Effects of elevated circulating cortisol levels on hydromineral status and gill tight junction protein abundance in the stenohaline goldfish. Gen Comp Endocr 175: 277-283.

Chasiotis, H. et al. (2012) Tight junctions, tight junction proteins and paracellular permeability across the gill epithelium of fishes: a review Resp Physiol and Neurobiol 184: 269-281.

Dangé, A. D. (1986) Branchial Na^+–K –ATPase activity in freshwater or saltwater acclimated tilapia, *Oreochromis* (*Sarotherodon*) *mossambicus*: Effects of cortisol and thyroxine. Gen Comp Endocrinol. 62: 341–343.

Darras, V.M. and Van Herck, S.L.J. (2012) Iodothyronine deiodinase structure and function: from ascidians to humans. J Endocrinol 215: 189-206.

Evans, D.H., Piermarini, P.M., Choe, K.P. (2005) The multifunctional fish gill: dominant site of gas exchange, osmoregulation, acid-base regulation, and excretion of nitrogenous waste. Physiol Rev. 85(1): pp. 97-177.

Fanning, A.S. and Anderson, J.M. (2009) Zonula occludens-1 and -2 are cytosolic scaffolds that regulate the assembly of cellular junctions. Ann N Y Acad Sci. 1165:113-20.

Geven, E.J.W., Nguyen, N.K., Van Den Boogaart, M., Spanings, F.A.T., Flik, G., Klaren, P.H.M. (2007) Comparative thyroidology: Thyroid gland location and iodothyronine dynamics in Mozambique tilapia (*Oreochromis mossambicus Peters*) and common carp (*Cyprinus carpio L.*). J Exp Biol 210: 4005–4015.

Günzel, D., Stuiver, M., Kausalya, P. J., et al. (2009). Claudin-10 exists in six alternatively spliced isoforms that exhibit distinct localization and function. J Cell Sci 122: 1507-1517.

Günzel, D., and Yu, A.S.L. (2013) Claudins and the Modulation of Tight Junction Permeability. Physiol Rev 93: 525-569.

Jones, I., Rogers, S.A., Kille, P., and Sweeney, G.E. (2002) Molecular expression of Thyroid Hormone Receptor Alpha during Salmonid Development. Gen Comp Endocrinol 125: 226-235.

Karnaky, K. J., Jr, Degnan, K. J. and Zadunaisky, J. A. (1977). Chloride transport across isolated opercular epithelium of killifish: a membrane rich in chloride cells. Science 195: 203-205.

Kelly, S.P., and Wood, C.M. (2001a) The physiological effects of 3,5',3'-triiodo-L-thyronine alone or combined with cortisol on cultured pavement cell epithelia from freshwater rainbow trout gills. Gen Comp Endocr 123, 280-294.

Kelly, S.P., and Wood, C.M. (2001b) Effect of cortisol on the physiology of cultured pavement cell epithelia from freshwater trout gills. Am J Physiol Regulatory Integrative Comp Physiol 281, R811-R820.

Kelly, S.P., Wood, C.M. (2002a) Cultured gill epithelia from freshwater tilapia (*Oreochromis niloticus*): Effect of cortisol and homologous serum supplements from stressed and unstressed fish. J Membrane Biol: 190 (1): pp. 29-42.

Kelly, S.P., Wood, C.M. (2002b) Prolactin effects on cultured pavement cell epithelia and pavement cell plus mitochondria-rich cell epithelia from freshwater rainbow trout gills. Gen Comp Endocr 128: 44-56.

Kolosov D, Bui P, Chasiotis H and Kelly SP (2013) Claudins in teleost fishes Tissue Barriers 1:3 e25391.

Kolosov D,m and Kelly S.P. (2013) A role for tricellulin in the regulation of gill epithelium permeability. Am J of Physiol Reg Int Comp Physiol. 304: R1139-R1148.

Kolosov, D., Chasiotis, H., Kelly, S.P. (2014) Tight junction protein gene expression patterns and changes in transcript abundance during development of model fish gill epithelia. J Exp Biol (217) 1667-1681.

Kolosov, D. and Kelly, S.P. (2017) Claudin-8d is a cortisol-responsive barrier protein in the gill epithelium of trout. J Mol Endocrinol. 59(3):299-310.

Kolosov, D. and Kelly, S.P. (2018) Tricellular tight junction-associated angulins in the gill epithelium of rainbow trout. Am J Physiol Regul Integr Comp Physiol. 315(2):R312-R322.

Laudet, V. (2011) The origins and evolution of vertebrate metamorphosis. Curr Biol 21: R726–R737.

Laurent, P. and Perry, S.F. (1990) Effects of cortisol on gill chloride cell morphology and ionic uptake in the freshwater trout, Salmo gairdneri. Cell Tissue Res. 259: 429–442.

Madsen, S. S., and Korsgaard, B. (1989). Time course effects of repetitive estradiol-17 and thyroxine injections on the natural spring molting of Atlantic salmon, *Salmo salar L*. J Fish Biol. 35: 119–128.

Madsen, S. S. (1990) Effect of repetitive cortisol and thyroxine injections on chloride cell number and Na^+-K^+-ATPase activity in gills of freshwater acclimated rainbow trout, *Salmo gairdneri*. Comp Biochem Physiol 95A: 171–175.

Marshall, W. S. and Grosell, M. (2006). Ion transport, osmoregulation and acid-base balance. In: The Physiology of Fishes 3rd Ed. (eds. D. H. Evans and J. B. Claiborne), pp. 177-230. Boca Raton FL: CRC Press.

Marshall, W.S., Breves, J.P., Doohan, E.M., et al. (2018) Claudin-10 Isoform Expression and Cation Selectivity Change With Salinity in Salt-Secreting Epithelia of *Fundulus heteroclitus*. J Exp Biol 221(1): jeb168906.

McCormick, S.D. et al. (1987) Photoperiod Control of Parr–Smolt Transformation in Atlantic Salmon (*Salmo salar*): Changes in salinity tolerance, gill Na+,K+-ATPase activity, and plasma thyroid hormones. Can J Fish Aquat Sci 44(8): pp. 1462-1468.

McCormick, S.D. (2001) Endocrine control of osmoregulation in teleost fish. Am Zool 41: 781–794.

McCormick, S.D. et al. (2007) Differential hormonal responses of Atlantic salmon parr and smolt to increased daylength: A possible developmental basis for smelting. Aquaculture 273 pp. 337–344.

McCormick, S.D.,Regish, A.M., and Christensen, A.K. (2009) Distinct freshwater and seawater isoforms of Na+/K+-ATPase in gill chloride cells of Atlantic salmon. J Exp Biol 212(24): 3994-4001.

McCormick, S.D., Farrell, A.P., Brauner, A.J. ed. (2013) Fish Physiology: Euryhaline Fishes. Academic Press, USA.

Miwa, S., et al (1988) Thyroxine surge in metamorphosing flounder larvae. Gen Comp Endocr 70: pp. 158-163.

Mullur, R., Liu, Y.Y., Brent, G.A. (2014) Thyroid hormone regulation of metabolism. Physiol Rev 94: 355–382.

Norris, D.O., and Carr, J.A. (2013) Vertebrate Endocrinology 5th ed. Academic Press. London, UK.

Odenwald, M.A., Choi, W., Kuo, W.T., Singh, G., Sailer, A., Wang, Y., Shen, L., Fanning, A.S. and Turner, J.R. (2018) The scaffolding protein ZO-1 coordinates actomyosin and epithelial apical specializations in vitro and in vivo. J Biol Chem 293(45):17317-17335.

Pelis, R.M., Zydlewski, J., and McCormick, S.D. (2001). Gill Na^+-K^+-$2Cl^-$ cotransporter abundance and location in Atlantic salmon: effects of seawater and smolting. Am J Physiol Reg Integr C 280:R1844 -R1852.

Perry, S. F. (1997). The chloride cell: structure and function in the gills of freshwater fishes. Annu Rev Physiol 59: 325-347.

Power, D.M., Llewellyn, L., Faustino, M., et al. (2001) Thyroid hormones in growth and development of fish. Comp Biochem Phys C 130(4): 447 – 459.

Richards, J.G., Semple, J.W., Bystriansky, J.S. et al. (2003) Na+/K+-ATPase alpha-isoform switching in gills of rainbow trout (*Oncorhynchus mykiss*) during salinity transfer. J Exp Biol 206(24): 4475-4486.

Qureshi, T.A., Sultan, R. (1976) Thyroid follicles in the head-kidney of teleosts. Anat Anz 139(4): pp. 332-336.

Sandbichler, A.M., Egg, M., Schwerte, T., et al. (2011) Claudin 28b and F-actin Are Involved in Rainbow Trout Gill Pavement Cell Tight Junction Remodeling Under Osmotic Stress. J Exp Biol 214(9): 1473-1487.

Sanders, J.P., Van der Geyten, S., Kaptein, E., et al. (1999) Cloning and Characterization of Type III Iodothyronine Deiodinase from the Fish *Oreochromis niloticus.* Endocrinology 140(8): 3666-3673.

Sardet, C., Pisam, M., and Maetz, J. (1979) The surface epithelium of teleostean gish gills. J Cell Biol. 80: 96–117.

Subash Peter, M.C., Lock, R.A., and Wendelaar Bonga, S.E. (2000). Evidence for an osmoregulatory role of thyroid hormones in freshwater Mozambique tilapia. Gen Comp Endocrinol. 120: 157–167.

Tagawa, M. et al. (1990) Changes in thyroid hormone concentrations during early development and metamorphosis of the flounder *Paralichthys olivaceus.* Zool Sci 7: pp. 93-96.

Tipsmark, C. K., Kiilerich, P., Nilsen, T. O., et al. (2008). Branchial expression patterns of claudin isoforms in Atlantic salmon during seawater acclimation and smoltification. Am J Physiol Regul Integr Comp Physiol 294, R1563-R1574.

Tse, W.K.F., Au, D.W.T., Wong, C.K.C. (2007) Effect of osmotic shrinkage and hormones on the expression of Na+/H+ exchanger-1, Na+/K+/2Cl- cotransporter and Na+/K+ -ATPase in gill pavement cells of freshwater adapted Japanese eel, *Anguilla japonica*. J Exp Biol 210(12): 2113-2120.

Virtanen, E. and Soivio, A. (1985) The patterns of T3, T4, cortisol and Na+K+-ATPase during smoltification of hatchery-reared Salmo salar and comparison with wild smolts. Aquaculture 45: pp. 97-109.

Wong, C.K.C. and Chan, D.K.O. (2001) Effects of cortisol on chloride cells in the gill epithelium of Japanese eel, *Anguilla japonica*. J Endocrinol 168: 185–192.

Wood, C.M., Kelly, S.P., Zhou, B. et al. (2002) Cultured gill epithelia as models for the freshwater fish gill. BBA-Biomembranes 1566(1): 72-83.

Zadunaisky J (1984) The chloride cell: the active transport of chloride and the paracellular pathways. In *Fish Physiology*. Hoar WS and Randall DJ ed. Academic Press, New York, NY. P. 129 – 176.

Chapter 4. Mummichog Gill and Operculum Exhibit Functionally Consistent *claudin-10* Paralog Profiles and Claudin-10c Hypersaline Response

4.1. Summary

Claudin (Cldn) -10 tight junction (TJ) proteins are hypothesized to form the paracellular Na^+ secretion pathway of hyposmoregulating mummichog (*Fundulus heteroclitus*) branchial epithelia. Organ-specific expression profiles showed that only branchial organs (the gill and opercular epithelium, OE) exhibited abundant *cldn-10* paralog transcripts, which typically increased following sea water (SW) to hypersaline (2SW) challenge. Post-translational properties, protein abundance, and ionocyte localization of Cldn-10c, were then examined in gill and OE. Western blot analysis revealed two Cldn-10c immunoreactive bands in the mummichog gill and OE at ~29 kDa and ~40 kDa. The heavier protein could be eliminated by glycosidase treatment, demonstrating the novel presence of a glycosylated Cldn-10c. Protein abundance of Cldn-10c increased in gill and OE of 2SW-exposed fish. Cldn-10c localized to the sides of gill and OE ionocyte apical crypts and partially colocalized with cystic fibrosis transmembrane conductance regulator and F-actin, consistent with TJ complex localization. Cldn-10c immunofluorescence intensity increased but localization was unaltered by 2SW conditions. In support of our hypothesis, *cldn-10*/Cldn-10 TJ protein dynamics in gill and OE of mummichogs and TJ localization are functionally consistent with the creation and maintenance of salinity-responsive, cation-selective pores that facilitate Na^+ secretion in hyperosmotic environment.

4.2. Introduction

Teleost fish gill and opercular epithelium (OE) contain high densities of ionocytes that are specialized to secrete Na^+ and Cl^- into sea water and hypersaline environments (Edwards and

Marshall, 2013; Evans et al., 2005; Marshall and Grosell, 2006). For marine teleost fish, a transcellular Cl^- secretion involving basolateral Na^+, K^+, $2Cl^-$ cotransporter NKCC1, driven by the Na^+ gradient produced by basolateral Na^+,K^+-ATPase (in association with an inwardly rectifying potassium channel), causes Cl^- accumulation intracellularly such that Cl^- exit is via passive diffusion through cystic fibrosis transmembrane conductance regulator (CFTR) anion channels into a cup-shaped apical microenvironment, the ionocyte apical crypt. In parallel, a cation-selective paracellular pathway employs a transepithelial positive electrical gradient of approximately +35-40 mV (Guggino, 1980; Marshall et al., 2017) to drive Na^+ down its electrochemical gradient from blood to sea water (Degnan and Zadunaisky, 1980; Pequeux et al., 1988). Paracellular Na^+ transport occurs through single-stranded, cation-permeable ('leaky') intercellular tight junctions (TJs) that exclusively form between marine fish ionocytes and a cell that resides adjacent to the ionocyte, the accessory cell (AC) (Karnaky, 1991; Sardet et al., 1979). Although some progress has been made in terms of elucidating which specific TJ proteins establish the required cation-selective pores between ionocytes and ACs (see below), there is a great deal that remains largely unknown.

Claudin (Cldn) proteins are incorporated into intercellular tight junctions (TJs) of vertebrate epithelia where they occupy a critically important role in the regulation of TJ permselectivity (Chasiotis et al., 2012; Krug et al., 2012; Krug et al., 2014). Some of these epithelial intercellular junctions are non-selective 'leaky' junctions, whereas others are selective to certain molecular species (e.g. cations or anions) and constitute cation or anion permeable “pores” (Shen et al., 2011). Because the gill epithelium of teleost fishes changes its transport characteristics from ion uptake in fresh water (FW) to ion secretion in SW, with concomitant changes in paracellular permeability of the junctions linking ionocytes and ACs, euryhaline species have been used to study the

functional dynamics of *cldn*/Cldn responses to these changing ion transport demands (for recent reviews see Chasiotis et al., 2012; Kolosov et al., 2013).

Several lines of evidence support a model involving insertion of Cldn-10 proteins to form (or contribute to the formation of) cation-selective pores between ionocytes and ACs of SW residing fishes. These include observations of restricted organ- and cell-specific *cldn-10*/Cldn-10 paralog distribution patterns, salinity-induced alterations in sub-cellular distribution as well as changes in abundance of *cldn*-10 transcript and Cldn-10 protein paralogs following salinity transfer or hormone treatment (Bossus et al., 2015; Bui and Kelly, 2014; Bui and Kelly, 2015; Bui et al., 2010; Kolosov et al., 2014; Loh et al., 2004; Marshall et al. 2018; Tipsmark et al., 2008, 2009; Trubitt et al., 2015). However, further studies on salt secretory epithelia of euryhaline teleost fishes are needed to discover exactly which Cldns are involved and how they form cation-selective pores.

The mummichog (*Fundulus heteroclitus*) is an important model organism that has provided significant genomic and physiological insights into molecular and cellular mechanisms that underlie gill function (Burnett et al., 2007; Cozzi et al., 2015; Whitehead et al., 2011). This is partly because mummichogs naturally inhabit, and in a laboratory setting readily acclimate to, salinities ranging from FW to strongly hypersaline conditions for extended periods of time (Griffith, 1974), and also because early observations revealed that the OE of this species is an excellent surrogate gill model that can be used for studies that are not possible to conduct using the architecturally complex gill itself (Degnan et al. 1977; Degnan and Zadunaisky 1980; Karnaky 1991, review Marshall and Grosell 2006). In addition, this species exhibits consistent differential regulation of transcripts encoding TJ proteins upon exposure to different salinities and diversifying selection between TJ protein transcripts in populations inhabiting different osmotic environments (see Reid et al 2017). Therefore, the mummichog is a robust model for examining TJ modifications

in response to salinity stress. To this end, we have recently examined *cldn-10c, -10d, -10e* and *-10f* mRNA abundance in mummichog gill following acclimation to increased salinity and described cation selectivity of the branchial salt secretory pore using the OE (Marshall et al., 2018). It was found that following acclimation of mummichogs from FW to SW, increased transcript abundance of *cldn-10d* and *-10e* occurred in the gill, and this was in line with salinity-induced changes of *cldn-10* paralogs in the gill tissues of other euryhaline fish species (see Marshall et al., 2018). A particularly novel observation was that acclimation of mummichogs to hypersaline conditions (i.e. from SW to 2SW) produced enhanced salt secretory activity of branchial trans- and paracellular pathways as well as a significant and sustained increase in the mRNA abundance of select *cldn-10* paralogs that had not been responsive to SW acclimation, i.e. *cldn-10c,* and *-10f* (Marshall et al., 2018). It has been reported that hypersaline stress causes further elaboration of TJ structure and enhanced ionic conductance (Cozzi et al., 2015) such that, even with a reduced transepithelial electromotive driving force, NaCl secretion can continue. Therefore our previous work suggests that *cldn-10* paralogs in the branchial tissues of mummichogs may exhibit a functionally tiered response to elevated environmental ion levels that is dictated by how high the salinity becomes. This would make physiological sense for an organism that, under normal circumstances, will experience tidal-driven fluctuations in the salt content of its surroundings that would range between FW above and SW below a halocline, but could also find itself isolated in an evaporating finite body of water (e.g. a tide pool) where salinity can often exceed that of SW.

The aforementioned observations provide an impetus to enhance our understanding of Cldn-10 TJ proteins in the mummichog, with an emphasis on several areas. First, despite the broadly acknowledged suitability of the OE as an appropriate surrogate gill model to study mechanisms of ion transport across the SW fish gill, no study has profiled and examined TJ

proteins in the OE. The OE is a flat epithelial sheet on the underside of bony opercula that cover the branchial cavity of fishes, but it is not part of the gill *per se*. Therefore, despite possessing ion transport characteristics and a cellular composition which mimics the gill, the OE could be viewed as skin, and the skin of fishes possesses a different TJ protein profile than the gill (see Kolosov et al., 2013). Therefore, the molecular physiology of OE TJs should be examined to show that they contribute to salt secretion using the same TJ proteins as the gill epithelium. Next, observations of mummichog gill and OE Cldn-10 TJ proteins should extend beyond the transcriptional level and include studies that examine changes in protein abundance as well as investigate protein localization in both the gill and OE. To address these gaps in our knowledge, the current work detailed *cldn-10* paralog expression profiles across organs of the mummichog and compared organ-specific *cldn-10* paralog mRNA abundance following acclimation of fish from SW to 2SW. Based on our observations, a custom synthesized antibody for mummichog Cldn-10c was produced to provide evidence of TJ formation and function in gill and OE. We examined Cldn-10c (1) post-translational characteristics, particularly O-glycosylation of the protein associated with TJ formation and function, (2) protein abundance in response to hypersaline (2SW) conditions, and (3) immunolocalization with reference to a transcellular ion transport protein (i.e. CFTR), that is associated with 'leaky' cation-permeable TJs, as well as actin (JLA20).

4.3. Materials and Methods

4.3.1. Animals

Adult mummichogs (*Fundulus heteroclitus* Linnaeus, 1766) of both sexes (7-15 g mass) were trapped in Ogdens Pond, Antigonish County, Nova Scotia, Canada in June and transported in coolers containing estuary water to the St. Francis Xavier University Animal Care Facility. The

fish were placed in full strength SW (32‰) in 450 L recirculating tanks at room temperature (20 ± 1ºC) under 12L:12D photoperiod under artificial lighting and were held for several weeks prior to experimentation. Salinity was monitored daily using a YSI Pro2030 (YSI Inc., Yellow Springs, OH, USA) conductivity meter; partial water exchanges were performed at the rate of 1/3 aquarium volume (same salinity and temperature) per 48 h period. For acclimation to hypersaline conditions, thirty fish were exposed to a flow-through salinity change, first to 45‰ SW for 48 h, then to 60‰ SW (2SW) for 6 days (following which samples were collected for RNA and protein isolation) and at days 11, 17 and 25 samples were collected for immunohistochemistry; SW was made hypersaline by addition of artificial sea salt (Instant Ocean, Blacksburg VA, USA). For acclimation to FW, fish were directly transferred to dechlorinated Antigonish tap water (0.1 mM NaCl, pH 6.7-6.9) for at least 10 days before use in immunofluorescence experiments. Fish were fed mealworms (*Tenebrio molitor*) three days a week and Nutrafin flakes (R.C. Hagen, Montreal, Quebec, Canada) twice daily, so that each fish consumed 1.0 g of food per 100 g of body weight per day. Fish were euthanized by single pithing followed by decapitation. For organ/tissue-specific profiling of *cldn-10* paralogs, brain, eye, gill, OE, heart, liver, kidney, posterior intestine (i.e. last third of total intestine length), skin (general body surface) and flank muscle were rapidly dissected, flash frozen in liquid N_2 and stored at -80ºC until further analysis. For immunohistochemistry, OE and gill filaments were dissected in and/or rinsed with modified Cortland's saline (composition in mmol l^{-1}: NaCl 159.9, KCl 2.55, $CaCl_2$ 1.56, $MgSO_4$ 0.93, NaH_2PO_4 2.97, $NaHCO_3$ 17.85, and glucose 5.55, bubbled with a 99% O_2/1.0% CO_2 gas mixture, pH 7.7-7.8, osmolality 317 mOsm kg^{-1}) prior to further processing and fixation (see below). Animal care and treatment occurred under approval 16-003-R2 by St. Francis Xavier University Animal Care Committee, following Canadian Council on Animal Care guidelines.

4.3.2. Total RNA Isolation and Quantitative Real-Time PCR Analyses

Samples for gene transcript expression profiles were homogenized in TRIzol reagent (Invitrogen Canada Inc., Burlington, ON, Canada) for total RNA isolation according to manufacturer's protocol. RNA pellets were resuspended in an appropriate volume of RNase-free water and quantified using a Nanodrop 2000 spectrophotometer (Thermo Fisher Scientific, Waltham, MA, USA) with sample quality determined by A260/A280 ratio. A fixed quantity of total RNA from each sample (2 μg) was treated with DNase I (Amplification Grade; Invitrogen Canada Inc.). First-strand synthesis was then carried out using SuperScript III^{TM} reverse transcriptase and Oligo $(dT)_{12-18}$ primers (Invitrogen Canada Inc.).

Quantitative-PCR (qPCR) experiments were carried out using iQ SYBR Green Supermix (Bio-Rad Laboratories, Inc., Mississauga, ON) in a CFX-96 Real-time System (Bio-Rad, Hercules, CA, USA) under the following conditions: 95 °C for 10 min, 40 cycles of 95°C for 30 s, 60°C for 60 s, read every cycle, 59°C to 95°C for melt curve, read every 0.5°C. PCR primers for *cldns-10c*, *-10d*, *-10e*, *-10f*, *cftr, and 18S RNA* were as previously described by Marshall et al. (2018). Standard curves were generated with stock mummichog gill cDNA in each qPCR assay as an internal control of each qPCR run. *18S RNA* was used as a reference gene and prior to analysis, *18S RNA* usage was validated statistically by comparing raw *Cq* values between organs/treatments to ensure no statistically significant changes occurred (P=0.882). Primer efficiency values averaged at 91.6% with specific values as follows; *18S* = 83.6%, *cldn-10c* = 83.52%, *cldn-10d* = 96.6%, *cldn-10e* = 105.5%, *cldn-10f* = 90.4%, and *cftr* = 90.0%. Transcript abundance calculations were as reported by Marshall et al. (2018). Organ-specific transcript abundance of *cldn-10s* and *cftr* are reported using *18S RNA* as a reference gene and expressed as fold change relative to levels in the SW fish gill. Transcript abundance of *cldn-10s* and *cftr* in gill, OE and skin following 2SW

acclimation are reported using *18S RNA* as a reference gene and for each organ, are expressed as fold change relative to SW levels.

4.3.3. Antibodies

The primary antibody used for detection of mummichog CFTR was mouse monoclonal anti-human CFTR (MAB25031, clone 24-1, R&D Systems, Minneapolis, USA) with the epitope at the carboxy terminus, a zone that is conserved in mummichog to human (Singer et al., 1998, 2008) and therefore is selective for this protein (Marshall et al., 2002). Custom synthesized anti-*F. heteroclitus* Cldn-10c affinity purified rabbit polyclonal antibody (developed by GenScript USA Inc, Piscataway, NJ, USA) was used for detection of mummichog Cldn-10c carboxy terminus; the immunogen sequence was: CISNTTRKTASNVYV. Cldn-10c was selected for antibody development because this paralog exhibited increased transcript abundance in gill tissue following acclimation from SW to hypersaline conditions (Marshall et al., 2018). F-actin immunofluorescence was detected using JLA20 mouse monoclonal antibody (Marshall et al., 2017) and α-5 mouse monoclonal antibody to the alpha (catalytic) subunit of chicken Na^+,K^+-ATPase, all three of which were obtained from Developmental Studies Hybridoma Bank (DSHB, University of Iowa, Iowa City, USA). Secondary antibodies used for immunofluorescence microscopy were goat anti-rabbit polyclonal immunoglobulin-G conjugated with Alexa Fluor 488 (A11001, Life Technologies Inc., Eugene, OR, USA) and goat anti-rabbit polyclonal immunoglobulin-G conjugated with DyLight 549 (111-505-003, Jackson ImmunoResearch Laboratories Inc., West Grove, PA, USA).

4.3.4. Immunoblots

Protein samples for immunoblotting of Cldn-10c were prepared from the phenol-ethanol fraction of the total RNA isolation solution according to manufacturer's protocol. The fractions were first washed with anhydrous ethanol to remove remaining nucleic acids in the solution, and protein samples were precipitated with 100% isopropanol followed by three washes (20 min each) in 0.3 M guanidine hydrochloride dissolved in 95% ethanol. Protein pellets were then washed once (20 min) with anhydrous ethanol prior to resuspension in 1% sodium dodecyl sulfate (1% SDS). Protein concentration of each sample was determined using a Micro bicinchoninic (BCA) Protein Assay Kit (Thermo Scientific, Rockford, IL) according to the manufacturer's instructions for the Microplate Procedure and samples were read using a Multiskan spectrophotometer (Thermo Fisher Scientific, Nepean, ON). For protein separation, tricine-SDS-PAGE electrophoresis was carried out with a 4% stacking gel and 10% separating gel in a Mini-PROTEAN Tetra Cell apparatus (Bio-Rad Laboratories, Inc.) with a Tris-Tricine buffer (25 mM Tris, 25 mM Tricine, 0.05% (w/v) SDS; Bioshop Canada, Burlington, ON). Identical amount of protein samples were treated with a sample buffer (Tris 60 mM; SDS 2%; glycerol 10%; Bromophenol Blue 0.0025%; 3% β-mercaptoethanol), heated (70°C, 15 min), and allowed to migrate at a constant voltage of 150 V.

Protein samples were blotted onto a PVDF membrane (0.45 μm pore size; Merck Millipore) with a chilled wet-transfer unit (Amersham Biosciences; 150 mA; 80 mins). After transfer, membranes were briefly rinsed in Tris-buffered saline with 0.1% Tween-20 (TBS-T; 20 mM Tris, 150 mM NaCl, pH 7.6) and blocked with a blocking solution (immunoblot blocking solution; 5% skim milk in TBS-T adjusted to 250 mM NaCl) for 1 h at room temperature. The membrane was then incubated at 4°C with Cldn-10c primary antibody solution (0.75 μg Cldn-10c primary antibody /mL immunoblot blocking solution) overnight. Immunogen peptide blocking was

performed by pre-incubating the Cldn-10c primary with peptide immunogen (1.5 μg Cldn-10c peptide immunogen/mL Cldn-10c primary antibody solution) overnight. An HRP conjugate secondary antibody (goat anti-rabbit; Bio-Rad Laboratories, Hercules, CA) and an ECL substrate (Pierce Biotechnology, Rockford, IL) were used for detection of Cldn-10c on PVDF membranes. Blots were imaged using DiaFilm Autoradiography Film (Diamed Lab Supplies Inc, Mississauga, ON) and digitized prior to densitometry analysis in Image Lab 6.0 software (Ver. 6.0.0 build 26; Bio-Rad Laboratories, Inc., Hercules, CA, USA). Blots were then treated with an acid stripping buffer and reprobed with an internal loading control (F-actin, JLA20, DHSB).

4.3.5. Deglycosylation of Cldn-10c

Deglycosylation of gill and OE protein samples was carried out with an Enzymatic Protein Deglycosylation Kit (EDEGLY, Millipore-Sigma). Protein samples from the gill and OE (100 μg in each case) were denatured (100°C, 5 min) and cooled to room temperature prior to addition of deglycosylation enzymes including PNGase F, O-Glycosidase, α-2(3,6,8,9)-Neuraminidase, β-1→4-Galactosidase, and β-N-Acetylglucosaminidase. The reaction mixture was incubated in a 37°C water bath for 6 h. Samples were used immediately for immunoblots after incubation. A negative-control experiment was performed to verify the deglycosylation kit buffer and detergent components have minimal effect on the mobility shift and intensity of the bands in the gill and OE samples.

4.3.6. OE Immunohistochemistry

OE from FW, SW and 2SW acclimated fish were dissected in Cortland's saline, excluding the underlying dermal chromatophore layers and whole mounts pinned to modeler's sheet wax (700-079, Rio Grande, Albuquerque, NM, USA). Preparations were rinsed three times in rinsing

buffer (TPBS) comprising 0.1% bovine serum albumin (BSA) with 0.05% Tween 20 in phosphate-buffered saline (PBS, composition in mmol l^{-1}: NaCl 137, KCl 2.7, Na_2HPO_4 4.3, and KH_2PO_4 1.4 at pH 7.4). OE were fixed for 2 h at −20°C in 80% methanol/20% dimethyl sulfoxide (DMSO), then rinsed in TPBS and immersed in a blocking solution (immunohistochemistry blocking solution) made with 5% normal goat serum, 0.1% BSA, 0.2% NaN_3 in TPBS, pH 7.4 for 1 h at 24ºC in the dark. The OE were then incubated in the primary antibodies Cldn-10c andJLA20 or CFTR (8 µg ml^{-1} in immunohistochemistry blocking solution) at 4°C overnight. Following three (5 min) rinses in PBS, the OE were exposed to the secondary antibodies (8 µg ml^{-1} in immunohistochemistry blocking solution) for 4 h at room temperature in the dark. After three final rinses in PBS, the OE were covered in a mounting medium (Fluoroshield™, Sigma-Aldrich, St. Louis, MO, USA) and slides were viewed in a single blind fashion. Negative controls were performed by immunogen peptide blocking; Cldn-10c immunogen peptide was pre-incubated with the primary antibody in immunohistochemistry blocking solution, then added to the OE. Subsequent handling of negative controls was performed identically as above. Images were collected with a laser scanning confocal microscope (FV300, Olympus, Markham, ON, Canada). In each OE, fields were randomly selected and *z*-stack series were collected using a 40X water (N.A. 1.15W) or 60X water objective (N.A. 1.20W), zoom of 3.0 and XYZ optical sections at increments of 0.50 µm (Marshall et al., 2017).

4.3.7. Gill Histology and Immunohistochemistry

Gill arches from SW fish were dissected, rinsed with Cortland's saline and fixed in 4% paraformaldehyde (PFA) pH 7.4, at 4 °C for 24 h. Fixation in 4% PFA provides mechanical support during vibratome sectioning. Following fixation, the gills were rinsed three times in phosphate-buffered saline (PBS; composition in mmol l^{-1}: NaCl 137, KCl 2.7, Na_2HPO_4 4.3, KH_2PO_4 1.4,

pH 7.4). The gill filaments were removed and embedded in 3% w/v agarose in PBS and allowed to set for 20 min at 4 °C. Filaments were sectioned by vibratome (Vibratome® Series 1000, Technical Products International, Inc., St. Louis, MO, USA) into 200 μm thick cross-sections and longitudinal sections (Barnes et al. 2014). The sections were immersed in immunohistochemistry blocking solution for 1 h at 24 ºC (in the dark) then incubated with primary antibodies (8 μg ml^{-1}), anti-CFTR and anti-Cldn-10c, in immunohistochemistry blocking solution overnight at 4 °C. Sections were then rinsed three times in TPBS rinsing buffer and exposed to the secondary antibody goat anti-mouse IgG complexed with Alexa Fluor 488 (8 μg ml^{-1}, Life Technologies Inc., Eugene, OR, USA) and goat anti-rabbit IgG DyLight 549 (8 μg ml^{-1}, Vector Laboratories, Burlingame, CA, USA) in immunohistochemistry blocking solution for 4 h at 24 C (in the dark). After three final rinses in TPBS rinsing buffer the sections were mounted in histology mounting medium (Fluoroshield™, Sigma-Aldrich). Negative (null) controls were performed by omitting the primary antibodies. Slides were viewed and images were collected with a laser scanning confocal microscope (FV300, Olympus). Optical section stacks were collected for final figures.

4.3.8. Statistics

All data are expressed as mean ± s.e.m. (n) where n represents the number of fish within the group. A Student's *t*-test was used to evaluate the effect of salinity on a target organ. Significant differences ($P<0.05$) are denoted with an asterisk (*). Ionocyte cell volume was calculated as oblate ellipsoids from XYZ confocal scans, n = 100 cells from 10 XYZ images, n = 4 animals per group, and statistical differences detected using unpaired two-tailed *t*-tests. All statistical analyses were performed using SigmaPlot for Windows Version 14.0 (Build 14.0.3.192; Systat Software, Inc., San Jose, CA, USA).

4.4. Chapter 4 Figures

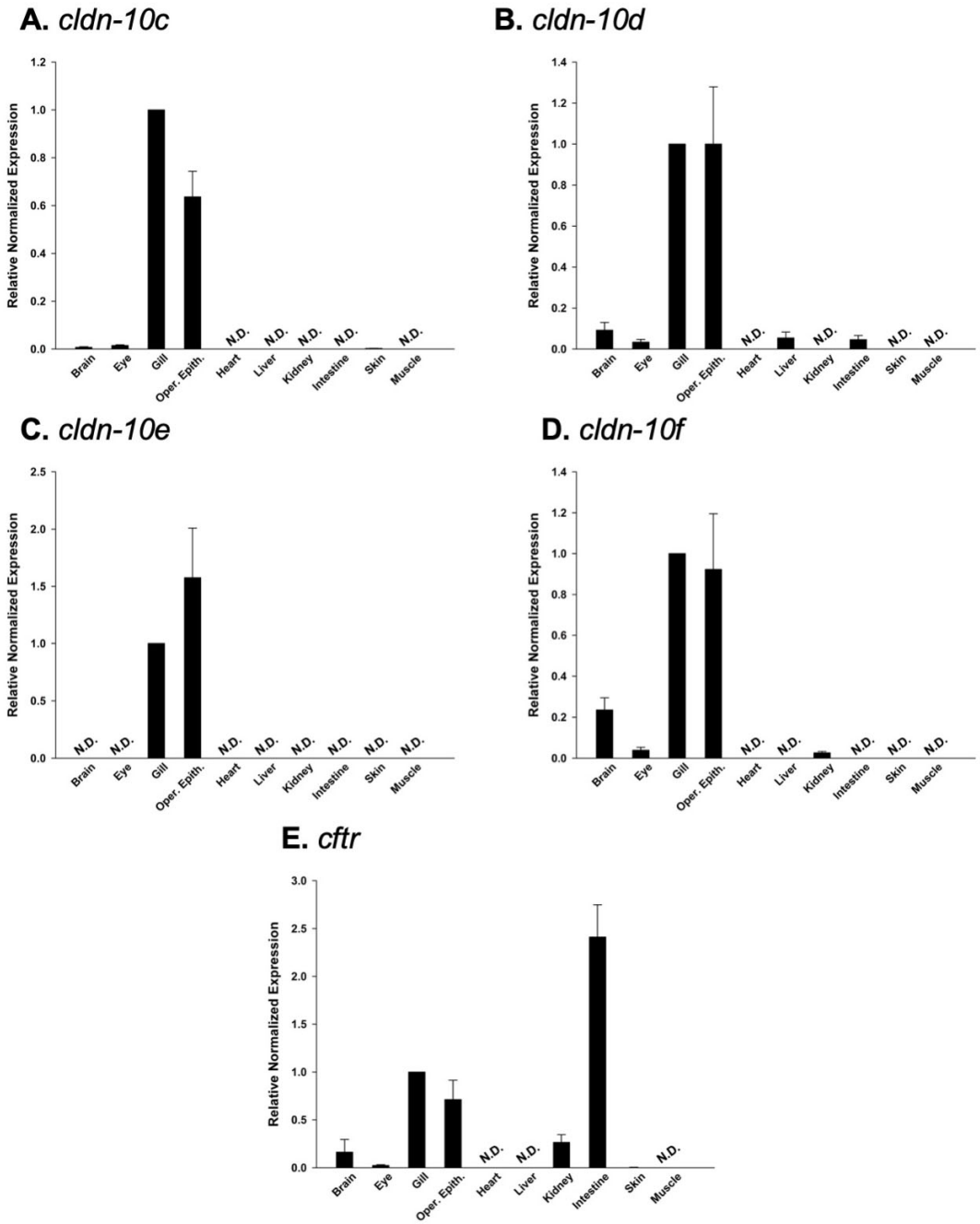

Figure 4-1. Organ-specific expression of claudin (*cldn*) (A) -*10c*, (B) -*10d*, (C) -*10e*, (D) -*10f*, and (E) cystic fibrosis transmembrane conductance regulator (*cftr*) in adult mummichogs acclimated to seawater. Transcript abundance was normalized using 18S RNA and expressed relative to the gill (assigned a value of 1.0) as a reference organ. All data expressed as mean values ±s.e.m. (n=5). N.D. = transcript not detected.

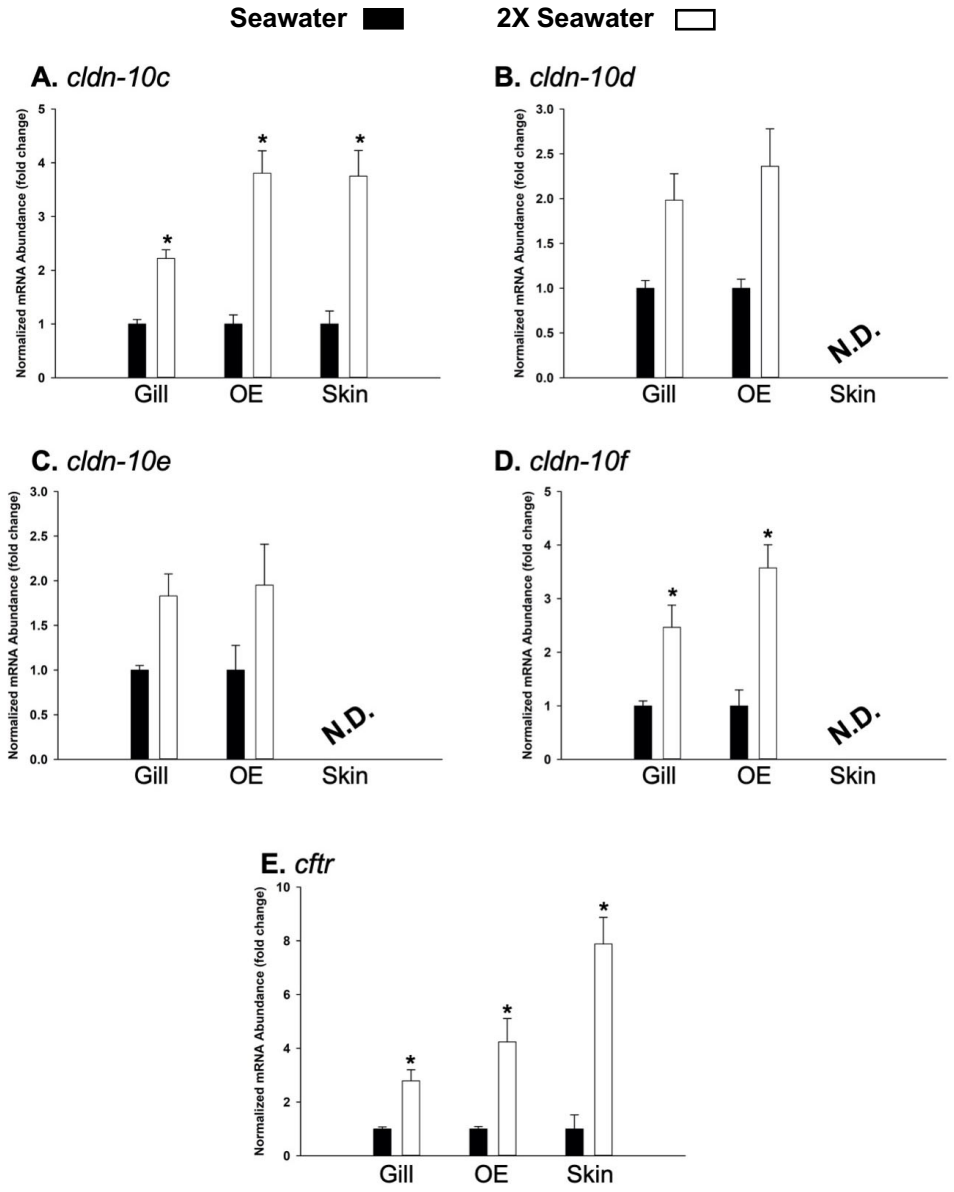

Figure 4-2. Transcript abundance of claudin (*cldn*) (A) -*10c*, (B) -*10d*, (C) -*10e*, (D) -*10f*, and (E) cystic fibrosis transmembrane conductance regulator (*cftr*) in mummichog gill, opercular epithelium (OE), and skin following acclimation of animals from seawater (SW; black bars) to hypersaline conditions (2SW; open bars). Transcript abundance was normalized using 18S RNA in the target tissue and 2SW transcript abundance in each organ was expressed relative SW assigned a value of 1. All data are expressed as mean values ±s.e.m. (n=5). An asterisk (*) denotes a significant difference between the SW and 2SW group as determined using a Student's t-test ($P \leq 0.05$). N.D. = transcript not detected.

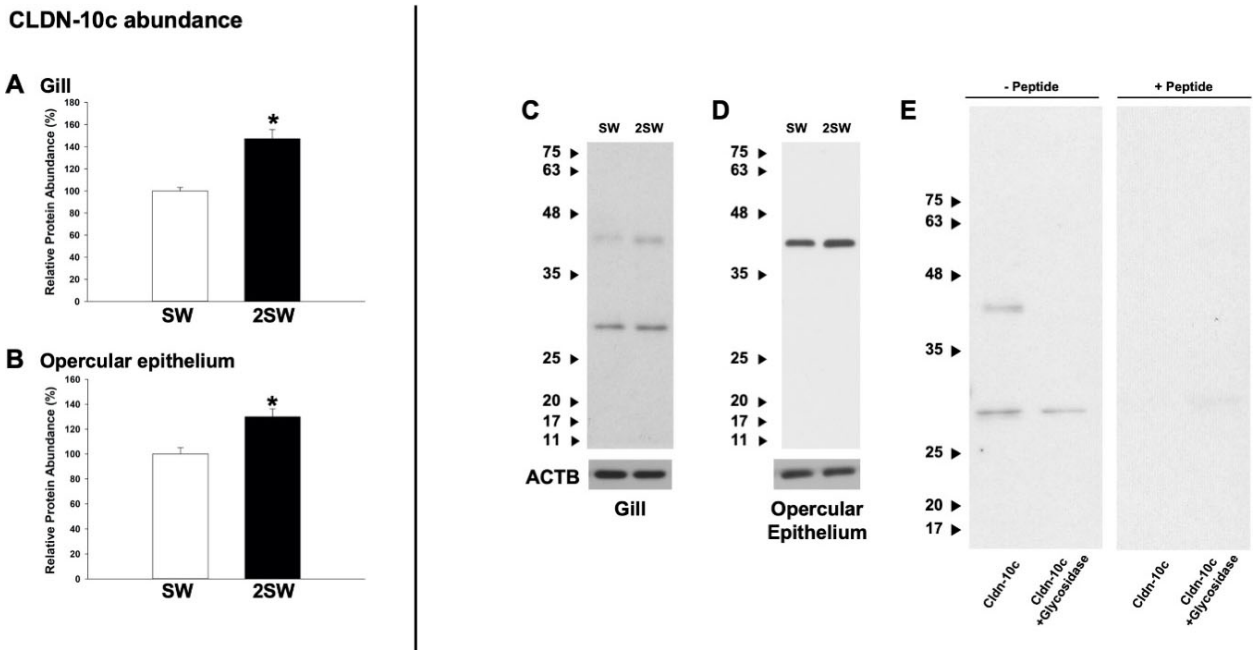

Figure 4-3. Protein abundance of claudin-10c (Cldn-10c) in (A) gill and (B) opercular epithelium of mummichogs acclimated to seawater (SW) or hypersaline (2SW) conditions. Panel (C) shows a Cldn-10c immunoblot using gill from SW and 2SW fish where two distinct bands at ~29 and ~40 kDa are apparent. In panel (D), the opercular epithelium (OE) reveals a singular ~40 kDa band. Panel (E) reveals that glycosidase treatment of gill samples results in the disappearance of the ~40 kDa immunoreactive band, and peptide blocking assay (+Peptide) results in an absence of anti-Cldn-10c immunoreactivity. Data in panels (A) and (B) are expressed as mean values ±s.e.m. (n=5). An asterisk (*) denotes a significant difference between the SW and 2SW group as determined using a Student's t-test ($P \leq 0.05$). ACTB = actin.

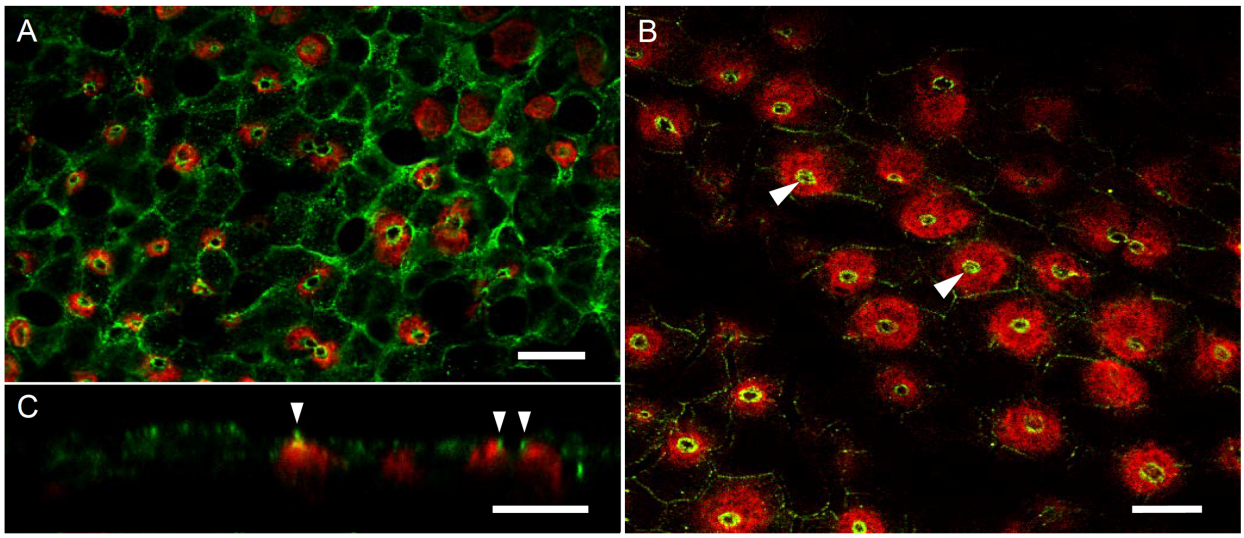

Figure 4-4. Immunohistochemistry of mummichog Cldn-10c (green) and Na^+,K^+-ATPase (red) in ionocytes of opercular epithelium from mummichogs acclimated to seawater (A; n =10) and hypersaline (2SW, B; n = 4). A) XY scan at the level of ionocyte apical crypts with ring-like Cldn-10c fluorescence around ionocyte crypt and some fluorescence in tight junctions between pavement cells. B) XY scan at the same level as (A) with intense fluorescent rings (arrowheads) in ionocyte crypts and enlarged hyperplastic cells. Panel (C) shows an XZ focal plane. Scale bars = 10 µm.

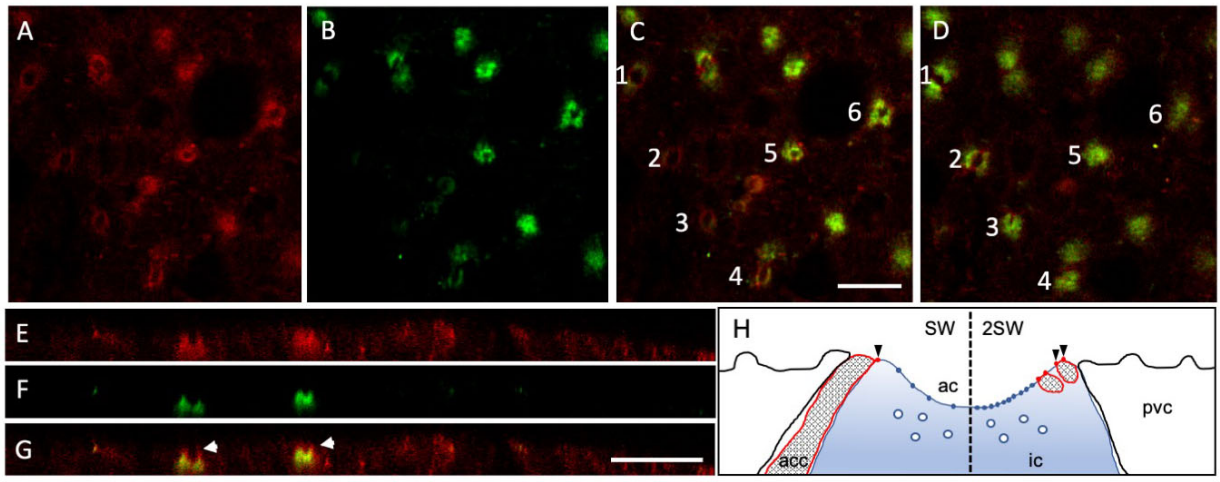

Figure 4-5. (Caption on next page)

Figure 4-5. Seawater opercular epithelium ionocytes A) Red: Cldn-10c, B) Green: CFTR anion channels. C) merged signals; near the surface of the epithelium with red rings apparent in superficial cells (cells 1, 2, 3 and 4) but in slightly deeper sections (cells 5 and 6) rings stain for CFTR also, yielding colocalization. D) Same frame and cells but 2 µm deeper: note that in cells 1, 2, 3 and 4, Cldn-10c is colocalized with CFTR and that cells 5 and 6 have closed appearance CFTR (indicating the bottom of the cup-shaped apical crypt) and no red stain. E) F) and G) are XZ scans through ionocytes E) Cldn-10c F) CFTR and G) Merge. Note that Cldn-10c immunofluorescence extends above the zone of colocalization with CFTR, arrow heads. n=10. Scale bars = 10 µm. Panel H) is a summary illustration of apical portion and apical crypt (ac) of an ionocyte (ic) with pavement cells (pvc), accessory cell (acc) as well as acc processes with Cldn-10c pores (red dots and arrowheads) positioned somewhat above the apical membrane-resident CFTR anion channels (blue dots), with more of the acc processes, Cldn pores and CFTR channels in 2SW (right), compared to SW control conditions (left). Sub-apical vesicles (white circles in ionocyte sub-apical region, commonly seen in TEM) are the presumed location of sub-apical CFTR.

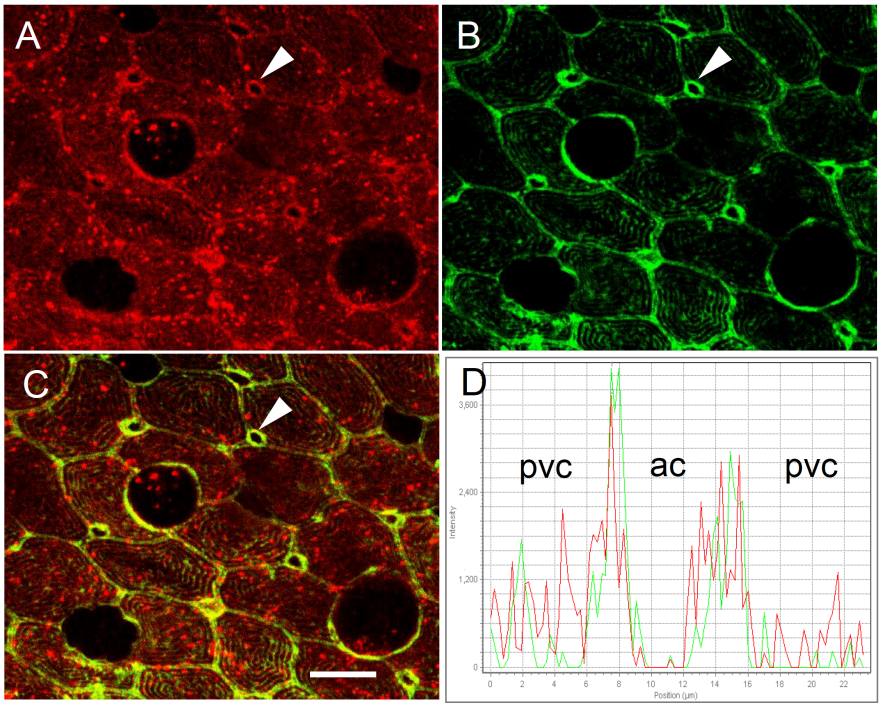

Figure 4-6. (Caption on next page)

Figure 4-6. Immunohistochemistry of ionocytes in opercular epithelium of SW mummichog showing distribution of Cldn-10c and JLA20 (F-actin), Cldn-10c (A; red) and actin (B; green) are localized in the apical crypts of ionocytes (white arrowheads highlight one of seven ionocytes in the images) and in the pavement cells. C) Actin colocalizes with Cldn-10c in the apical crypt of ionocytes and in the TJs of the pavement cells (yellow in merged image; N = 6). D) A line scan across an apical crypt shows both green and red fluorescence overlapping at the edges of the apical crypt. Scale bar: 10µm.

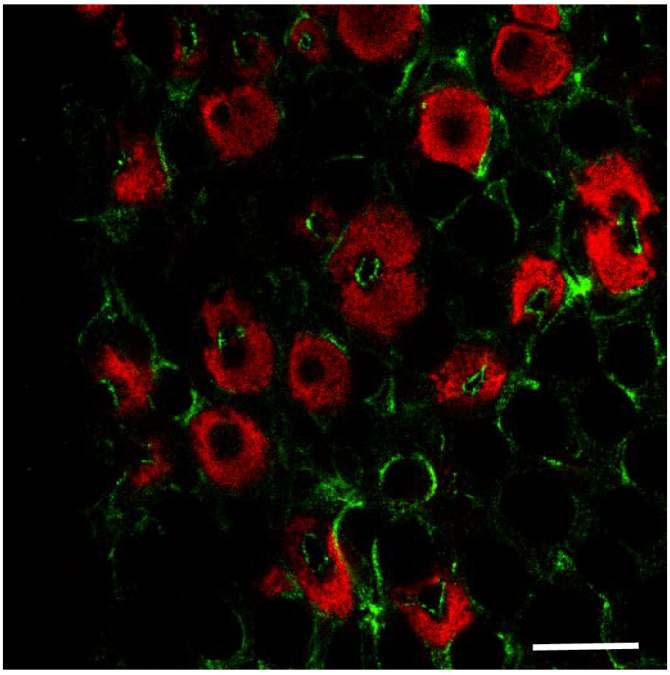

Figure 4-7. Cldn-10c immunofluorescence in freshwater (FW) acclimated mummichog opercular epithelium ionocytes (n=4 animals). Green is anti-Cldn-10c; Red is α-5 anti Na^+, K^+-ATPase. Image was collected 10 µm below the surface of the epithelium, showing some unexposed ionocytes with Cldn immunofluorescence and pairs of enlarged ionocytes. There was no positive Cldn immunofluorescence at the plane of the surface of the epithelium. Scale bar = 20 µm.

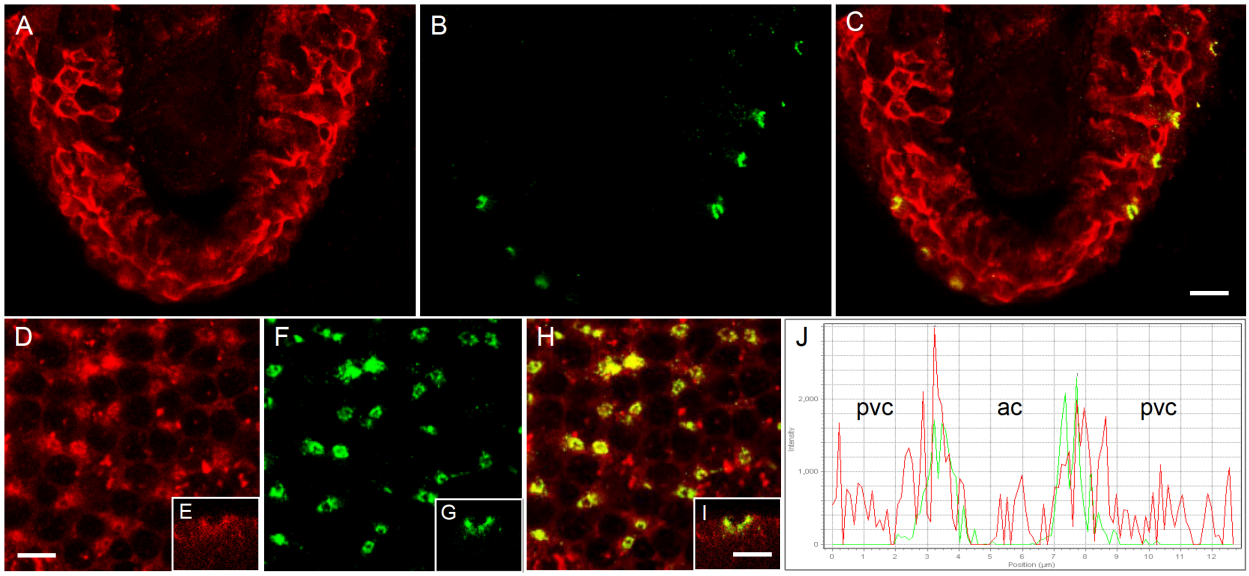

Figure 4-8. Immunohistochemistry of SW mummichog gill cross-sections (A-C) and longitudinal sections across the surface of the posterior gill filament (D-I) showing the distribution of Cldn-10c and CFTR anion channels. (A) Cldn-10c (red) is localized to the margins of the apical crypt (ac) of ionocytes and to a lesser extent in the pavement cells (pvc). (B) CFTR (green) is localized solely across the apical crypts of ionocytes. (C) Colocalization of Cldn-10c and CFTR in the apical crypt of ionocytes (yellow). In the longitudinal gill sections, Cldn-10c (D, XZ side view E) and CFTR (F, XZ side view G) colocalize in the apical crypt (H, I XZ side view) shown here by the overlapping red and green fluorescence in the line scan graph (J). (n=6) ac: apical crypt, pvc: pavement cells. Scale bar: 10 µm for A, B, C, F, H. Scale bar: 5µm for E, G, I.

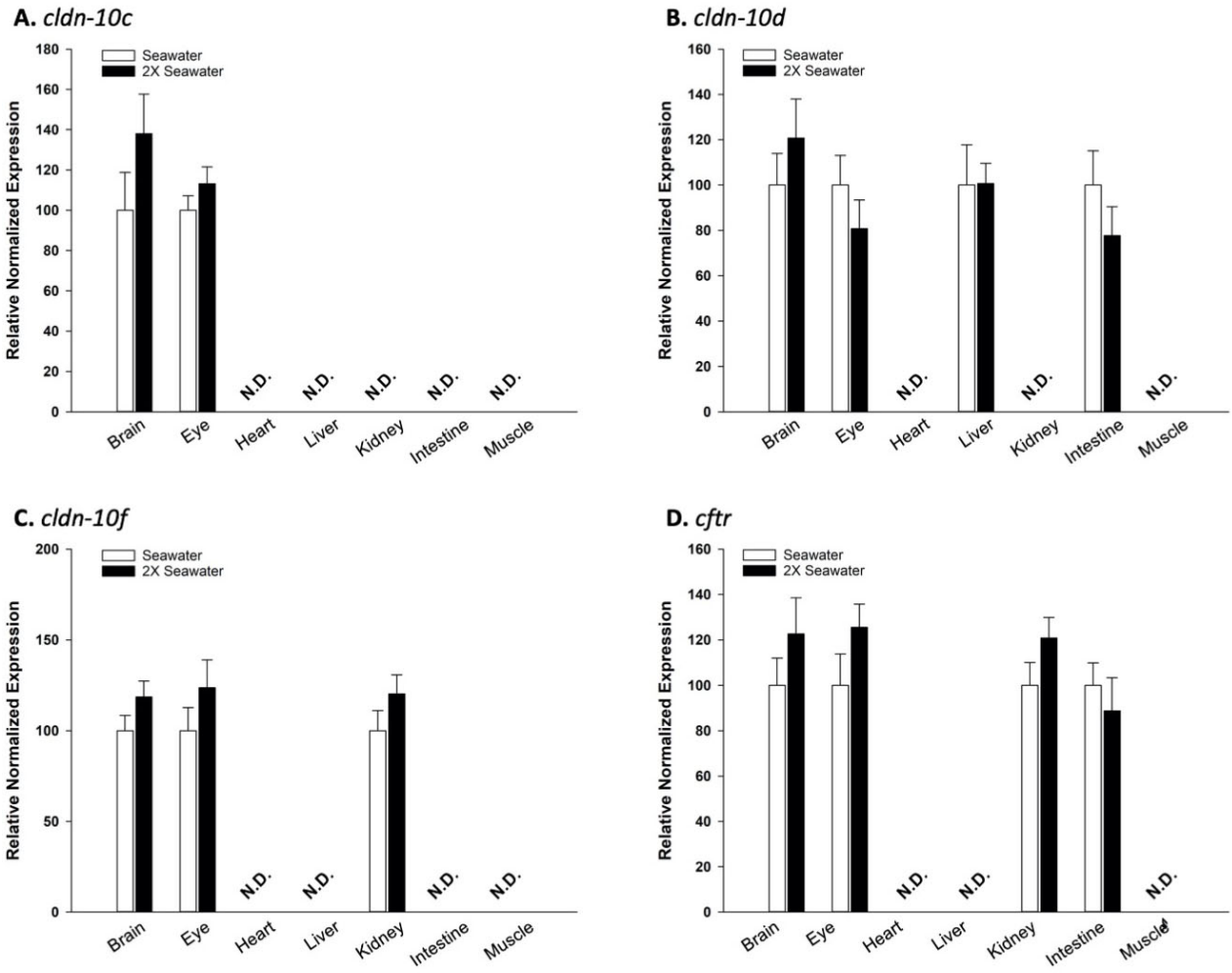

Supplemental Figure 4-1. Transcript abundance of claudin (*cldn*) (A) -*10c*, (B) -*10d*, (C) -*10f*, and (D) cystic fibrosis transmembrane conductance regulator (*cftr*) in mummichog brain, eye, heart, liver, kidney, intestine, and muscle following acclimation of animals from seawater (SW; open bars) to hypersaline conditions (2SW; black bars). Transcript abundance was normalized using 18S RNA in the target tissue and 2SW transcript abundance in each organ was expressed relative SW assigned a value of 100. All data are expressed as mean values ±s.e.m. (n=5). No significant difference between the SW and 2SW group was found in any organ using a Student's t-test ($P \leq 0.05$). N.D. = transcript not detected.

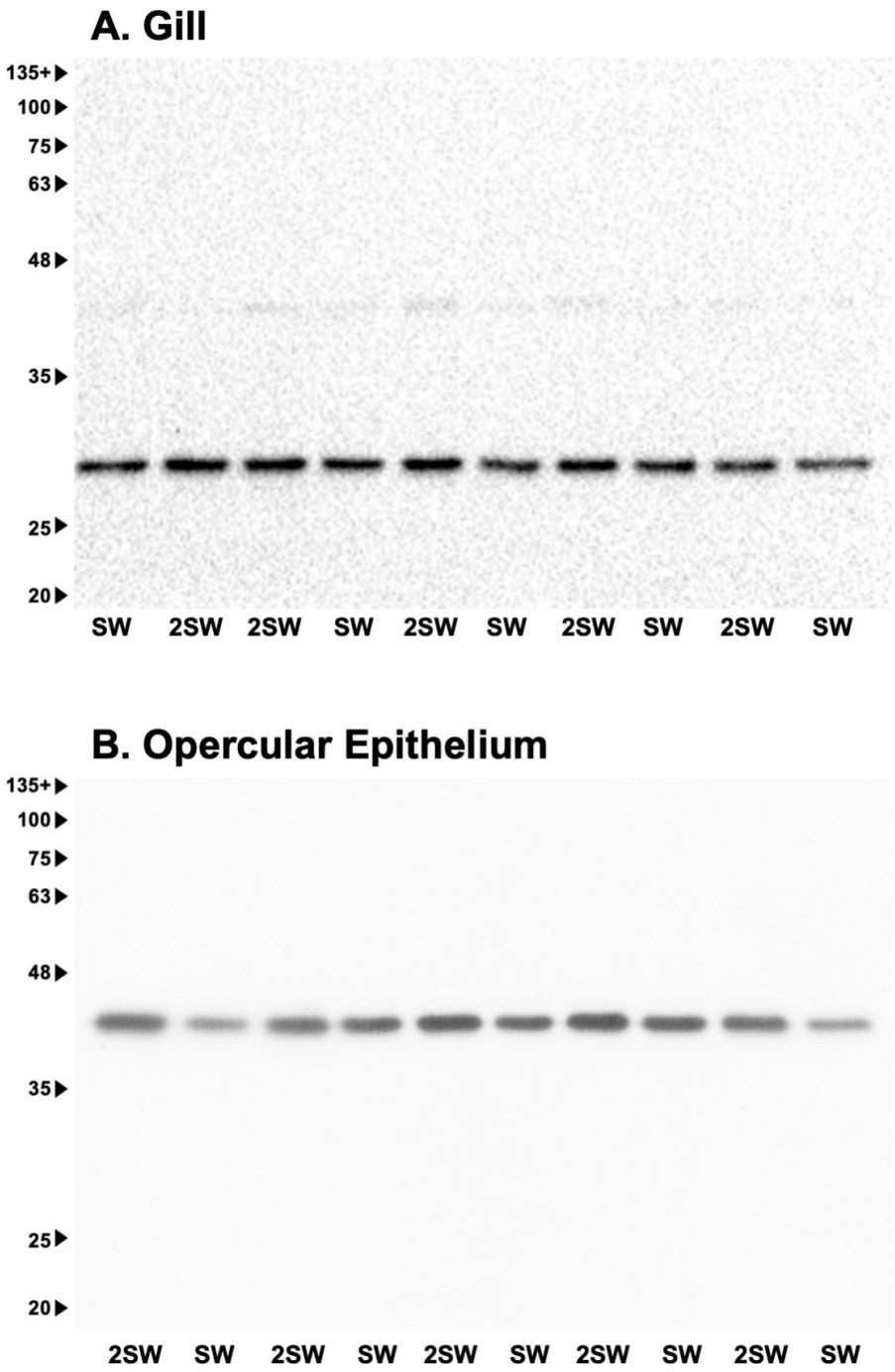

Supplemental Figure 4-2. Western blots showing protein abundance of claudin-10c (Cldn-10c) in (A) gill and (B) opercular epithelium (OE) of mummichogs acclimated to seawater (SW) or hypersaline (2SW) conditions.

4.5. Results

4.5.1. Organ-specific distribution of cldn-10 paralogs and salinity response

Examination of various mummichog organs, as well as flank muscle revealed that all *cldn-10* paralogs were predominantly expressed in the gill and OE, irrespective of their presence or absence in other organs (**Figure 4-1 A-D**). Notably, *cldn-10e* was found exclusively in the gill and OE but in no other organ/organ biopsy examined in this study. In terms of broad distribution, and at low levels, *cldn-10c, -10d* and *-10f* transcripts were expressed in the brain and eye (**Figure 4-1 A-D**). All *cldn-10* paralogs were absent from the heart and muscle (**Figure 4-1 A-D**). In other organs composed mainly of epithelial tissue (i.e. liver, kidney, posterior intestine, and skin), no *cldn-10* paralog was found to be present in all. That is, no *cldn-10* paralog was broadly distributed across these organs. Instead, individual select *cldn-10* paralog mRNA was found in each organ. Specifically, *cldn-10c* was found in skin (**Figure 4-1A**), *cldn-10d* in liver as well as posterior intestine (**Figure 4-1B**) and *cldn-10f* in kidney (**Figure 4-1D**), all at low levels relative to gill and OE. The distribution of *cftr* mRNA was broader than most *cldn-10* paralogs, but similar in that it was found to be quite dominant in the gill and OE (**Figure 4-1E**). However, *cftr* mRNA of fish residing in SW was most abundant in the posterior intestine (**Figure 4-1E**).

Following acclimation of fish from SW to 2SW, a significant increase in gill *cldn-10c* ($P<0.01$), *-10d* ($P=0.024$), *-10e* ($P=0.049$) and *-10f* ($P<0.01$) mRNA abundance occurred (**Figure 4-2 A-D**). In the OE of fish acclimated to 2SW, *cldn-10c* ($P<0.01$), *-10d* ($P=0.05$) and *-10f* ($P<0.01$) mRNA abundance significantly increased while and *-10e* ($P=0.20$) was not significantly different (Figure 2 A-D). Transcript abundance of *cldn-10c* was also observed to significantly increase ($P<0.01$) in the skin of fish acclimated from SW to 2SW (**Figure 4-2A**), but when present, *cldn-10* paralog mRNAs in all other organs were not found to alter in response to salinity (**Supplemental Figure**

4-1). Acclimation of fish from SW to 2SW also elicited a significant increase in gill, OE, and skin *cftr* mRNA abundance (all $P<0.01$; Fig. 2E), but no salinity-induced change in *cftr* mRNA abundance was found to occur in other organs (**Supplemental Figure 4-1**).

4.5.2. Cldn-10c abundance in the gill and OE

Salinity acclimation from SW to 2SW resulted in a significant increase in Cldn-10c abundance in both the gill (**Figure 4-3A**, **Supplemental Figure 4-2**) and OE (**Figure 4-3B**, Supplemental **Figure 6-2**). Immunoblot of gill tissues showed two distinct bands with MWs of ~29 kDa and ~40 kDa, with the predicted MW of the Cldn-10c sequence at 29 kDa (XP_012728690). When considering the prominent 29 kDa bands in the gill, immunoblot showed significant increase in 29 kDa band intensity in 2SW (126.76 ±7.49%) when compared to SW (100 ±5.16%; $P<0.01$). A single band at 40 kDa was detected in the OE (**Figure 4-3D**). An enzymatic deglycosylation protocol was carried out using gill tissues and, following this, only a single band at 29 kDa was observed (**Figure 4-3E**). No bands were present in Western blots generated with gill and OE samples incubated with anti-Cldn-10c primary antibody in combination with immunopeptide.

Immunohistochemistry

4.5.3. Claudin-10c in OE

Effect of hypersaline conditions: Cldn-10c immunofluorescence in SW acclimated fish OE consistently appeared in the apical crypts of ionocytes as incomplete or complete rings (**Figure 4-4A**) slightly (1-2 μm) above (**Figure 4-4B**) the immunofluorescence of Na^+,K^+-ATPase, which served as a marker for mitochondrion-rich ionocytes (n = 10 epithelial preparations on day 10 of 2SW acclimation). TJs between pavement cells (PVCs) were often observed to be variably positive for Cldn-10c (**Figure 4-4A**). Deeper into the epithelium (10-14 μm), there regularly

appeared Cldn-10c immunopositive ionocytes (i.e. as defined by the parallel presence of Na^+, K^+-ATPase immunoreactivity) also appearing as ring-like shapes. This intraepithelial staining we inferred as unerupted ionocytes (data not shown). Exposure to 2SW (n = 4, exposures 5, 11, 17 and 25 days in 2SW) did not alter the localization of Cldn-10c and Na^+,K^+-ATPase immunofluorescence (i.e. Cldn-10c immunofluorescence was still in the apical crypts of ionocytes) and there was weakly positive signal in the TJs between PVCs. In addition, ionocyte cell size, indicated by the Na^+, K^+-ATPase positive area, was markedly larger (**Figure 4-4B**, 2SW exposure 17 days). The width of the Cldn-10c positive rings appeared wider, typically 0.5 μm, compared to 0.3 μm in SW, often the rings were double lines (arrow in **Figure 4-4C**) and the signal stronger in the 2SW ionocytes. The estimated volume of ionocytes in SW was 576 $\pm$ 34.3 μm^3 (n = 100 cells from 10 images) but after exposure to 2SW for 11, 17 and 25 days, ionocyte volume was significantly ($P < 0.001$, unpaired two tailed *t*-test) larger at 1492 $\pm$ 88.7 μm^3(n = 100 cell from 10 images) However, there was no significant change ($P = 0.3549$) in the overall ionocyte density (number of ionocytes per unit area); in SW 49.3 $\pm$ 5.1 cells per 0.015 mm^2 versus 2SW at 40.3 $\pm$ 8.1 cells per 0.015 mm^2 (n = 10 areas of 0.015 mm^2 per sample).

4.5.4. Proximity of Cldn-10c relative to CFTR and actin

In the SW OE, Cldn-10c was detected in apical crypts (**Figure 4-5 A-G**) as seen in images collected using the red channel for Cldn-10c and the green channel to localize CFTR. CFTR distribution is cup-like, down the sides of the apical crypts and across the bottom of the crypts, whereas, Cldn-10c occurred slightly (1-2 μm) higher along the margins of the apical crypt than CFTR and was colocalized with CFTR along the sides of the apical crypts but was absent from the bottom of the crypt (XY scans **Figure 4-5 A-D** and XZ scans, **Figure 4-5 E-G**). **Figure 4-5H** diagrammatically summarizes the findings of more cation-permeable claudin-10c and more anion-

conductive CFTR in 2SW than in SW controls and the close relative positions of the two proteins in the ionocytes. Cldn-10c was also detected in the PVCs of the OE but most prominently in the apical crypts of ionocytes (arrowhead) (**Figure 4-6A**). Actin immunofluorescence was present in the microridges on the upper surface of pavement cells and in the rings surrounding ionocyte apical crypts (**Figure 4-6B**). Cldn-10c colocalized considerably with actin in the apical crypts and in the TJs between pavement cells (**Figure 4-6C** and **D**).

FW acclimated mummichog opercular epithelia had some ionocytes below the surface in the OE that appeared to stain for Cldn-10c, localized to the apical crypts (**Figure 4-7**). However, many of Na^+, K^+-ATPase positive ionocytes were negative for Cldn-10c (**Figure 4-7**). Irrespective, the Cldn-10c positive ionocytes were not exposed to the surface of the epithelium and instead were buried 10 μm or more in the epithelium.

4.5.5. Claudin-10c in gill

The cellular localization and distribution of Cldn-10c in SW fish gill filaments were similar to that observed in OE ionocytes. Specifically, some immunofluorescence was observed in pavement cells (**Figure 4-8A**), but it was at a high intensity in apical crypts of ionocytes. CFTR immunofluorescence was present in ionocyte apical crypts (**Figure 4-8B**) where CFTR colocalized with Cldn-10c (**Figure 4-8C**). In a different plane, distribution of Cldn-10c was further evident in the pavement cells and with prevalent immunofluorescence in the ionocyte apical crypts (**Figure 4-8D** and **E**). CFTR (**Figure 4-8F** and **G**) was obvious in the apical crypt rings of ionocytes, as was colocalization of the two proteins (**Figure 4-8H** and **I**); the colocalization was also confirmed by line scan graph (**Figure 4-8J**).

4.6. Discussion

4.6.1. Overview

The current study provides a first look at organ-specific profiles of *cldn-10* paralogs in the mummichog, *F. heteroclitus* and, with respect to externally exposed ion-secreting epithelia, shows that the gill and OE exhibit an almost identical *cldn-10* paralog profile. Because recent evidence supports the view that *cldn-10* paralogs are essential components of the paracellular Na^+ secretory pathway of the SW-residing mummichog gill (Marshall et al., 2018), this observation underscores the OE as an important and appropriate surrogate model of gill epithelium. Furthermore, salinity-induced changes in the transcript and protein abundance of *cldn-10* paralogs in gill and OE (i.e. changes occurring following acclimation from SW to 2SW) mirrored one another, thus supporting the view that these organs exhibit functionally consistent paracellular properties using the same TJ proteins. This idea is additionally supported by observations of the cellular and sub-cellular localization of Cldn-10c protein in OE and gill, using a custom antibody to the carboxy terminus. Specifically, Cldn-10c is a hypersaline responsive paralog at the transcriptional level (Marshall et al. 2018) and, in this study, was shown to exhibit parallel changes in protein abundance. Furthermore, Cldn-10c exhibited robust localization in gill and OE ionocytes where co-immunofluorescence with CFTR further demonstrated that Cldn-10c in this species is associated with intercellular junctions adjoining apical crypts. Finally, the current study detected a heavier anti-Cldn-10c reactive band in both the gill and OE that was eliminated by deglycosylation enzymes. This band was more intense in the OE and in both gill and OE under hypersaline conditions. Our findings suggest a mechanism that could assist in the maintenance of elevated functional Cldn-10c under conditions of extreme salinity (i.e. a hypersaline environment) as protein glycosylation has been associated with environmentally stressful circumstances (e.g. Ernst

et al., 1994; Kazemi et al., 2010). This also suggests that under natural conditions, the molecular physiology of the OE TJ complex may be better prepared for rapid exposure to hypersaline conditions.

4.6.2. Organ-specific cldn-10 paralog and cftr mRNA expression/abundance and salinity response

The TJ protein Cldn-10 has been documented in multiple forms in teleost fishes and these are now quite broadly reported to exhibit restricted organ-specific distribution patterns that are often dominated by the gill (Loh et al., 2004; Tipsmark et al., 2008; Bui and Kelly, 2014; Kolosov et al., 2014). In addition, Cldn-10 proteins (or the genes that encode them) in the gill epithelium are also well-documented to respond to alterations in environmental salinity, such that they typically increase following transfer of euryhaline fishes from FW to SW (e.g. Tipsmark et al., 2008; Bui et al., 2010; Bui and Kelly, 2014; Marshall et al., 2018) or from SW to 2SW, as was observed more recently (Marshall et al., 2018). The current study shows that *cldn-10* transcript distribution patterns in the mummichog were found to occur predominantly in the gill as well as in the OE. While the observations of gill *cldn-10* abundance are largely confirmatory, an OE *cldn* profile has yet to be reported for any fish species. Nevertheless, the presence of TJ strands in mummichog OE have been well illustrated by transmission electron microscopy (e.g. Karnaky, 1991), and the OE is an established surrogate model for studying the ion transport properties of the marine fish gill (Degnan et al., 1977; Marshall et al., 1997; Marshall and Grosell, 2006). Therefore, observations of *cldn-10* paralogs in the OE that qualitatively and quantitatively match those of the gill provide evidence that the molecular components, which facilitate paracellular Na^+ secretion across the OE are, if not the same, very similar to those of the gill epithelium. In turn, these observations also

underscore the suitability of the OE as a model for studying marine fish ion transport. Indeed, further emphasizing this conclusion is the response of OE *cldn-10* paralogs following acclimation of animals from SW to 2SW, which closely align with the response of *cldn-10* paralogs in the gill. That is, *cldn-10c* and *-10f* were the *cldn-10* paralogs that exhibited robust and clear-cut elevations in mRNA abundance in the gill and OE following 2SW acclimation in this study and these *cldn-10* paralogs also exhibited robust and sustained elevations in gill tissues following acclimation to 2SW in a previous study (Marshall et al., 2018).

Because the OE is a flat epithelial sheet that is often referred to as "skin", it is important to note that the molecular physiology of OE *cldn-10s* does not resemble the epidermal epithelium. Specifically, only one *cldn-10* paralog (*cldn-10c*) was found to be expressed in the general integument of the mummichog, and in this organ *cldn-10c* transcript abundance was markedly lower than *cldn-10c* transcript abundance in the gill and OE. This indicates that the molecular physiology of OE TJs resembles the gill more than the skin. The presence of *cldn-10c* in the skin would be consistent with the low level Cldn-10c immunofluorescence we observed in branchial junctions between PVCs. More specifically, because branchial PVCs as well as epidermal cells are connected by multi- stranded junctions that exhibit low permeability (Chasiotis et al. 2012; Kolosov et al. 2013; Sardet et al. 1979), apparently some copies of pore-forming claudins can exist in these locations without coming together to form organized single-stranded ion pores. Nevertheless, *cldn-10c* transcript abundance in the skin of the mummichog in this study did increase in response to 2SW acclimation. At this stage, it can be suggested that increased mummichog skin *cldn-10c* is unlikely to contribute to overall salt and water balance, because *cldn-10c* abundance is low and the ion-transport capacity of the cutanenous epithelium of most teleost fishes, beyond the larval stage, is limited. Indeed, comparable observations and a similar

conclusion was drawn by Bui and Kelly (2014) with respect to low levels of *cldn-10* transcript abundance in the puffer fish skin versus the gill epithelium. Nevertheless, a physiological role for select Cldn-10 proteins seems likely in the skin, but will require further study.

Transcript-encoding *cldn-10* paralogs were also present in the brain and eye (*cldn-10c, -10d*, and *-10f*) as well as the kidney (*cldn-10f*), liver and posterior intestine (*cldn-10d*). Transcript abundance in these organs was considerably lower than that observed in the gill and OE, and in no case did transcript abundance alter following exposure to 2SW. However, these observations do suggest that Cldn-10 proteins have a physiological role to play in barrier tissues that are not directly exposed to the external environment in the way that the gill and OE are. But we are far from understanding all the complexities of Cldn-10 protein involvement in teleost fish homeostasis. Transcript encoding *cldn-10* in the central nervous system illustrate this point, as *cldn-10* paralogs have been reported in the nervous tissue of several teleost species (see Kolosov et al., 2013), but species-specific differences in which form dominates seem to occur. For example, in the mummichog brain *cldn-10d* and *cldn-10f* are predominant, whereas *cldn-10e* was not detected. This contrasts with the rainbow trout brain where *cldn-10e* is present but *cldn-10c* and *-10d* are absent (Kolosov et al., 2014). This difference between species was further seen in *cldn-10* paralog expression in ocular tissues, and contrasting both are observations derived from *Fugu rubripes*, where no *cldn-10* expression was detected in the brain, while *cldn-10b* and *-10c* were detected in the eye (Loh et al., 2004). Taken together with observations of selective *cldn-10* presence in the liver, kidney and posterior intestine, organ-specific *cldn-10* distribution appears to highlight the significance and importance of diverse strategies in the maintenance of physiological barriers and ion balance.

4.6.3. Cldn-10c in the Gill and OE

Transcriptional changes in branchial *cldn-10s* during and following salinity acclimation have been documented in several teleost species, with increases in teleost Cldn-10 protein abundance documented in the spotted green pufferfish (Bui and Kelly, 2014). In the current study, acclimation to 2SW resulted in elevated Cldn-10c in the mummichog gill and OE. An anti-Cldn-10c custom antibody detected a 29 kDa band in the gill, consistent with the MW prediction of a 255 residue sequence (XP_012728690). In addition, a ~40 kDa band in both the gill and the OE was also detected throughout this study. The 40 kDa band exhibited similar immunoreactivity as the predicted sequence, which could suggest a peptide that has a similar epitope to the Cldn-10c carboxy terminus sequence (against which the primary antibody was raised), potentially leading to non-specific interactions. However, BLAST searches of the *F. heteroclitus* genome failed to reveal any full-length matches and only two hits at 43% similarity (GABA receptor type 5 and Frizzled-10, neither of which are associated with epithelial ion transport) and no matches for the highly immunogenic last 8 residues (KTASNVYV-COOH). Further analysis suggests an alternative hypothesis, that the MW shift of Cldn-10c may be a product of post-translational modification. *In silico* analysis of Cldn-10c sequence revealed 22 potential O-glycosylation sites (NetOGlyc 4.0; Technical University of Denmark). An estimate of 22 glycosylation sites would shift the MW by 4.8 kDa with each glycosylation site presumably modified with a 220 Da glycoside. Whereas simple glycosylation in serine and threonine glycosidation is typical, there exists a possibility where the glycoside-units may be further elongated by glycan repeats (Nakada, 2014; Ogawa et al., 2018). The 40 kDa immunoreactive band was absent after glycosidase incubation, indicating that the observed 40 kDa band may be a heavily glycosylated protein. Whereas the current study has not explored potential interplay between phosphorylation and

glycosidation that may alter the integrity of TJ components (Butt et al., 2012), an *in silico* prediction of YinYang sites using YinOYang 1.2 (Gupta and Brunak, 2002) revealed seven potential YinYang sites in the mummichog *cldn-10c* sequence, five near the carboxy terminus. Hence further investigation of mummichog *cldn-10c* regulation is warranted. Nevertheless, a MW shift towards 40 kDa that is greater in the OE samples was detected, to a point where analyses of the 29 kDa band in the OE is delimited due to experimental resolution. Experimental evidence for the glycosylation of Cldn TJ proteins is scarce, and most glycosylation information on Cldns is based on sequence information. Here we conclude that Cldn-10c can be glycosylated in the mummichog gill and OE epithelium, with a predominant form in the OE that seems likely to have functional significance.

Glycosylation is a post-translational modification that is associated with sub-cellular functions that include signal-transduction, protein localization, and protein stability (for review, see Moremen et al., 2012) and there is evidence to support protein glycosylation as an intrinsic cellular response to environmental stressors that enhances the stability of proteins (Ernst et al., 2009; Watanabe et al., 2004; Kazemi et al., 2010). Notably, these observations include glycosylation of CFTR, an ion transporting protein in a salt-stressed ion transporting epithelium (see Ernst et al., 1994). Taken together with observations in this study, it can be suggested that glycosylation of Cldn-10c in branchial tissues may be a mechanism that allows externally exposed mummichog ion-regulating epithelia to cope with the heightened environmental challenge of hypersaline conditions. Furthermore, because the putative glycosylated form is dominant in the OE, this may mean that the OE is better equipped for a rapid exposure to hypersaline conditions. This idea, however, will require further exploration.

The increase in Cldn-10c abundance underlines the importance of its potential contribution in

the formation of TJ pores that drive cation permeability. The high transcript versus comparatively modest (but still significant) increase in Cldn-10c protein abundance suggests a potentially high turnover rate of *cldn-10c* mRNA. The dual increases in *cldn-10c* and *cftr* transcripts (which mirror one another) and the resulting Cldn-10c abundance further strengthens the idea that Cldn-10c plays an important role in modulating epithelium permeability in response to hypersaline surroundings.

4.6.4. Claudin-10 immunohistochemistry and salinity response

In OE and gill there is a close-fitting association of Cldn-10c immunofluorescence in the TJs of Na^+-K^+-ATPase-enriched ionocytes that have CFTR in the apical membrane. Importantly, immunogen peptide was able to block Cldn-10c immunofluorescence in SW opercular epithelia and omission of the primary antibody also produced negligible fluorescence. The close association of Cldn-10c and CFTR in the OE (fixed in methanol-DMSO) and in the gill (fixed in paraformaldehyde) demonstrates the robust binding ability of the custom Cldn-10c antibody and also supports the use of the OE as a model for ionocyte function in the marine teleost gill. The claudin immunofluorescence in XZ scans was clearly located more apically than Na^+, K^+-ATPase, consistent with a TJ position. Cldn-10c immunofluorescence was also colocalized with CFTR in part, along the sides of the apical crypts in XZ scans, but Cldn-10c was absent from the bottom of the cup-shaped apical membrane, where only CFTR was present. We infer that the Cldn-10c was not in the apical membrane but rather, in the TJ complex.

Actin is present near epithelial TJs and immunohistochemistry revealed that Cldn-10c and F-actin were co-localized in the apical crypt area and to a lesser extent in the TJ between pavement cells, consistent with actin involvement in TJ maintenance and a TJ localization for Cldn-10c. Cldn-10c localization in association with gill and OE ionocytes was similar to that previously observed in human conjunctival epithelium (Yoshida et al., 2009) in that there was punctate

distribution of human CLDN-10 in conjunctiva associated with specialized transport cells, rather than a general staining of TJs, as was observed for CLDN-1, -4 and -7. Despite being present in both ionocytes and PVCs of the gill and OE, overall Cldn-10c was enriched in mummichog ionocytes. In the puffer fish gill epithelium, Cldn-10d and -10e were also found to be enriched in ionocytes (Bui and Kelly, 2014), but based on molecular and cell isolation techniques, were proposed to be absent from PVCs (Bui et al., 2010). Similarly, *cldn-10c* and *-10d* were proposed to be absent from gill PVCs of rainbow trout and enriched in ionocytes (Kolosov et al., 2014). But *cldn-10e* transcript was found in both ionocytes and PVCs of rainbow trout, suggesting that species-specific differences in the presence (or absence) of *cldn-10s* in different branchial epithelium cells occurs. Nevertheless, we can conclude that immunohisochemical evidence places Cldn-10c in or in close association with mummichog branchial TJs, especially in the apical crypts of ionocytes and closely associated with important transport proteins CFTR and Na^+,K^+-ATPase as well as F-actin associated with TJ complex function..

Hypersaline conditions produced marked hyperplasia of ionocytes in the OE, similar to that previously observed in branchial ionocytes of hypersaline tolerant fishes (Gonzalez 2012), and an apparent increase in the thickness of the Cldn-10c immunofluorescent rings, consistent with a need to increase ion transport rate in the higher salinity. We have observed a significant increase in opercular epithelium transepithelial potential in hypersaline conditions *in vitro*, such that the electrical driving force for Na^+ extrusion rises from +35-40 mV in sea water to +45-50 mV in 2SW, accompanied by an increase in epithelial conductance (Marshall et al., 2017) along with elaborations in ionocyte-AC TJs (Cozzi et al., 2015). Ion substitution experiments demonstrated that the isolated OE selects for Na^+ and against Li^+, Rb^+, and Cs^+ (Marshall et al. 2018), evidence that paracellular claudin-10 pores are Na^+-selective. Our results are consistent with those of

Ouatara et al. (2009), who observed a marked increase in ionocyte size in tilapia (*Sarotherodon melanotheron*) gill epithelium without an apparent increase in cell density, following exposure to hypersaline conditions. Therefore all evidence suggests that hypersaline conditions enhances Cldn-10c presence in the TJs of ionocytes and increases the cell capacity for ion transport in the form of cation-selective pores that comprise a Na^+-selective paracellular pathway essential for NaCl secretion.

4.7. Conclusions and Perspectives

The current study presents further evidence that Cldn-10 proteins play a key role in regulating salt secretion across the branchial tissues of fishes acclimated to or living in SW or hypersaline conditions. Of particular note is the idea that in the mummichog, Cldn-10 proteins exhibit a functional response to hyperosmotic condition, and that Cldn-10c in this species is an important component in the formation of TJ pores that contribute to the permselectivity properties of branchial epithelia under SW and hypersaline conditions. This most likely contributes to the ability of these fish to accommodate paracellular cation secretion under such extreme conditions. We are also able to conclude that the molecular physiology of genes encoding Cldn-10 proteins in the mummichog exhibit a consistent response to hypersaline conditions in the gill and OE, providing the first evidence that the molecular machinery of the cation-selective TJ complex of the OE and gill epithelium are the same. But it is also clear from this study (and others) that while we can make some generalizations about Cldn-10 TJ proteins, the specific presence and role of different Cldn-10 in branchial epithelia and other barrier tissues in fishes will not be uniform, and this warrants further study. Indeed, future studies that also address the functional significance Cldn glycosylation in fishes will also be of interest.

4.8. References

Barnes, K.R., Cozzi, R.R.F., Robertson, G.N. and Marshall, W.S. (2013). Cold acclimation of NaCl secretion in a eurythermic teleost: Mitochondrial function and gill remodeling. *Comp. Biochem. Physiol. A Molec. Integ. Physiol.* 168, 50-62.

Bossus, M. C., Madsen, S. S. and Tipsmark, C. K. (2015). Functional dynamics of claudin expression in Japanese medaka (*Oryzias latipes*): Response to environmental salinity. *Comp. Biochem. Physiol. A-Mol. Integr. Physiol.* 187, 74-85.

Bui, P. and Kelly, S. P. (2014). Claudin-6, -10d and -10e contribute to seawater acclimation in the euryhaline puffer fish *Tetraodon nigroviridis*. *J. Exp. Biol.* 217, 1758-1767.

Bui, P. and Kelly, S. P. (2015). Claudins in a primary cultured puffer fish (*Tetraodon nigroviridis*) gill epithelium model alter in response to acute seawater exposure. *Comp. Biochem. Physiol. A-Mol. Integr. Physiol.* 189, 91-101.

Bui, P., Bagherie-Lachidan, M. and Kelly, S. P. (2010). Cortisol differentially alters claudin isoforms in cultured puffer fish gill epithelia. *Mol. Cell. Endocrinol.* 317, 120-126.

Burnett, K. G., Bain, L. J., Baldwin, W. S., Callard, G. V., Cohen, S., Di Giulio, R. T., Evans, D. H., Gomez-Chiarri, M., Hahn, M. E., Hoover, C. A. et al. (2007). *Fundulus* as the premier teleost model in environmental biology: Opportunities for new insights using genomics. *Comp. Biochem. Physiol. D-Genomics and Proteomics* 2, 257-286.

Butt, A.M., Khan, I.B., Hussain, M., Idress, M., Lu, J., Tong, Y. (2012) Role of post translational modifications and novel crosstalk between phosphorylation and O-beta-GlcNAc modifications in human claudin-1, -3 and -4. *Mol. Biol. Rep.* 39,1359-1369.

Chasiotis, H., Kolosov, D., Bui, P. and Kelly, S. P. (2012). Tight junctions, tight junction proteins and paracellular permeability across the gill epithelium of fishes: A review. *Respir. Physiol. Neuro.* 184, 269-281.

Cozzi, R. R. F., Robertson, G. N., Spieker, M., Claus, L. N., Zaparilla, G. M. M., Garrow, K. L. and Marshall, W. S. (2015). Paracellular pathway remodeling enhances sodium secretion by teleost fish in hypersaline environments. *J. Exp. Biol.* 218, 1259-1269.

Degnan, K. J., Karnaky, K. J. Jr. and Zadunaisky, J. A. (1977). Active chloride transport in the invitro opercular skin of a teleost (*Fundulus heteroclitus*), a gill-like epithelium rich in chloride cells. *J. Physiol. lond.* 271,155-191.

Degnan, K. J. and Zadunaisky, J. A. (1980). Passive sodium movements across the opercular epithelium: The paracellular shunt pathway and ionic conductance.. *J. Membr. Biol.* 55, 175-185.

Edwards, S. L. and Marshall, W. S. (2013). Principles and patterns of osmoregulation and euryhalinity in fishes. In *Euryhaline Fishes (Fish Physiology Vol 33)* (ed. S. D. McCormick, A. P. Farrell and C. J. Brauner), pp. 1-44. San Diego: Academic Press.

Ernst, S.A., Crawford, K.M., Post, M.A. and Cohn, J.A. (1994). Salt stress increases abundance and glycosylation of CFTR localized at apical surfaces of salt gland secretory cells. *Am. J. Physiol*. 267, C990-1001.

Evans, D. H., Piermarini, P. M. and Choe, K. P. (2005). The multifunctional fish gill: Dominant site of gas exchange, osmoregulation, acid-base regulation, and excretion of nitrogenous waste. *Physiol. Rev.* 85, 97-177.

Gonzalez, R.J. (2012). The physiology of hyper-salinity tolerance in teleost fish: a review. *J Comp Physiol B* 182, 321–329.

Griffith, R. W. (1974). Environment and salinity tolerance in the genus *Fundulus*. *Copeia* 1974, 319-331.

Guggino, W. B. (1980). Salt balance in embryos of *Fundulus heteroclitus* and *F. bermudae* adapted to seawater. *Am. J. Physiol. Reg. Integ. Comp. Physiol.* 238, R42-R49.

Gupta, R. and Brunak, S. (2002) Prediction of glycosylation across the human proteome and the correlation to protein function. Pacif. Sympos. Biocomput. 7, 310-322.

Karnaky, K. J. Jr. (1991). Teleost osmoregulation: Changes in the tight junction in response to the salinity of the environment. In *The Tight Junction.* (ed. M. Cereijido), pp. 175-185. Boca Raton, USA: CRC Press.

Kazemi, Z., Chang, H., Haserodt, S., McKen, C. and Zachara, N.E. (2010). O -Linked β- N -acetylglucosamine (O-GlcNAc) Regulates Stress-induced Heat Shock Protein Expression in a GSK-3β-dependent Manner. *J. Biol. Chem.* 285, 39096–39107.

Kolosov, D., Bui, P., Chasiotis, H. and Kelly, S. P. (2013). Claudins in teleost fishes. *Tissue Barriers* 1, e25391.

Kolosov, D., Chasiotis, H. and Kelly, S. P. (2014). Tight junction protein gene expression patterns and changes in transcript abundance during development of model fish gill epithelia. *J. Exp. Biol.* 217, 1667-1681.

Krug, S. M., Guenzel, D., Conrad, M. P., Lee, I. M., Amasheh, S., Fromm, M. and Yu, A. S. L. (2012). Charge-selective claudin channels. *Ann. NY Acad. Sci.* 1257, 20-28.

Krug, S. M., Schulzke, J. D. and Fromm, M. (2014). Tight junction, selective permeability, and related diseases. *Semin. Cell Dev. Biol.* 36, 166-176.

Loh, Y., Christoffels, A., Brenner, S., Hunziker, W. and Venkatesh, B. (2004). Extensive expansion of the claudin gene family in the teleost fish, *Fugu rubripes*. *Genome Res.* 14, 1248-1257.

Marshall, W.S., Bryson, S.E., Darling, P., Whitten, C., Patrick, M., Wilkie, M., Wood, C.M., and Buckland-Nicks, J. (1997) NaCl Transport and Ultrastructure of Opercular Epithelium From a Freshwater-Adapted Euryhaline Teleost, Fundulus heteroclitus. *J. Exp. Zool.* 277, 23-37.

Marshall, W. S., Emberley, T. R., Singer, T. D., Bryson, S. E. and McCormick, S. D. (1999). Time course of salinity adaptation in a strongly euryhaline estuarine teleost, *Fundulus heteroclitus*: A multivariable approach. *J. Exp. Biol.* 202, 1535-1544.

Marshall, W.S., Lynch, E.M. and Cozzi, R.R.F. (2002). Redistribution of immunofluorescence of CFTR anion channel and NKCC cotransporter in chloride cells during adaptation of the killifish *Fundulus heteroclitus* to sea water. *J. Exp. Biol.* 205, 1265-1273.

Marshall, W. S. and Grosell, M. (2006). Ion transport, osmoregulation and acid-base balance. *In*: *The Physiology of Fishes* 3rd Ed. (*eds*. D. H. Evans and J. B. Claiborne), pp. 177-230. Boca Raton FL: CRC Press.

Marshall, W.S., Cozzi, R.R.F., Spieker, M. (2017). WNK1 and p38-MAPK distribution in ionocytes and accessory cells of euryhaline teleost fish implies ionoregulatory function. *Biology Open* 7, 956-966.

Marshall, W.S., Breves, J.P., Doohan, E.M., Tipsmark, C.K., Kelly, S.P., Robertson, G.N. and Schulte, P.M. (2018). Claudin-10 isoform expression and cation selectivity change with salinity in salt-secreting epithelia of *F. heteroclitus.* *J. Exp. Biol.* 221: 1: DOI 10.1242/jeb168906.

Moremen, K.W., Tiemeyer, M. and Nairn, A. V. (2012). Vertebrate protein glycosylation: diversity, synthesis and function. *Nat. Rev. Mol. Cell Biol.* 13, 448–62.

Nakada H. (2014) Map 2: Biosynthetic Pathways of O-Glycans. In *Handbook of Glycosyltransferases and Related Genes* (ed. N. Taniguchi, K. Honke, M. Fukuda, H. Narimatsu, Y. Yamaguchi, and T. Angata) pp. 631-635. Tokyo: Springer.

Ogawa, M., Senoo, Y., Ikeda, K., Takeuchi, H., and Okajima, T. (2018) Structural Divergence in O-GlcNAc Glycans Displayed on Epidermal Growth Factor-like Repeats of Mammalian Notch1. *Molecules* 23: E1745.

Ouattara, N.G., Bodinier, C., Negre-Sadargues, G., D'Cotta, H. Messad, S. Charmantier, G., Panfili, J. and Baroiller, J.-F. (2009) Changes in gill ionocyte morphology and function following transfer from fresh to hypersaline waters in the tilapia *Sarotherodon melanotheron*. *Aquaculture* 290, 155-164.

Pequeux, A., Gilles, R. and Marshall, W.S. (1988). NaCl transport in gills and related structures: *In*: Advances in Comparative and Environmental Physiology I. NaCl Transport in Epithelia (ed. R. Greger). pp. 1-73. Berlin: Springer-Verlag.

Reid, N.M., Jacksin, C.E., Gilbert, D., Minx, P., Montague, M.J., Hampton, T.H., Helfrich, L.W., King, B.L., Nacci, D.E., Aluru, N., Karchner, S.I., Colbourbe, J.K., Hahn, M.E., Shaw, J.R., Oleksiak, M.F., Crawford, D.L., Warren, W.C. and Whitehead, A. (2017) The landscape of extreme genomic variation in the highly adaptable Atlantic killifish. *Genome Biol. Evol.* 9, 659-676.

Sardet, C., Pisam, M. and Maetz, J. (1979). The surface epithelium of teleostean fish gills, cellular and junctional adaptations of the chloride cell in relation to salt adaptation. *J. Cell. Biol.* 80, 96-117.

Shen, L., Weber, C. R., Raleigh, D. R., Yu, D. and Tumer, J. R. (2011). Tight junction pore and leak pathways: A dynamic duo. *Annu. Rev. Physiol.* 73, 283-309.

Singer, T.D., Tucker, S.J., Marshall, W.S. and Higgins, C.F. (1998). A divergent CFTR homologue: Highly regulated salt transport in the euryhaline teleost *F. heteroclitus. Am. J. Physiol. Cell Physiol.* 274, C715-C723.

Singer, T.D., Keir, K.R., Hinton, M., Scott, G.R., McKinley, R.S. and Schulte P.M. (2008). Structure and regulation of the cystic fibrosis transmembrane conductance regulator (*CFTR*) gene in killifish: A comparative genomics approach. *Comp. Biochem. Physiol.* D *Genomics and Proteomics* 3, 172-185.

Tipsmark, C. K., Jorgensen, C., Brande-Lavridsen, N., Engelund, M., Olesen, J. H. and Madsen, S. S. (2009). Effects of cortisol, growth hormone and prolactin on gill claudin expression in Atlantic salmon. *Gen. Comp. Endocrinol.* 163, 270-277.

Tipsmark, C. K., Kiilerich, P., Nilsen, T. O., Ebbesson, L. O. E., Stefansson, S. O. and Madsen, S. S. (2008). Branchial expression patterns of claudin isoforms in Atlantic salmon during seawater acclimation and smoltification. *Am. J. Physiol.-Regul. Integr. Comp. Physiol.* 294, R1563-R1574.

Trubitt, R. T., Rabeneck, D. B., Bujak, J. K., Bossus, M. C., Madsen, S. S. and Tipsmark, C. K. (2015). Transepithelial resistance and claudin expression in trout RTgill-W1 cell line: Effects of osmoregulatory hormones. *Comp. Biochem. Physiol. A-Mol. Integr. Physiol.* 182, 45-52.

Watanabe, I., Zhu, J., Recio-Pinto, E. and Thornhill, W.B. (2004). Glycosylation affects the protein stability and cell surface expression of Kv1.4 but Not Kv1.1 potassium channels. A pore region determinant dictates the effect of glycosylation on trafficking. *J. Biol. Chem.* 279, 8879–85.

Whitehead, A., Roach, J. L., Zhang, S. and Galvez, F. (2011). Genomic mechanisms of evolved physiological plasticity in killifish distributed along an environmental salinity gradient. *Proc. Natl. Acad. Sci. U. S. A.* 108, 6193-6198.

Yoshida, Y., Ban, Y. and Kinoshita, S. (2009). Tight junction transmembrane protein claudin subtype expression and distibution in human corneal and conjunctival epithelium. *Invest. Ophthalmol. Vis. Sci.* 50, 2103-2108.

Chapter 5. Peri-metamorphic Tight Junction-associated Gene Expression Patterns in the Sea Lamprey (*Petromyzon marinus*) Gill

5.1. Summary

Anadromous sea lamprey (*Petromyzon marinus*) are jawless vertebrates that have an indirect development life cycle characterized by three phases; (1) a protracted stenohaline larval period, (2) seven metamorphosing stages (S1 – S7) and (3) an adult. During anadromous sea lamprey metamorphosis, morphological and physiological alterations prepare the sea lamprey for seawater (SW) residency and life as a parasitic/raptorial adult. This study examined peri-metamorphic transcript abundance of genes encoding sea lamprey tight junction (TJ) proteins in the gill to provide some insight into how gill TJs might alter in association with lamprey metamorphosis. Genes encoding TJ proteins including MARVEL-domain containing TJ-associated proteins occludin (*ocln*), occludin-a (*ocln-a*), and tricellular TJ-protein tricellulin (*tric*), as well as claudin (*cldn*) family (*-3b*, *-10*, *-14*, *-18*, *-19*) proteins were examined. Transcript abundance of *ocln* and *ocln-a* in the gill did not significantly alter from larval through to metamorphosis stage 7. However, in post-metamorphic young adults residing in freshwater (FW), gill *ocln* abundance significantly elevated while *ocln-a* abundance significantly decreased. No peri-metamorphic alterations in *tric* mRNA abundance were observed. Transcript encoding Cldn-14 was not detected in the gill before, during or after metamorphosis and *cldn-3b* and *-19* mRNA abundance were unaltered. However, at the onset of metamorphosis, *cldn-18* mRNA abundance increased, peaked at S3 and then significantly reduced in young adults. In contrast, *cldn-10* mRNA abundance increased significantly at S6, but was unaltered at any other period. Therefore, gill Cldn TJ protein gene expression patterns (most to least abundant) of FW animals alter during metamorphosis, but remain the same pre- and post-metamorphosis (*cldn-3b* > *-19* > *-18* > *-10*).

Acclimation of post-metamorphic animals to full strength SW (35 ‰) reduced gill *ocln*, *cldn-3b*, *cldn-10* and *cldn-19* and increased *ocln-a* and *tric* mRNA abundance. Data suggest that migration from FW to SW may have a greater impact on transcriptional regulation of gill TJ proteins in sea lamprey than metamorphic events.

5.2. Introduction

Sea lamprey (*Petromyzon marinus*; Linnaeus 1758) in the order Petromyzontiformes belongs to one of the only two surviving groups of jawless (Agnatha) vertebrates. In this regard, there is considerable interest in understanding the physiology and functional genomics of these basal vertebrates, as they are often suggested to provide essential information on vertebrate evolution (Smith et al., 2013). A feature of all lamprey genera is the indirect development life cycle that consists of a protracted larval phase followed by a spontaneous and synchronized metamorphosis which results in radical morphological and physiological changes (Potter, 1980; Potter et al., 1978a, 1978b; Potter and Beamish, 1977; Youson, 2003). Sea lamprey are anadromous animals (although landlocked populations exist), and as such, metamorphosis in these organisms is not only associated with profound alterations in functional morphology, but also with physiological adjustments that accommodate a new life stage that transitions from freshwater (FW) to seawater (SW) (Bartels et al., 2011; Johnson et al., 2016; Potter, 1980; Patrick Reis-Santos et al., 2008; Swink and Johnson, 2014). But while a considerable number of studies have examined various aspects of metamorphosis and this FW to SW transition, there are very few studies that have addressed the molecular physiology associated with metamorphosis and SW entry in lamprey in important osmoregulatory organs (see Kolosov et al. 2020).

5.2.1. Indirect Development in the Sea Lamprey Life Cycle

Indirect development allows an organism to exploit distinct ecological niches at different life cycle stages or when one habitat becomes unfavorable (Dawson et al. 2015). Indirect development is a relatively rare occurrence amongst chordate groups, notably appearing in urochordates, fishes and amphibians (Laudet, 2011). Fishes, as an assemblage of over 28,000 species (Nelson, 2006), are the largest and arguably the most diverse vertebrate group. Yet despite having great biodiversity, true metamorphosis is only observed in the suborder Elopomorpha (*e.g.* tarpons and eels), order Pleuronectiformes (*e.g.* flatfishes), and in the order Petromyzontiformes (Youson 1988; Manzon 2011).

The sea lamprey is characterized by having a protracted larval phase, which is as burrowing filter feeder that resides in FW, followed by a synchronous metamorphosis into young adults that are ready to migrate (Potter et al., 1978b). In describing the various metamorphic stages of sea lamprey life cycle, Youson and Potter (1979) utilized external morphological features such as eye development, oral disc morphology and dentition, changes in body coloration, as well as fin profile to categorize the sea lamprey metamorphic period into seven distinct stages (S1 - S7). Therefore, morphological characters alone can allow the differentiation of the sea lamprey life cycle into nine stages; a discrete a larval stage, S1 – S7 of metamorphosis and finally a fully metamorphosized young adult. This system of characterization using hallmarks of lamprey morphology during development provides a map to navigate the developmental time points when attempting to understand how physiological changes take place in association with metamorphosis.

5.2.2. Physiology of Sea Lamprey Metamorphosis

The precise trigger of synchronous sea lamprey metamorphosis is not completely understood but has been proposed to arise as a combination of both endogenous and exogenous

factors (Holmes et al., 1999; Kao et al., 2002; Richards and Beamish, 1981; Youson, 1997). In amphibians and teleost fishes, metamorphosis is primarily induced by the product of the thyroid hormones (e.g. thyroxine and the de-iodized triiodothyronine) (Laudet, 2011). In lamprey, a decrease in circulating thyroid hormone may trigger metamorphosis but does not otherwise play a significant part in lamprey development (Manzon and Manzon, 2017; Youson, 1997). In contrast, environmental factors (i.e. photoperiod and water temperature) and body composition (i.e. body length and lipid composition) are considered to be major triggers in lamprey metamorphosis (Holmes et al., 1994; O'Boyle and Beamish, 1977; Purvis, 1980).

During metamorphosis, sea lamprey undergo major morphological changes that include the development of the eye and teeth, changes in the shape of the oral hood, enlargement of the dorsal and caudal fins, as well as major change in coloration (Hilliard et al., 1983; Youson and Potter, 1979). Furthermore, significant reorganization of internal organs occurs in sea lamprey, and these are critical for life as parasitic adults (Youson, 1985). In addition, anadromous lamprey (such as *P. marinus*) will be required to re-organize their osmoregulatory physiology from strategies that deal with passive ion loss and water loading in FW to strategies that manage dehydration and salt loading in SW. Therefore, it is no surprise that with respect to branchial physiology, difference in cellular composition and biochemistry of the gill have been documented between the different life cycle stages as well as in migrating sea lamprey (Bartels et al., 2011; Bartels and Potter, 2004; McCormick et al., 2009). Indeed, the blood osmolality of young adult sea lamprey residing in FW following metamorphosis is significantly greater than that of larval fish (~265 mOsmol kg-1 versus ~ 225 mOsmol kg-1) (Bartels and Potter, 2004). Therefore, there is evidence to suggest that either ion transport mechanisms that enhance ion acquisition or those that mitigate ion loss may be altered in association with metamorphic events. Nevertheless, few

studies have considered how lamprey epithelia maintain selective paracellular barriers to solute movement.

5.2.3. Tight Junction Complex in Aquatic Vertebrates

The tight junction (TJ) complex is a hallmark of vertebrate epithelia that forms the occluding barrier between adjacent epithelial cells to mediate paracellular permeability and directional solute transport (Anderson and Van Itallie, 2009; Angelow et al., 2008; Van Itallie and Anderson, 2006). In fishes, TJ and TJ-associated proteins have become a major focal point in understanding piscine physiology and the overall maintenance of salt and water homeostasis (Chasiotis et al., 2012a; Kolosov et al., 2013a). TJ assembly and TJ associated gene transcripts are closely associated with environmental osmolality as well as regulation by endocrine factors. Moreover, TJ proteins have also been demonstrated to associate with specific cell types in the branchial epithelium (Kolosov et al., 2014). While there is an increasing abundance of literature supporting the roles of TJ and TJ-associated proteins in bony fishes, TJ physiology in lampreys remain relatively unexplored.

The presence of occluding junctions in lampreys was identified using freeze-fracture replicas and ultra-thin sections, and the morphology of these junctional complexes was shown to alter in response to changing environmental salt content (Bartels et al., 2011; Bartels and Potter, 2004). Molecular characterization of lamprey TJs was first utilized to consider transcriptional regulation of claudin (Cldn) TJ proteins in developing embryos (Mukendi et al., 2016), as TJ regulation in development has been demonstrated in other vertebrate models (Abuazza et al., 2006). The molecular physiology of the lamprey TJ complex and TJ proteins in salinity acclimation was first introduced through an investigation on MARVEL-domain associated TJ proteins (occludin, *ocln*; occludin-a, *ocln-a*; tricellulin, *tric*) in larval sea lamprey acclimated to FW and ion-poor FW

(Kolosov et al., 2017). In a more recent study, select genes encoding Cldn TJ proteins were also examined in larval sea lamprey and young adults in association with salinity alterations (Kolosov et al., 2020). In both cases, alterations in transcript and protein abundance of specific TJ proteins suggest an important role for TJs in this basal vertebrate in association with changes in environmental conditions and life stage, and this provides a strong rationale to support a more detailed investigation on the role that TJs and TJ proteins might play in gill remodeling during the peri-metamorphic period of the sea lamprey life cycle.

5.2.4. Objectives

Evidence from gill remodeling and identification of TJ components and salinity response has provided a foundation to further examine changes in molecular physiology of TJs in sea lamprey metamorphosis. I hypothesize that TJ assembly changes occur during sea lamprey metamorphosis in preparation for migration and acclimation to a new aquatic environment. To address this, the objective of this study was to examine for transcriptional change in genes encoding select TJ proteins in association with defined periods of metamorphosis of the sea lamprey. In addition, the transcriptional response of these genes was also examined in post-metamorphic young adults following acclimation to SW. Taken together, this will provide insight into the molecular physiology of the gill epithelium TJ complex during two major life events in the sea lamprey, metamorphosis and SW entry.

5.3. Materials and Methods

5.3.1. Animal Husbandry

Larval sea lampreys were collected from tributaries of the Richibucto River June of 2016 and June of 2017, New Brunswick, using pulsed DC backpack electrofishing (Mode LR20, Smith-

Root, Vancouver, WA). The animals were kept in 30 L static aquaria filled with well water (pH ~8.1, alkalinity ~250 mg/L $CaCO_3$) at Wilfrid Laurier University Aquatic Care Facility (Waterloo, Canada). A layer of sand was provided as burrowing substrate. Water was replaced weekly and animals were maintained under a constant photoperiod (12 hours light: 12 hours dark). Ammocoetes were fed a slurry of baker's yeast on a weekly basis (1 g/animal). All animal care and experimental protocols were approved by the Wilfrid Laurier Animal Care Committee and followed Canadian Council of Animal Care guidelines.

5.3.2. Sea Lamprey Gill Tissue Sampling

Sea lamprey ammocoetes that were identified as candidates for metamorphosis based on Holmes and Youson (1994) and were housed separately by life cycle stages in aquaria as described above. Animals were weighed every 2 weeks to follow changes in body mass of transforming and non-transforming animals between July and December. Gill sampling was conducted between June to December 2016 and July 2017 to February 2018 for a total of six times. During each sampling period, lampreys were anaesthetized and then euthanized with buffered tricaine methanesulfonate (MS-222) followed by the immediate gill collection. A group of young adults (n = 10) were then acclimated to increased salinity every 3 days from 33%, 66%, and 100% SW (35‰). Samples were kept in – 80 °C until experiment.

5.3.3. Total RNA Isolation and cDNA Synthesis

Sea lamprey gill samples were homogenized in 1 mL TRIzol reagent (Life Technologies, Carlsbad, USA) for 10 seconds using a power homogenizer (PRO Scientific, Oxford, USA), and total RNA isolation was carried out following the manufacturer's protocol. Each of the RNA samples were resuspended in nuclease-free water and quantified using a SkanIT Multiskan

Spectrum spectrophotometer (Thermo Scientific, Napean, ON). Sample integrity was referenced by with A260/A280 ratio. cDNA synthesis was immediately carried out following RNA isolation. Identical amounts (2 μg) of total RNA from each samples were treated with ezDNase™ Enzyme at 37 °C for 2 min (Life Technologies), followed by a reverse transcriptase reaction using SuperScript™ IV VILO™ Master Mix (Life Technologies) for cDNA synthesis under the following conditions: 25°C for 10 min, 50°C for 10 min, and 85°C for 5 min. Control experiments with no reverse transcriptase and a no template controls were carried out alongside the experimental samples.

5.3.4. qPCR Experiments and Gene Normalization

Quantitative polymerase chain reaction (qPCR) experiments were conducted using a CFX Connect™ Real-Time PCR Detection System (Bio-Rad Laboratories, Inc., Mississauga, ON) with Bio-Rad CFX Maestro 1.1 Software (Bio-Rad Laboratories, Inc.; Version 4.1.2433.1219). qPCR experiments were carried out using iQ SYBR Green Supermix (Bio-Rad Laboratories, Inc.) under the following conditions: 95 °C for 10 min, 40 cycles of 95°C for 30 s, primer specific annealing temperature (T_A) for 60 s, extension at 72 °C for 30 s, read every cycle, one degree below T_A to 95°C for melt curve, read every 0.5°C. PCR primers were previously verified and primer sequence, annealing temperature, and accession number are summarized in **Table 4-1** (Kolosov et al. 2017; Kolosov et al. 2020). A standard curve was generated with stock ammocoete gill cDNA in each qPCR assay as internal control. Transcript abundance were normalized to sea lamprey elongation factor-1α (*ef-1a*) gene. The use *ef-1a* was validated by statistically comparing raw Cq values between developmental stages and between salinity treatments. No statistically significant variation in *ef-1a* abundance was detected between experimental groups.

5.3.5. Statistical Analysis

All data are expressed as mean ± S.E.M. (n) where n represents the number of fish within the group. One-way analysis of variance (ANOVA) was conducted on changes in gene transcript during metamorphosis with Holm-Šídák post-hoc test. Student's t-test was conducted on changes in gene transcript of juvenile sea lamprey SW acclimation. All statistical analyses were conducted using SigmaPlot for Windows Version 14.0 (Build 14.0.3.192; Systat Software, Inc., San Jose, CA, USA).

Table 5-1. Primer sequence information for mRNA transcript analysis of tight junction associated genes in the development and metamorphosis of sea lamprey (*P. marinus*).

Gene	Name	Primer Sequence (5'→ 3')	Annealing Temperature (ºC)	Amplicon Size	Accession Number
ef-1α	Elongation factor 1α	F: GTGGGTCGTGTTGAGACTGG	60	208	KU726618
		R: GGTCGTTCTTGCTGTCAC			
cldn-3b	Claudin-3b	F: CTGGATGAACTGCGTGGTG	59	237	MN380218
		R: CCCGACAGGATGAAGATGA			
cldn-10	Claudin-10	F: ATGATAACCTCCGTATTCTTG	54	226	MN380219
		R: ACTTTGCCCCGATGA			
cldn-14	Claudin-14	F: GGATGAGCACGGGATTCTTC	61	224	MN380217
		R: GGAGACGATGAGGCAGAGG			
cldn-18	Claudin-18	F: AGGTTCTTTCAGGTGGT	60	130	MN380220
		R: AGTTTGGTCTTGGTGCTG			
cldn-19	Claudin-19	F: ACAACAAAACCCGCAAGAAC	60	181	MN380220
		R: ACCCAGCCCACAAACAGAG			
ocln	Occludin	F: CTACACCACAGAGCCCGAGT	60	321	KU721849
		R: GAGAGCCGCACCTTCAGC			
ocln-a	Occludin-a	F: ACCTCATCACCATCATCTG	54	247	KU721850
		R: ACCAGCATAAAGCCACAC			
tric	Tricellulin	F: CACATCCCCAAGCCTCTG	60	208	KU726618
		R: CCACTCGCTCCATCTCCTG			

5.4. Chapter 5 Figures

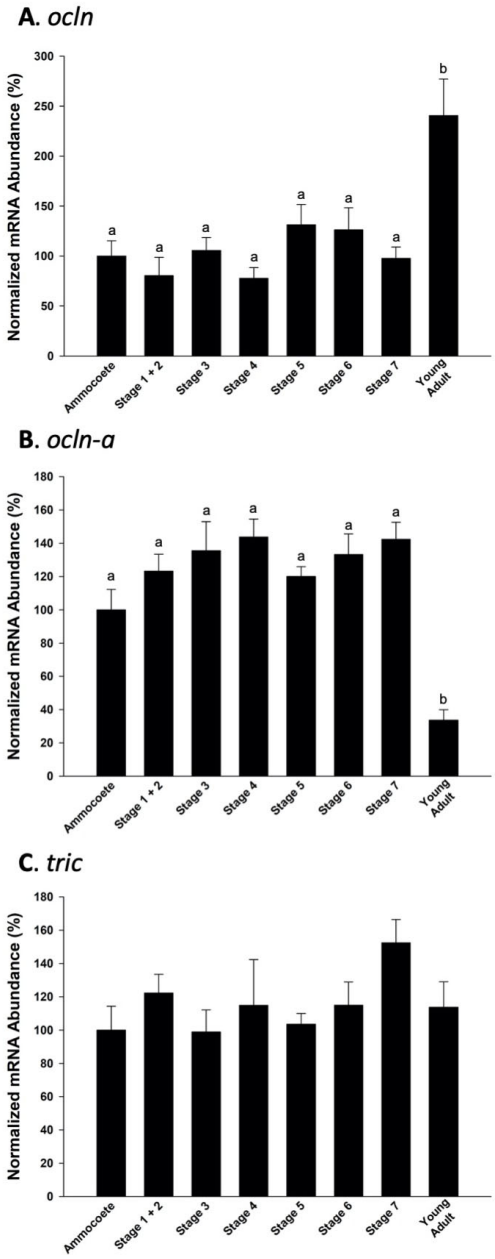

Figure 5-1. Changes in gill TJ protein (A) *ocln*, (B) *ocln-a*, and (C) *tric* transcript abundance in metamorphosing sea lampreys. Data are normalized to elongation factor-1α and standardized to ammocoetes. Letters denote difference by one-way ANOVA ($P<0.05$). All data denoted as mean ± S.E.M. (ammocoete n = 12; Stage 1 and 2 n = 7; Stage 3 n = 5; Stage 4 n = 4; Stage 5 n = 10; Stage 6 n = 7; Stage 7 n = 12; young adults n = 8).

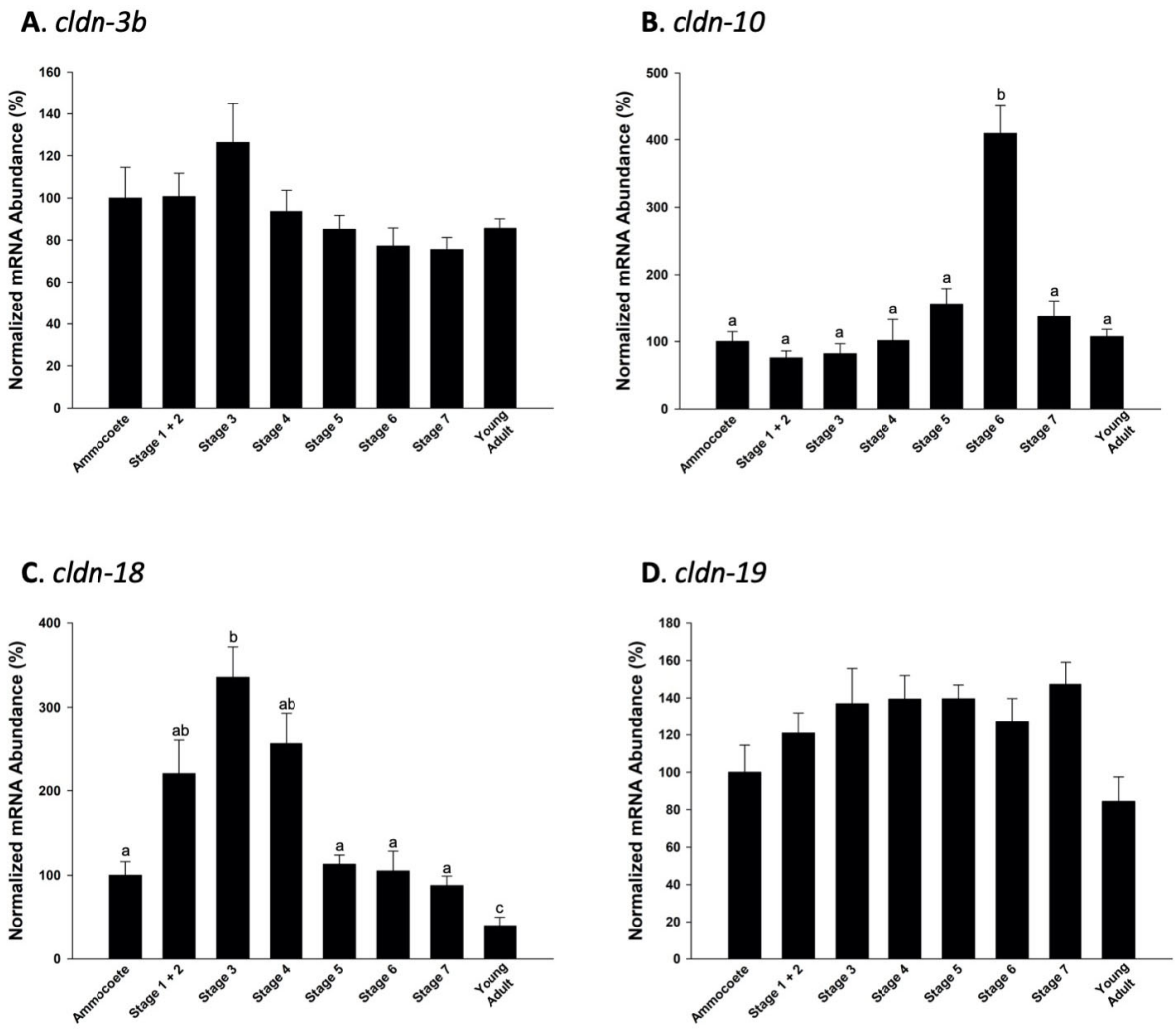

Figure 5-2. Changes in gill claudin (*cldn*) TJ proteins transcript abundance in metamorphosing sea lampreys. Data are normalized to elongation factor-1α and standardized to ammocoetes. Letters denote difference by one-way ANOVA ($P<0.05$). All data denoted as mean ± S.E.M. (ammocoete n = 12; Stage 1 and 2 n = 7; Stage 3 n = 5; Stage 4 n = 4; Stage 5 n = 10; Stage 6 n = 7; Stage 7 n = 12; young adults n = 8).

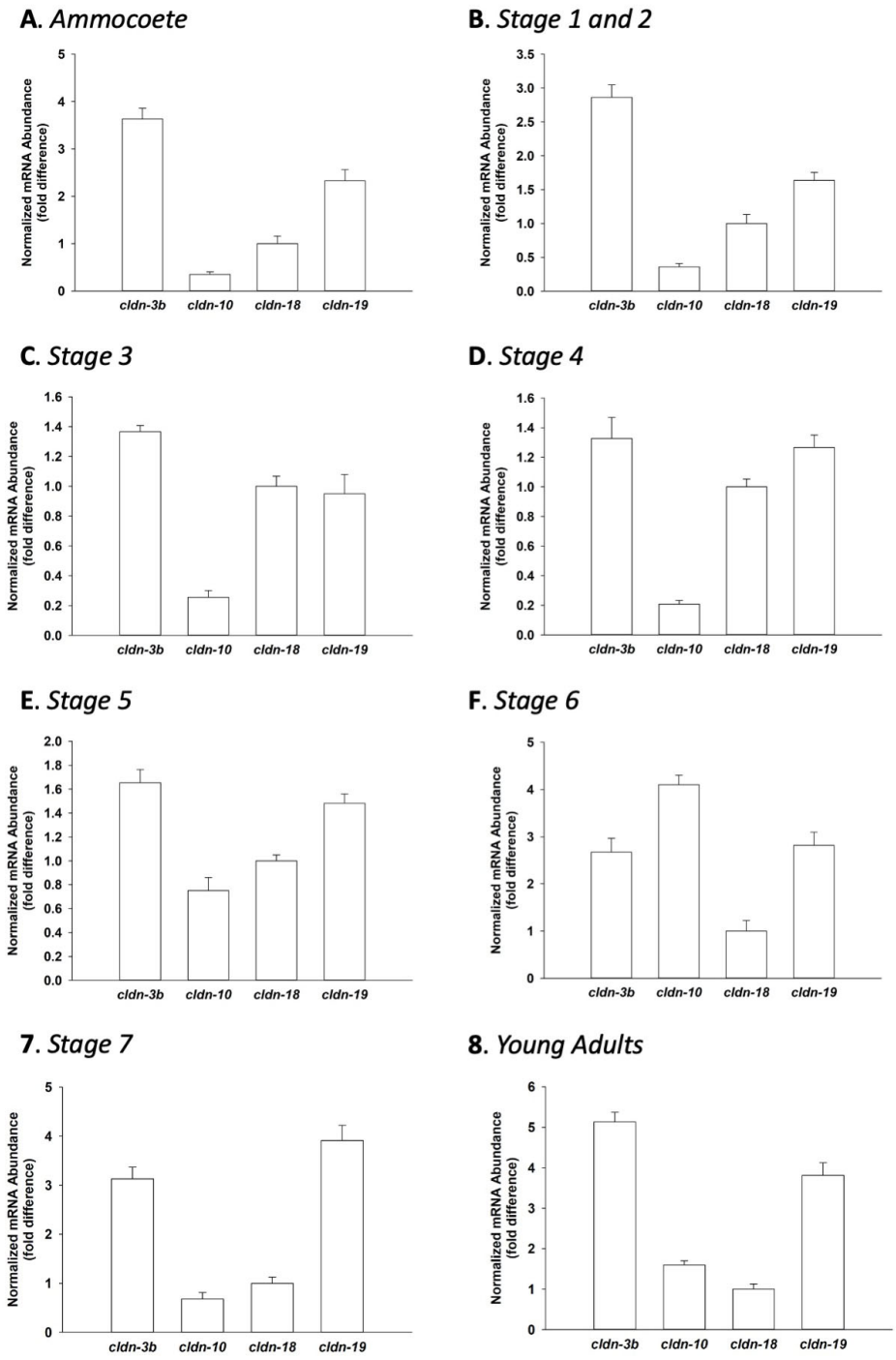

Figure 5-3. Normalized mRNA abundance of *cldn-3b*, *-10*, *-18*, and *-19* in the sea lamprey gill tissue from ammocoete to young adults. Data are normalized to elongation factor-1α and standardized to *cldn-18*.

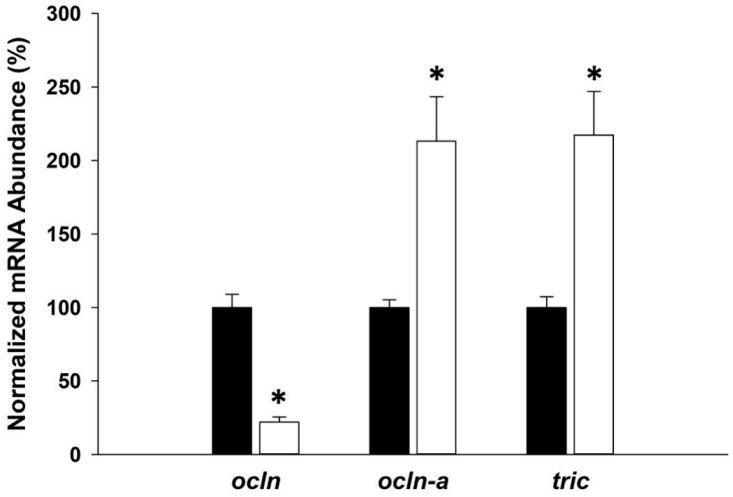

Figure 5-4. Effects of seawater exposure (35‰, open bar) on gill TJ mRNA transcript in young adult sea lampreys. Data are normalized to elongation factor-1α and standardized to freshwater (closed bar). Significant difference by Student's t-test denoted by Asterisk (*). All values denoted as mean ±S.E.M. (n = 8-9).

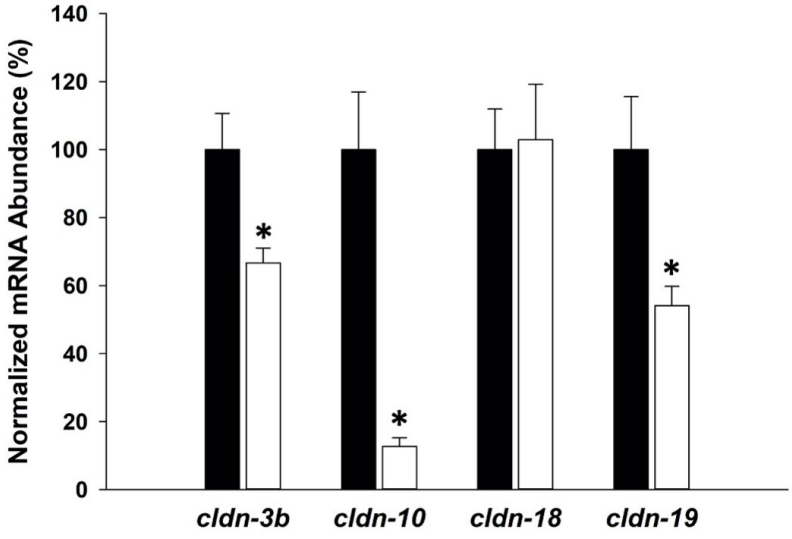

Figure 5-5. Effects of seawater exposure (35‰, open bar) on gill claudin (*cldn*) mRNA transcript in young adult sea lampreys. Data are normalized to elongation factor-1α and standardized to freshwater (closed bar). Significant difference by Student's t-test denoted by Asterisk (*). All values denoted as mean ±S.E.M. (n = 8-9).

5.5. Results

In the gill, mRNA abundance of MARVEL-domain containing TJ-associated genes *ocln*, *ocln-a*, and *tric* did not significantly alter from larva through stages S1 – S7 of metamorphosis (**Figure 5-1**). However, following metamorphosis, the gill of young adult lamprey exhibited significantly elevated mRNA abundance of *ocln* and significantly decreased mRNA abundance of *ocln-a* (**Figure 5-1A** and **1B**). Transcript abundance of *tric*, however, remained unchanged in the gill of post-metamorphic lamprey (i.e. *tric* mRNA abundance did not change at all during the peri-metamorphic period examined) (**Figure 5-1C**). Transcript abundance of various *cldn* family TJ proteins were examined in this study including *cldn-3b*, *-10*, *-14, -18*, and *-19* (**Figure 5-2**). No significant alteration in mRNA abundance was detected for either *cldn-3b* or *-19* during the entire peri-metamorphic period examined (**Figure 5-2A** and **2D**). However, a significant increase in *cldn-10* mRNA transcript abundance was observed during S6 of metamorphosis (**Figure 5-2B**). Furthermore, mRNA abundance of *cldn-18* increased immediately at the onset of metamorphosis with a peak at S3 (**Figure 5-2C**). Transcript abundance of *cldn-18* then attenuated, and a significant reduction (relative to larval fish and all metamorphic periods) in the gill of young adults was observed (**Figure 5-2C**). Transcript encoding Cldn-14 was not detected in the gill tissue in any of the life cycle stages examined (data not shown). As a consequence of transcriptional alterations during metamorphosis, expression patterns of *cldn* genes (i.e. most to least abundant) were found to vary during the S1 – S7 periods of metamorphosis (**Figure 5-3**).

SW acclimation of young adult sea lamprey resulted in significant changes in mRNA abundance of TJ-associated genes. These included a significant reduction in gill *ocln* abundance coupled with significant increase in gill *ocln-a* and *tric* abundance (**Figure 5-4**). With the exception of *cldn-18*, which did not respond to SW acclimation, all other *cldn* (i.e. *cldn-3b*, *-10*,

and -*19*) mRNA abundance significantly decreased in the gill SW acclimated lamprey (**Figure 5-5**).

5.6. Discussion

5.6.1. Overview

This study considered peri-metamorphic transcriptional events in the gill TJ complex of the sea lamprey. The indirect development of sea lamprey is discernable by dramatic morphological and physiological changes that include alterations in the gill epithelium. Data from the current investigation suggest that select TJ proteins (e.g. Cldn-18 and -10) exhibit marked alterations in abundance during defined stages of metamorphosis, while other proteins (e.g. Ocln and Ocln-a) alter upon the completion of metamorphosis. Only *cldn-18* was found to exhibit alterations in transcript abundance in both situations, while mRNA abundance of *tric*, *cldn-3b* and *cldn-19* did not significantly change at any point during the peri-metamorphic period examined in this study. In contrast, when young adult lamprey were acclimated from FW to SW (to simulate post-metamorphic SW entry), all but one gene encoding the TJ proteins examined in this study exhibited a significant change in mRNA abundance. This would suggest that adjustments in the molecular architecture of the gill TJ complex of lamprey upon SW entry has a much more profound impact on TJ form and function than changes that occur during metamorphosis. However, from a transcriptional standpoint there are two interesting trends to note: (1) The most responsive TJ-associated gene during the peri-metamorphic period, *cldn-18*, is also the only TJ-associated gene (in this study) that does not exhibit an alteration in abundance following acclimation to SW. Because transcript abundance of *cldn-18* in young adults is significantly lower than larval lamprey or lamprey in S1 – S7, this may indicate that the contribution of Cldn-18 to gill epithelium barrier

properties in SW is organized in advance of SW entry; (2) Changes in transcript abundance of *ocln* and *ocln-a* in post-metamorphic lamprey held in FW (i.e. an increase in *ocln* and decrease in *ocln-a*) are reversed when these fish are acclimated to SW (i.e. *ocln* mRNA abundance decreases and *ocln-a* increases). This suggests that post-metamorphic alterations in Ocln and Ocln-a contribute to the maintenance of salt and water balance in a more active FW lamprey life stage, but that this contribution is reversed in SW. Taken together, the current study provides a first look at peri-metamorphic alterations in gill TJ-associated genes of a basal vertebrate and provides insight into gill MARVEL-domain associated TJ proteins in SW acclimation of lamprey.

5.6.2. Tight Junction Transcript Changes in Metamorphic Sea Lampreys

Developmental changes associated with basal vertebrate TJs were first examined in the context of *cldn* regulation during sea lamprey morphogenesis (Mukendi et al., 2016). In contrast, the current study examines changes in TJ-associated gene transcripts with respect to sea lamprey metamorphosis. Consequently, we examined how changes in TJ profile may contribute to osmoregulatory strategies in larval, metamorphic and young adult sea lamprey. Despite remaining in FW during metamorphosis (and for at least a short while afterwards), the gills of sea lamprey undergo cellular rearrangement and compositional alterations during metamorphosis (Bartels et al., 2015, 2011; Bartels and Potter, 2004). However, these changes appear to occur later in metamorphosis (Peek and Youson 1979) than changes in other organs such as the intestine, kidney, liver and endostyle (Ooi and Youson 1979; Youson and Connelly 1978; Youson and Sidon 1978; Youson et al 1977). Nevertheless, adjustments in the gill epithelium cell-type and cell-type abundance can potentially alter TJ architecture as TJ proteins were previously demonstrated in teleosts to be associated with specific gill cell types (Bui and Kelly, 2014; Chen et al. 2020).

A major alteration in TJ protein transcript associated with sea lamprey gill during metamorphosis was observed in *cldn-18*. This first occurred at the onset of metamorphosis (S1 + S2) and peaked at S3. Altered *cldn-18* mRNA abundance was followed by an increase in *cldn-10* transcript abundance that peaked with S6 of metamorphosis. All other genes examined did not show transcriptional changes during S1 to S7 phase despite significant differences occurring in *ocln* (increased) and *ocln-a* (decreased) abundance in post-metamorphic young adults. The association of TJ transcript to the composition of the sea lamprey gill organ is not well understood. However, Peek and Youson (1979) have provided elegant descriptions of the cellular changes in the gills of metamorphosing sea lamprey. There are four main types of epithelial cells overlaying the lamprey gill organ: intercalated mitochondria-rich (MR) cells, ammocoete MR cells, pavement cells, and chloride cells (Bartels and Potter, 2004). The presence and absence of specific cell types are dependent on each lamprey life cycle, as well as adult lamprey migration and salinity tolerance. In metamorphosing sea lampreys, the cells of the gill epithelium begin to transform as the animal switches from an unidirectional respiratory current to a tidal flow around the start of S3 (Peek and Youson, 1979). The change in respiratory current is crucial for the change in feeding strategy. Furthermore, while it is not known whether sea lamprey metamorphosis is directly regulated by thyroid hormone, thyroid hormone levels that increased through the ammecoete stage decreases sharply in metamorphosing lampreys, and is lowest in S3 lampreys (Youson et al., 1994).

Post S3 sea lampreys were previously found to tolerate salinity above 10 ‰ and with increased salinity tolerance at each successive stages (Patrick Reis-Santos et al., 2008). This ability to tolerate increasing salinity was previously highlighted as changes in Na^+-K^+-ATPase activity and regulation (P. Reis-Santos et al., 2008). While the functional significance of various claudins in sea lampreys are not well understood, changes in TJ transcript may contribute to the increased

salinity tolerance to elevated environmental osmolality. Despite current data suggesting *cldn-18* does not respond to salinity in the gill organ, however, there were two notable observation from the study by Kolosov and colleagues (2020): (1) *cldn-18* is ubiquitously expressed in all tissues, and (2) *cldn-18* responds to salinity change only in the kidney and intestine. The change in *cldn-18* may be critical during the initiation of organ remodeling. It can also be noted that changes in gill *cldn-18* also occurs concurrently with the extensive remodeling of the metamorphosing S3 sea lamprey kidney, where the morphology and functions of adult lamprey appears in S4 (Youson and Ooi, 1979). A second notable change observed in the current study is the sharp increase in *cldn-10* in S6 metamorphosing lampreys. In teleosts, *cldn-10* isoforms are highly associated with ionocytes (Chen et al 2020). While it is not known whether sea lamprey *cldn-10* is also associated with ionocytes, the chloride cells of adult lampreys begin to function during S6 metamorphosis (Peek and Youson, 1979). All genes examined in the current study are present in every life cycle stage with the exception of *cldn-14*. Transcript of *cldn-14* was absent in the gill of sea lampreys in a previous study (Kolosov et al., 2020). The absence of *cldn-14* transcript in the current study in surveying all life cycle stages and SW transfer provides further evidence that *cldn-14* may not be associated with the gill organ, or potentially an epithelium in direct contact with the aquatic medium.

Two genes encoding for Ocln TJ protein have previously been identified in sea lampreys with different sequence identity to mammalian Ocln protein (Kolosov et al. 2017). Moreover, the two identified Ocln and Ocln-a in sea lampreys have distinct localization profile in the gill organ and different response to IPW acclimation (Kolosov et al. 2017). Current data further distinguish the functional difference between the Ocln and Ocln-a as young adult lampreys showed contrasting changes in mRNA abundance between the two genes upon SW acclimation. The increase in *ocln*

in young adults may be a required barrier as the lampreys completes metamorphosis. Finally, the change in *ocln-a* may coincide with the time the adult lamprey gill cells begin to function.

5.6.3. Transcript Changes in Seawater Acclimated Sea Lampreys

In recent studies, salinity associated changes in TJ assembly have been a major focus in piscine osmoregulation (Chasiotis et al., 2012a; Kolosov et al., 2013b). Branchial epithelia of hypoosmoregulating fishes are crucial in driving the unidirectional extrusion of excess Na^+ and Cl^- ions while maintaining the overall barrier integrity (Evans et al., 2005). The recent study from Kolosov and colleages (2020) has reported on changes in the mRNA abundance of various *cldn* TJ-associated genes in the gill of young adult sea lamprey acclimated to 60% SW (~ 20 ‰) for 3 days. In this regard, it was found that even after this comparatively short period in saline waters that are likely to be experienced in the estuarine reaches of migration routes, significant changes in the transcript abundance of several *cldns* occur (Kolosov et al 2020). The current work considers the molecular physiology of TJs in the young adult lamprey gill following acclimation to full strength SW (~ 35 ‰) for a period of three days, which would be consistent with SW entry proper, and much of the data is in-line with previous observations. More specifically, reductions in the mRNA abundance of gill *cldn-3b* and *cldn-10* were observed while gill *cldn-18* transcript abundance did not alter in response to elevated salinity (Kolosov et al., 2020). However, in this study, a reduction in *cldn-19* transcript abundance in SW was also noted. The reason for the decrease in the various gill claudins in seawater is not clear. As mentioned earlier, teleost cldn-10 isoforms are highly associated with ionocytes for the selective extrusion of Na^+ in the aquatic environment (Bui and Kelly, 2014; Chen et al 2020). However, the agnathan lineage did not experience the further genome duplication events that occurred in jawed vertebrates including

teleost (Osório and Rétaux, 2008). Sea lampreys may not have the diversity and functional specialization in TJ proteins as more derived vertebrates.

Transcription regulation of MARVEL-domain containing TJ proteins in response to SW acclimation has provided surprising results in the current study. While precise roles of both Ocln and Ocln-a in lampreys is currently not known, previous examination on IPW response of Ocln/Ocln-a in larval lampreys did not suggest potential barrier functions in line with Goldfish study (Chasiotis et al., 2012b; Kolosov et al., 2017). More surprisingly, transcript abundance of *ocln* and *tric* in SW acclimated juvenile lampreys respond in a manner similar to ammocoete in IPW acclimation. A potential explanation for the increase in *ocln-a* may suggest (1) Ocln-a may be associated with specific cell population of the lamprey branchial epithelium, much akin to the association of cldn-10 in teleost (Bartels and Potter, 2004; Bui and Kelly, 2014; Kolosov et al., 2014); or (2) an increase in ocln-a may be required to maintain the overall integrity of the epithelium as a global decrease is observed in various TJ transcripts upon SW acclimation. A hypothesis to the current observation is that the increase in MARVEL-domain containing proteins *ocln-a* and *tric* in full strength SW are critical in the maintenance of the overall barrier properties and integrity of the gill epithelium, whereas the decrease in gill claudins can be important for allowing the extrusion of monovalent sodium ions to the aquatic environment. This idea will require further examination.

5.7. Conclusions and Perspectives

The current study examined the transcriptional regulation of TJ protein associated genes in the gill of metamorphosizing sea lamprey and the response to SW acclimation. While sea lamprey remains a relatively novel model for understanding the molecular physiology of the TJ complex,

current experiments suggest potentially complex lamprey TJ regulation that is comparable to more derived fishes. In light of the current findings, one significant gap in the current knowledge is whether there are highly orchestrated compensatory mechanisms as each of the osmoregulatory organ takes its functions in metamorphosing sea lampreys. Furthermore, the development of primary cultured surrogate gill model can be highly advantageous to understand whether TJ components are specific to certain cells on the gill epithelium, and whether they respond to specific endocrine factors *in vitro*.

5.8. References

Abuazza, G., Becker, A., Williams, S.S., Chakravarty, S., Truong, H.-T., Lin, F., Baum, M. (2006) Claudins 6, 9, and 13 are developmentally expressed renal tight junction proteins. Am J Physiol Renal Physiol 291: F1132-41.

Anderson, J.M., Van Itallie, C.M. (2009) Physiology and function of the tight junction. Cold Spring Harb. Perspect. Biol. 1, a002584.

Angelow, S., Ahlstrom, R., Yu, A.S.L. (2008) Biology of claudins. Am J Physiol - Ren Physiol 295.

Bartels, H., Docker, M.F., Krappe, M., White, M.M., Wrede, C., Potter, I.C. (2015) Variations in the presence of chloride cells in the gills of lampreys (Petromyzontiformes) and their evolutionary implications. J Fish Biol 86: 1421–1428.

Bartels, H., Fazekas, U., Youson, J.H., Potter, I.C. (2011) Changes in the cellular composition of the gill epithelium during the life cycle of a nonparasitic lamprey: Functional and evolutionary implications. Can J Zool 89: 538–545.

Bartels, H., Potter, I.C. (2004) Cellular composition and ultrastructure of the gill epithelium of larval and adult lampreys: Implications for osmoregulation in fresh and seawater. J Exp Biol 207: 3447–3462.

Bui, P., Kelly, S.P. (2014) Claudin-6, -10d and -10e contribute to seawater acclimation in the euryhaline puffer fish Tetraodon nigroviridis. J Exp Biol 217: 1758–1767.

Chasiotis, H., Kolosov, D., Bui, P., Kelly, S.P. (2012a) Tight junctions, tight junction proteins and paracellular permeability across the gill epithelium of fishes: a review. Respir Physiol Neurobiol 184: 269–81.

Chasiotis, H., Kolosov, D., Kelly, S.P. (2012b) Permeability properties of the teleost gill epithelium under ion-poor conditions. Am J Physiol Regul Integr Comp Physiol 302: R727-39.

Dawson, H.A., Quintella, B.R., Almeida, P.R., Trebble, A.J., Jolley, J.C. (2015) The Ecology of Larval and Metamorphosing Lampreys. In Lampreys: Biology, Conservation and Control. Docker MF ed. Springer, Oregon, USA. P.75-125.

Evans, D.H., Piermarini, P.M., Choe, K.P. (2005) The multifunctional fish gill: dominant site of gas exchange, osmoregulation, acid-base regulation, and excretion of nitrogenous waste. Physiol Rev 85: 97–177.

Hilliard, R.W., Bird, D.J., Potter, I.C. (1983) Metamorphic changes in the intestine of three species of lampreys. J Morphol 176: 181–196.

Holmes, J.A., Beamish, F.W., Seelye, J.G., Sower, S.A., Youson, J.H. (1994) Long-term influence of water temperature, photoperiod, and food deprivation on metamorphosis of sea lamprey, *Petromyzon marinus*. Can J Fish Aquat Sci 51: 2045–2051.

Holmes, J.A., and Youson, J.H. (1994) Fall condition factor and temperature influence the incidence of meta- morphosis in sea lampreys, *Petromyzon marinus*. Can J Zool 72:1134–1140.

Holmes, J.A., Chu, H., Khanam, S.A., Manzon, R.G., Youson, J.H. (1999) Spontaneous and induced metamorphosis in the American brook lamprey, *Lampetra appendix*. Can J Zool 77: 959–971.

Johnson, N.S., Brenden, T.O., Swink, W.D., Lipps, M.A. (2016) Survival and metamorphosis of larval sea lamprey (*Petromyzon marinus*) residing in Lakes Michigan and Huron near river mouths. J Great Lakes Res 42: 1461–1469.

Kao, Y.H., Youson, J.H., Vick, B., Sheridan, M.A. (2002) Differences in the fatty acid composition of larvae and metamorphosing sea lampreys, *Petromyzon marinus*. Comp Biochem Physiol - B Biochem Mol Biol 131: 153–169.

Kolosov, D., Bui, P., Chasiotis, H., Kelly, S. (2013a) Claudins in teleost fishes. Tissue Barriers 1–15.

Kolosov, D., Bui, P., Donini, A., Wilkie, M.P., Kelly, S.P. (2017) A role for tight junction-associated MARVEL proteins in larval sea lamprey (*Petromyzon marinus*) osmoregulation. J Exp Biol 220: 3657–3670.

Kolosov, D., Bui, P., Wilkie, M.P., Kelly, S.P. (2020) Claudins of sea lamprey (*Petromyzon marinus*) – organ-specific expression and transcriptional responses to water of varying ion content. J Fish Biol 96: 768–781.

Kolosov, D., Chasiotis, H., Kelly, S.P. (2014) Tight junction protein gene expression patterns and changes in transcript abundance during development of model fish gill epithelia. J Exp Biol 217: 1667–1681.

Laudet, V. (2011) The origins and evolution of vertebrate metamorphosis. Curr Biol 21: R726–R737.

Manzon, R.G. (2011) Thyroidal regulation of life history transitions in fish. In: Mechanisms of life history evolution: The Genetics and Physiology of Life History Traits and Trade-Offs. Flatt T, Heyland A ed. (eds) Mechanisms of life history evolution: the genetics and physiology of life history traits and trade-offs. Oxford University, Oxford, pp 72–86.

Manzon, R.G., Manzon, L.A. (2017) Lamprey metamorphosis: Thyroid hormone signaling in a basal vertebrate. Mol Cell Endocrinol 459: 28–42.

McCormick, S.D., Regish, A.M., Christensen, A.K. (2009) Distinct freshwater and seawater isoforms of Na+-K+-ATPase in gill chloride cells of Atlantic salmon. J Exp Biol 212: 3994–4001.

Mukendi, C., Dean, N., Lala, R., Smith, J., Bronner, M.E., Nikitina, N. V. (2016) Evolution of the vertebrate claudin gene family: Insights from a basal vertebrate, the sea lamprey. Int J Dev Biol 60: 39–51.

Nelson, J.S. (2006) Fishes of the World. 4th ed. John Wiley and Sons, Inc. New Jersey, USA.

O'Boyle, R.N., Beamish, F.W.H. (1977) Growth and intermediary metabolism of larval and metamorphosing stages of the landlocked sea lamprey, *Petromyzon marinus L*. Environ Biol Fishes 2: 103–120.

Osório, J., Rétaux, S. (2008) The lamprey in evolutionary studies. Dev Genes Evol 218 :221–235.

Peek, W.D., Youson, J.H. (1979) Transformation of the interlamellar epithelium of the gills of the anadromous sea lamprey, *Petromyzon marinus L.*, during metamorphosis. Can J Zool 57: 1318–1332.

Potter, I.C. (1980) Ecology of Larval and Metamorphosing Lampreys. Can J Fish Aquat Sci 37: 1641–1657.9

Potter, I.C., Beamish, F.W.H. (1977) The freshwater biology of adult anadromous Sea lampreys *Petromyzon marinus*. J Zool 181: 113–130.

Potter, I.C., Wright, G.M., Youson, J.H. (1978a) Metamorphosis in the anadromous sea lamprey, *Petromyzon marinus L*. Can J Zool 56: 561–570.

Potter, I.C., Wright, G.M., Youson, J.H. (1978b) Metamorphosis in the anadromous sea lamprey, *Petromyzon marinus L*. Can J Zool 56: 561–570.

Purvis, H.A. (1980) Effects of Temperature on Metamorphosis and the Age and Length at Metamorphosis in Sea Lamprey (*Petromyzon marinus*) in the Great Lakes. Can J Fish Aquat Sci 37: 1827–1834.

Reis-Santos, P., McCormick, S.D., Wilson, J.M. (2008) Ionoregulatory changes during metamorphosis and salinity exposure of juvenile sea lamprey (*Petromyzon marinus L.*). J Exp Biol 211: 978–988.

Reis-Santos, P., McCormick, S.D., Wilson, J.M. (2008) Ionoregulatory changes during metamorphosis and salinity exposure of juvenile sea lamprey (*Petromyzon marinus L.*). J Exp Biol 211: 978–988.

Richards, J.E., Beamish, F.W.H. (1981) Initiation of feeding and salinity tolerance in the pacific lamprey *Lampetra tridentata*. Mar Biol 63: 73–77.

Smith, J.J., Kuraku, S., Holt, C., et al. (2013) Sequencing of the sea lamprey (*Petromyzon marinus*) genome provides insights into vertebrate evolution. Nat Genet 45: 415–421.

Swink, W.D., Johnson, N.S. (2014) Growth and Survival of Sea Lampreys from Metamorphosis to Spawning in Lake Huron. Trans Am Fish Soc 143: 380–386.

Van Itallie, C.M., Anderson, J.M. (2006) Claudins and Epithelial Paracellular Transport. Annu Rev Physiol 68: 403–429.

Youson, J.H. (1988) First metamorphosis. In: Hoar WS, Randall DJ (eds) Fish physiology, vol 11. Academic Press, San Diego, pp 135–196.

Youson, J.H. (2003) The biology of metamorphosis in sea lampreys: endocrine, environmental, and physiological cues and events, and their potential application to lamprey control. J Great Lakes Res 29: 26–49.

Youson, J.H. (1997) Is lamprey metamorphosis regulated by thyroid hormones? Am Zool 37: 441–460.

Youson, J.H., M, P.E., Leatherland John F (1994) Concentrations of insulin and thyroid hormones in the serum of landlocked sea lampreys (*Petromyzon marinus*) of three larval year classes, in larvae exposed to two temperature regimes, and in individuals during and after metamorphosis. Gen Comp Endocrinol 94: 294–304.

Youson, J.H., Ooi, E.C. (1979) Development of the renal corpuscle during metamorphosis in the lamprey. Am J Anat 155: 201–221.

Youson, J.H., Potter, I.C. (1979) A description of the stages in the metamorphosis of the anadromous sea lamprey, *Petromyzon marinus L*. Can J Zool 57: 1808–1817.

Youson J.H. (1985) Organ Development and Specialization in Lamprey Species. In: Foreman R.E., Gorbman A., Dodd J.M., Olsson R. (eds) Evolutionary Biology of Primitive Fishes. NATO ASI Series (Series A: Life Sciences), vol 103. Springer, Boston, MA pp.141-164.

Chapter 6. Development of a Primary Cultured Sea Lamprey (*Petromyzon marinus*) Gill Epithelium

6.1. Summary

Primary culture techniques have played significant roles in understanding the physiology of the branchial epithelium in various fish species. The use of primary culture and surrogate gill models has not only allowed transport studies to be conducted on an otherwise architectural complex organ, it has also contributed vastly to a mechanistic approach to physiological and toxicological studies. The current study reports on the development of a primary cell culture technique using larval sea lamprey (*Petromyzon marinus*) gill cells and gill explants to reliably establish a lamprey gill epithelium model in both tissue culture wells and on permeable supports. Outgrowth from gill explants produced a consistent area of coverage up to and after ~ 20 days in culture, producing epithelia that were ~ 10 mm in diameter. In cell culture inserts outgrowth from gill explants was sufficient to cover cell culture inserts with a growth area of 0.3 cm^2 and these cells formed an epithelium that generated an appreciable increase in transepithelial electrical resistance (TER) to a plateau of ~ 600 Ω cm^2. Molecular profiling of cultured preparations revealed transcripts of tight junction (TJ) assembly proteins that included claudins (*cldn*) *-3b*, *-18*, and *-19*, as well as occludin-a (*ocln-a*) and tricellulin (*tric*). Transcript encoding *cldn-10* and *-14* were absent from the cultured preparation, as was *ocln*/Ocln. Western blotting verified the presence of Ocln-a in the gill explants. We examined the response of cultured preparations to 11-deoxycortisol, but only transient effect on TER was observed following treatment with 10 ng/mL 11-deoxycortisol. The current work provides the first model gill epithelium for the study of basal vertebrate (agnathan) branchial function.

6.2. Introduction

Primary culture gill epithelium models derived from the gill of teleost fishes have advanced the understanding of branchial physiology and contributed critically to environmental monitoring and toxicological studies. The use of surrogate gill models to consider mechanistic questions in gill ion transport physiology was first introduced using the seawater-acclimated killifish (*Fundulus heteroclitus*) opercular skin, which helped to define mechanisms of Cl^- transport across teleost branchial epithelia (Karnaky et al. 1977). The opercular epithelium, and other isolated preparations, are comparatively simple flat epithelia that exhibit the same cellular composition as the gill epithelium but overcome the architectural complexity of the organ (Karnaky and Kinter 1977; Marshall 1977). However, isolated tissues/organs are limited by having a finite period of viability, and in the early 90s the first primary culture model fish gill epithelium was developed by Pärt and colleagues (1993) using the rainbow trout (*Oncorhynchus mykiss*). Since the initial introduction, new techniques have been developed for several fish species using various solid and permeable supports (Wood and Part 1997; Fletcher et al. 2000; Kelly and Wood 2002; Bui et al. 2010; Chasiotis and Kelly 2011).

Primary culture of fish gill cells provides advantages over *in vivo* studies that include minimizing the number of animals sacrificed for experiments (Bury et al. 2014). However, the key advantage primary cultured gill models are that they can provide a tissue-specific mechanistic view on cellular regulation in response to physiological and environmental changes. Primary culture of fish gill cells has provided knowledge on the endocrine regulation of the branchial epithelium in several teleost species. These endocrine regulations include corticosteroid (Kelly and Wood 2001; Chasiotis and Kelly 2011), luteotropic (Kelly and Wood 2002), and thyroid hormone (Kelly and Wood 2001) regulation of the gill epithelium. Furthermore, asymmetrical culture condition in

primary culture allows an examination of the branchial epithelium in response to alterations in osmotic gradient (Gilmour et al. 1998). Primary culture has also allowed toxicological exposure including heavy metals such as copper to be conducted directly on gill cells (Nogueira et al. 2020). The numerous advantages of primary culture provide valuable insights in both basic and applied biological research.

Lampreys are basal vertebrates belonging to the superclass Agnatha that includes all extant jawless fishes (Nelson 2006). The sea lampreys (*Petromyzon marinus*), in particular, has gained considerable research interests in terms of population control strategies as this parasitic species has significant economic impact in the Great Lakes of North America. However, despite being an invasive specie, there has also been considerable interests in lamprey physiology and biological adaptations. Extant jawless fishes share similar morphological traits as their evolutionary ancestors (Gess et al. 2006). Understanding the evolutionary perspective of jawless fishes have been proposed to link key findings in the evolution of more derived vertebrate characteristics (Smith et al. 2013). In the context of membrane transport properties of the gill epithelium, one should highlight the evolutionary significance of the vertebrate tight junction (TJ) assembly that has been demonstrated to partake a critical part in the regulation of salt and water balance in aquatic vertebrates.

The TJ complex is a hallmark of the vertebrate epithelium that forms intercellular junctions on the apical-lateral position between epithelial cells (González-Mariscal et al. 2003). The TJ complex mediates paracellular permeability and has been demonstrated to play significant roles in piscine physiology (for review see Chasiotis et al. 2012; Kolosov et al. 2013). Most notably, endocrine regulations of primary cultured branchial epithelia are directly associated with modulation of the TJ assembly components (Bui et al. 2010; Chasiotis et al. 2010; Chasiotis and

Kelly 2011, Kolosov and Kelly 2013). The molecular physiology of the TJs and TJ proteins in fishes have advanced since their identification in the Japanese puffer (Loh et al. 2004). In lampreys, TJs have been identified and described in the gills using electron microscopy and, in this organ, they have been observed to undergo significant morphological alterations in association with salinity change (Bartels and Potter 1991; Bartels and Potter 1993; Bartels and Potter 2004). The idea that this would occur in conjunction with alterations in the molecular physiology of the TJ complex is supported by the molecular and biochemical identification of MARVEL-associated and claudin (Cldn) family TJ proteins in the sea lamprey (Kolosov et al. 2017; Kolosov et al. 2020), which selectively exhibit alterations in mRNA and protein abundance in responce to environmental salinity changes (Kolosov et al. 2017; Kolosov et al. 2020). But how these changes in gill TJ physiology might be linked to the endocrine system in lamprey, as occurs in teleost fishes, remains unexplored. Close and colleagues (2010) have provided evidence that 11-deoxycortisol is the main corticosteroid in sea lamprey where it plays a role in the stress response and salinity acclimation. Corticosteroids have been reported to tighten vertebrate epithelia (i.e. reduce paracellular permeability) by increasing the abundance of a variety of barrier-forming TJ proteins in fishes (Bui et al. 2010; Chasiotis et al. 2010; Chasiotis and Kelly 2011, Kolosov and Kelly 2013). These studies have invariably used primary cultured models to establish this tightening effect, therefore it would be useful to develop and utilize a comparable primary culture system for the sea lamprey gill to consider the hypothesis that corticosteroids may tighten the epithelia of a basal vertebrate also.

The current study reports on the development of a primary culture model system derived from the gill tissue of the larval sea lamprey (*P. marinus*). The first objective was to establish a reliable methodology to generate a confluent primary culture epithelium composed of larval sea

lamprey gill cells on both solid substrate as well as on permeable supports. The latter allows the barrier properties of the epithelium to be examined. Once this had been established, I sought to examine the molecular physiology of the TJ complex, which largely dictates the resistive properties of high resistance epithelia such as the fish gill. Finally, I exposed the cultured preparations to 11-deoxycortisol to see if this hormone would impact the electrophysiology of the model gill epithelium.

6.3. Materials and Methods

6.3.1. Animals

Sea lamprey ammocoetes were collected from tributaries of the Richibucto River, New Brunswick, using pulsed DC backpack electrofishing (Mode LR20, Smith-Root, Vancouver, WA). Fish were housed in York University aquatics facilities in 200 L opaque polystyrene aquaria supplied with flow-through, dechlorinated City of Toronto tap water (10-12°C; approximate composition in μM: Na^+ 590; Cl^- 920; Ca^{2+} 900; K^+ 50; pH 7.4). Fish were kept under a constant photoperiod (12 h light : 12 h dark) and polyester fiber was added to each aquarium as substrate into which larvae could burrow. Water was aerated gently with an air curtain. Animals were fed once weekly with commercial active dry yeast (Lesaffre Yeast Corporation, WI, USA) at approximately 0.125 g of dry yeast per liter holding volume. Fish were size matched for each gill explant experiments conducted. Animal husbandry and all experiments were conducted in accordance with Canadian Council on Animal Care (CCAC) guidelines and under an approved York University Animal Care Committee protocol.

6.3.2. Preparation of Explant Culture Substrate and Reagents

Tissue culture surfaces were coated with type I collagen (15 µg·cm^{-2}; Collagen, Type I solution from rat tail; Millipore Sigma, St-Louis, MO, USA) and fibronectin solution (1 µg·cm^{-2}; Fibronectin from bovine plasma; Millipore Sigma) prior to experiments. Coated culture substrates (tissue culture wells and inserts) used immediately after coating for experiments. Preparation for lamprey explant culture reagents and media were similar to trout primary gill cell culture as described by Kelly et al. (2000). A 30 mL wash solution (WASH) was prepared containing 200 units/mL penicillin-streptomycin solution (Pen Strep; Gibco, Grand Island, USA), 0.4 mg/mL Gentamicin (Gibco), and 2.5 µg/mL Amphotericin B (Gibco) in sterile phosphate buffered saline (PBS, pH 7.7). Culture media was prepared with Leibovitz's L-15 Medium (L-15, Gibco) containing 100 units/mL Pen Strep, 0.05 mg/mL Gentamicin, and 10% fetal bovine serum (FBS, Qualified, Canadian Origin, Gibco). Preparation of all explant solutions followed aseptic technique in a Class II biosafety cabinet.

6.3.3. Preparation of Stock 11-Deoxycortisol Solution and 11-Deoxycortisol Treatment Media

A stock solution of 11-deoxycortisol (Reichstein's Substance; Sigma-Aldrich, Oakville, ON) was prepared by dissolving 11-deoxycortisol in 100% ethanol to make a 10 mg/mL stock solution. The stock solution was stored at - 30°C in single use aliquots. Prior to use, the stock aliquot was diluted with L-15 to prepare each final working concentration for an experiment. The final ethanol volume required to dissolve 11-deoxycortisol is less than 1% of the final media volume and did not have an effect on the culture preparation.

6.3.4. Gill Tissue Isolation and Explant Preparation

The anterior end of sea lamprey ammocoete was severed using a sharp razor blade just posterior to the last pair of the gill slits (anterior to the heart). The separated region was then opened lengthwise along the ventral midline from the anterior end at the bottom of the mouth to the posterior position of the initial cut. Gill arches were carefully (and cleanly) removed from the cartilage and bathed immediately in ice-cold L-15 medium. Eight arches were dissected from each sea lamprey posterior to the first set of gill arches, which were always excluded. The gill arches were cut into smaller pieces of approximately 4 filaments each. Each piece was considered a single explant. The explants were rinsed with PBS (pH 7.7) prior to transferring into a sterile 50 mL conical tube containing 10 ml WASH in the bio-safety cabinet. Explants were washed a total of three times (10 mL for 10 min each at 4 °C) with intermittent vigorous agitation during each incubation period. The explants were then used after being thoroughly rinsed with ice-cold PBS (pH 7.7) to remove all WASH.

Explants were placed directly on prepared culture surface using sterile forceps. A single filament bundle is placed in the center of the culture substrate as starting explant. A minimum volume of prepared media was added directly on top of the dissected explant. In 12 and 24 well cell culture plates (BD Falcon, culture areas = 3.5 cm^2 and 1.9 cm^2, respectively), the initial media volume used was 250 µL for explants in 12 well tissue culture plates and 150 µL in 24 well plates (BD Falcon, culture areas = 3.5 cm^2 and 1.9 cm^2, respectively). One well in each culture plate is kept without explant and filled with sterile distilled water to maintain overall humidity. Initiation of gill explants on 24 well permeable supports (Transparent PET Membrane, 0.3 cm^2 culture area, 0.4 µm pore size, 1.6 x 10^6 pores/cm^2) is similar to the tissue culture plates, but complete media was kept in the basolateral compartment and in contact with the PET membrane. The initial L-15

volume used for inserts was 50 µL for the apical surface and 600 µL for the well (basolateral side) in 24 well plates. The tissue culture plates were sealed around the edge with parafilm, and the explants were incubated in an air atmosphere incubator at 18°C. For the first five days, 50 µL of L-15 was added per day regardless of wells or inserts culture with minimal disturbance to the explant tissue. On day six, media was exchanged with a volume that is double the initial volume (i.e. 500 µL in 12 well plates). Media is then refreshed every other day with a doubling of media volume at every second media exchange until the volume equals to 5 mL for 12 well plates and 2 mL for 24 well plates. The media volume for cultured epithelium on 24 well insert was 350 µL in the apical compartment and 800 µL in the basolateral compartment.

6.3.5. Measurement of Explant Diameter Measurements and Transepithelial Electrical Resistance

Images of complete explant preparations were captured using an Olympus digital camera (OM-D E-M5 Mark II) adapted to an inverted phase contrast microscope for explant imaging diameter measurements. Average diameter measurements were estimated in ImageJ software by first drawing a calibrated rectangle enclosing the culture explant. The estimated diameter was then calculated as the average of the width, height, and diagonal length across the rectangle drawn.

The measurement of transepithelial electrical resistance (TER) across confluent lamprey gill epithelia grown on permeable cell culture filter supports for conducted using STX-2 chopstick electrodes connected to an EVOM epithelial voltohmmeter (World Precision Instruments, Sarasota, FL). TER was expressed as ohms per centimeter squared ($\Omega \cdot cm^2$) after correcting for the background resistance of the culture insert.

6.3.6. Transcript Abundance of TJ-Encoding Genes in Gill Explant Preparations

Gill epithelium preparations on permeable inserts with measurable plateau in TER were collected for total RNA isolation and cDNA synthesis. Culture media was first aspirated from both the apical and basolateral side of the culture insert then, the gill explant was removed using sterile fine forceps. A fixed volume (200 µL) of TRIzol reagent (Life Technologies, Burlington, ON, Canada) was used to lyse the cells directly on the culture insert, and the volume was adjusted to 500 µL for total RNA isolation following the manufacturer's protocol. RNA pellets were resuspended in RNase-free water and quantified using a Nanodrop 2000 spectrophotometer (Thermo Fisher Scientific, Waltham, MA, USA) with sample quality determined by A260/A280 ratio. A fixed quantity of total RNA (2 µg) was treated with ezDNase™ Enzyme (Life Technologies, Burlington, ON, Canada), and first-strand synthesis was carried out using SuperScript™ IV VILO™ Master Mix (Life Technologies) following the manufacturer's protocol.

Quantitative polymerase chain reaction (qRT-PCR) experiments were conducted using a CFX Connect™ Real-Time PCR Detection System (Bio-Rad Laboratories, Inc., Mississauga, ON) with iQ SYBR Green Supermix (Bio-Rad Laboratories, Inc.) under the following conditions: 95 °C for 10 min, 40 cycles of 95°C for 30 s, primer specific annealing temperature (T_A) for 60 s, read every cycle. A melt curve analysis was conducted one degree below T_A to 95°C, read every 0.5°C for each qRT-PCR experiment. PCR primers were previously verified and are summarized in **Table 5-1** (Page 192**,** Kolosov et al. 2017; Kolosov et al. 2020). Stability of reference gene (elongation factor-1α) was confirm prior to expression profile analysis. Analysis of transcripts encoding TJ proteins were conducted using Bio-Rad CFX Maestro 1.1 Software (Bio-Rad Laboratories, Inc.; Version 4.1.2433.1219).

6.3.7. Western Blotting

Protein fractions from total RNA isolation was reserved for Western blotting of sea lamprey OCLN and OCLN a. Protein pellets were precipitated with 100% isopropanol followed by three washes (20 min each) in 0.3 M guanidine hydrochloride solution. Pellets were then washed once (20 min) with anhydrous ethanol (Sigma-Aldrich) and pooled (two per sample) prior to dissolving in 1% sodium dodecyl sulfate (1% SDS) with 4 M urea solution (with ultrapure water). Protein concentration of the suspension was determined using a Micro bicinchoninic (BCA) Protein Assay Kit (Thermo Scientific, Rockford, IL) according to the manufacturer's instructions and using a Multiskan spectrophotometer (Thermo Fisher Scientific, Nepean, ON). For protein separation, 5 µg of total protein was first treated with a sample buffer (Tris 60 mM; SDS 2%; glycerol 10%; Bromophenol Blue 0.0025%; 3% β-mercaptoethanol) and heated (70°C, 15 min). SDS-PAGE electrophoresis was carried out with a 4% stacking gel and 10% separating gel in a Mini-PROTEAN Tetra Cell apparatus (Bio-Rad Laboratories, Inc.) with a tris-glycine buffer and allowed to migrate at a constant voltage (150 V).

Electrophoresis sample was blotted onto an Immobilon® PVDF membrane (0.45 µm pore size; Merck Millipore) with a chilled wet-transfer unit (Amersham Biosciences; 150 mA; 80 mins). Membrane was then briefly rinsed in Tris-buffered saline with 0.1% Tween-20 (TBS-T; 20 mM Tris, 50 mM NaCl, pH 7.6) and blocked with a blocking solution (5% skim milk in TBS-T) for 1 h at room temperature. Following this, the membrane was incubated overnight at 4°C with custom antibodies against sea lamprey OCLN or OCLN-a (Kolosov et al. 2017). A commercial secondary antibody (Bio-Rad Laboratories, Mississauga, ON) was used to detect the primary antibodies on the membrane. Blots were imaged using a ChemiDoc™ Gel Imaging System (Bio-Rad Laboratories, Mississauga, ON).

6.3.8. Statistical Analysis

All data are expressed as mean ± S.E.M. (n) where n represents the number of pooled or individual model preparations. In observing changes in TER of lamprey explant in response to 11-deoxycortisol media, two-way analysis of variance (ANOVA) with Tukey's post-hoc test was conducted on daily changes in resistance between groups. All statistical analyses were performed using SigmaPlot for Windows Version 14.0 (Build 14.0.3.192; Systat Software, Inc., San Jose, CA, USA).

6.4. Chapter 6 Figures

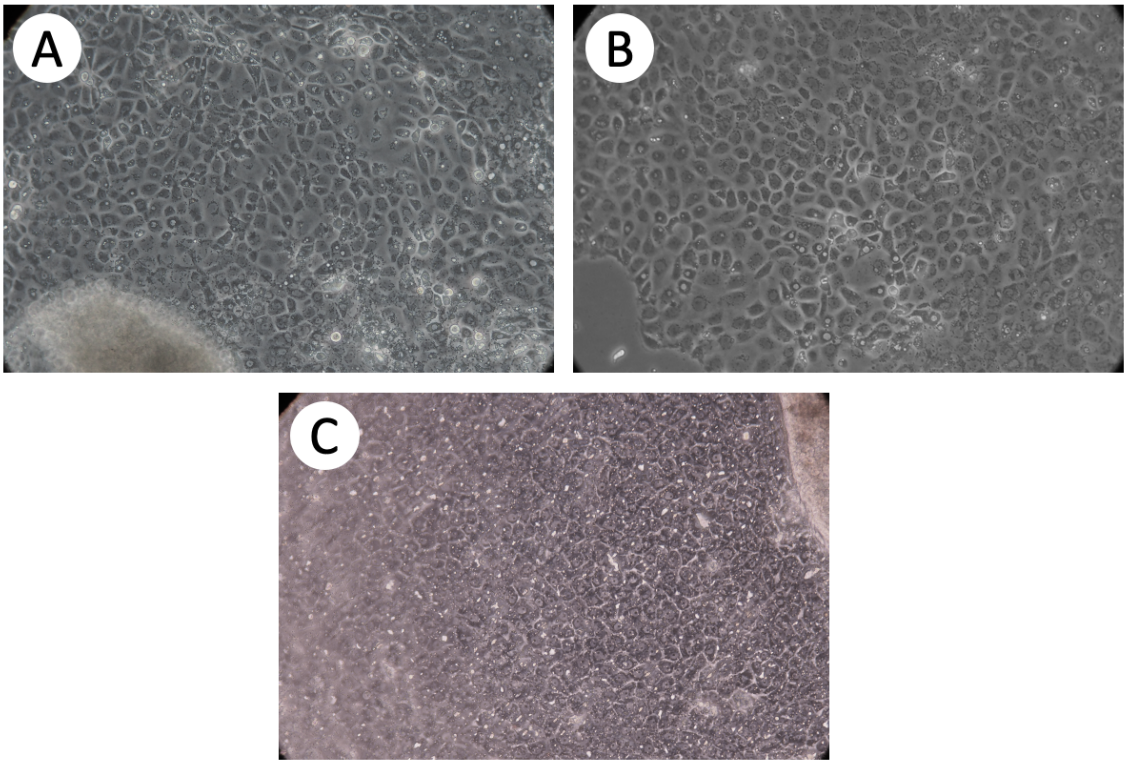

Figure 6-1. Phase contrast images of cultured sea lamprey gill outgrowth in tissue culture wells at close proximity to the original explant (A) and at the edge of proliferation (B). The gill explant was also able to attach to trans-well permeable tissue culture inserts (C)

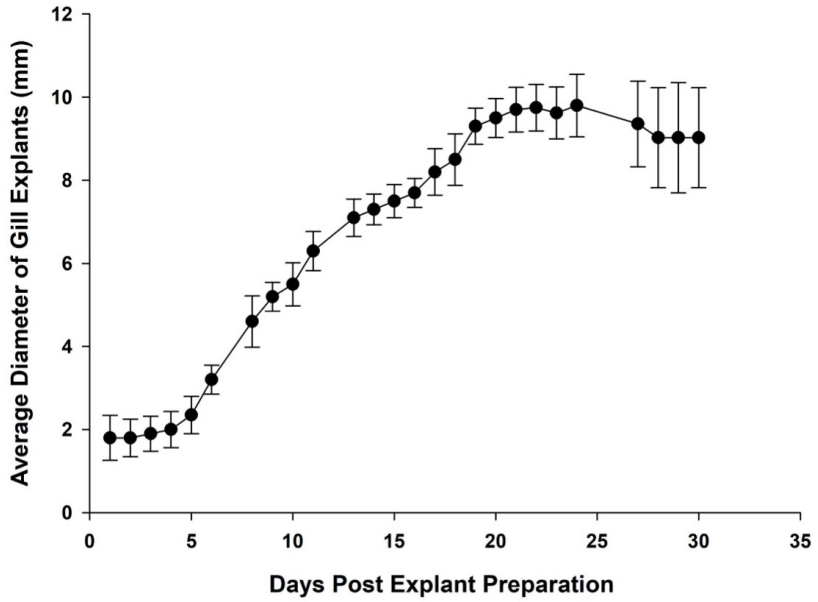

Figure 6-2. Growth curve of sea lamprey gill outgrowth average diameter over time in cultured wells. Data are expressed as means ± S.E.M. (n = 40 up to day 15, samples were gradually taken for experiment after day 15).

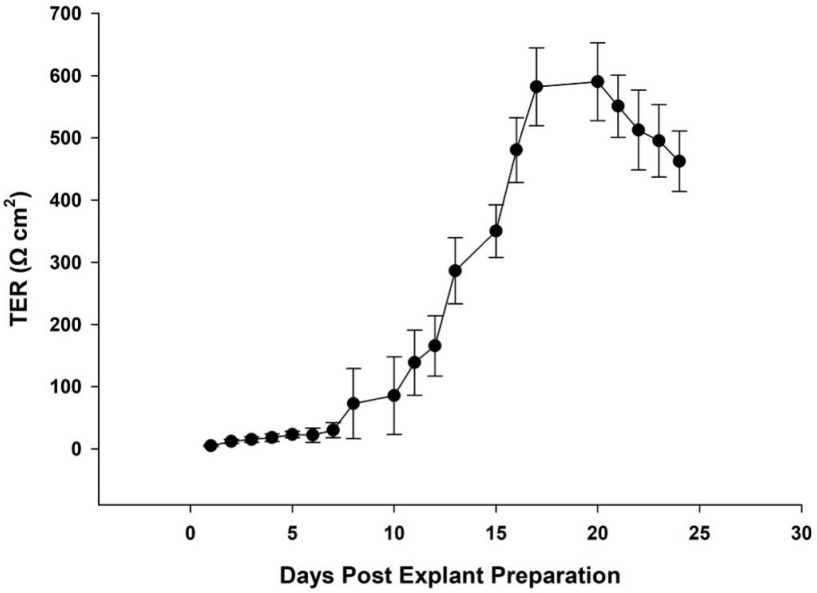

Figure 6-3. Changes in transepithelial electrical resistance (TER) in cultured ammocoete gill epithelium in 24-wells permeable inserts (culture area = 0.3 cm^2). Data are expressed as means ± S.E.M. (n = 6 fish, each fish represents an average of two cultured inserts).

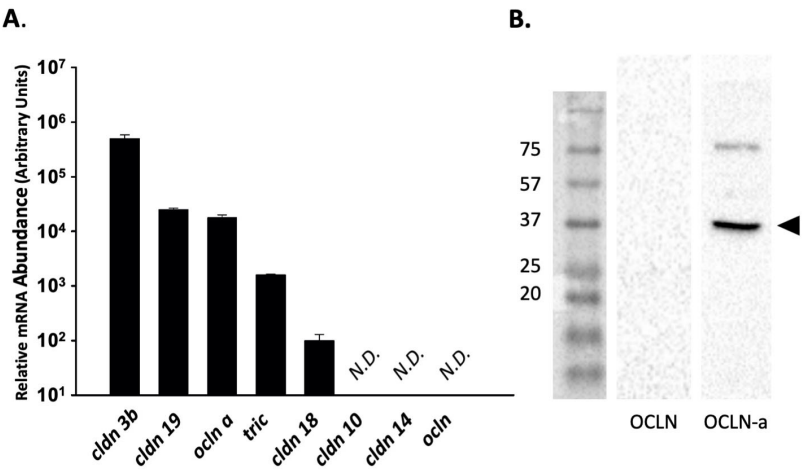

Figure 6-4. Relative mRNA transcript abundance of TJ encoding genes including claudins (*cldn*) *-3b*, *-10*, *-14*, *-18*, *-19*, occludin (*ocln*), occludin-a (*ocln-a*), and tricellulin (*tric*) in cultured sea lamprey gill epithelium. (A). Data are normalized to elongation factor-1α and expressed as means ± S.E.M. (n = 10). N.D. = not detected. Western blot with total protein homogenate with the gill explant detects the presence of OCLN-a, but not OCLN in the preparation (B).

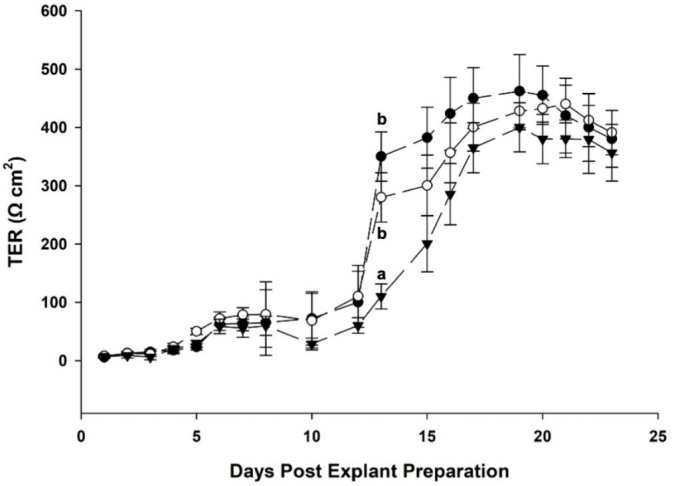

Figure 6-5. Changes in transepithelial electrical resistance (TER) in cultured ammocoete gill explants in 24-wells permeable inserts treated immediately after preparation with 0 (dark circle), 1 (open circle), and 10 (triangle) ng/mL 11-deoxycortisol per mL culture media. Data are expressed as means ± S.E.M (n = 6 – 8). Letters denotes a significant difference between groups by two-way analyses of variance (ANOVA; P≤0.05).

6.5. Results

Larval sea lamprey gill explants develop a confluent outgrowth of gill cells on solid (**Figure 6-1A** and **1B**) and cell culture insert (**Figure 6-1C**) surfaces when they are coated with type I collagen and fibronectin. Upon successful attachment to the substratum, the gill cells migrate, and significant outgrowth can normally be observed following approximately five days in culture. Cells in the epithelial outgrowth demonstrates polygonal morphology under light microscopy where each individual cell in the outgrowth can be identified (**Figure 6-1**). The gill cells gradually migrate outward across the substratum and the diameter of the outgrowth plateaus around 9-21 days after the preparation is first started when space is not limited (**Figure 6-2**). Moreover, the outgrowth can be maintained for a prolonged period (i.e. + 30 days) without alteration in cell morphology or significant detachment of cell outgrowth. Nevertheless, there appears to be a limit on the distance from the distal edge of the outgrowth to the edge of the original gill explant, with the diameter of solid substrate preparations exhibiting an upper plateau of ~ 10 mm (**Figure 6-2**).

Culture gill explants maintained in 24-well permeable culture inserts showed negligible transepithelial electrical resistance (TER) until the explant outgrowth achieve confluence on the permeable culture membrane at day 8-10 (**Figure 6-3**). Following the formation of a confluent preparation, TER values increased until a plateau of ~ 600 $\Omega \cdot cm^2$ was reached and maintained for ~ 5 days (**Figure 6-3**). Following this, TER values began to decline. Quantitative PCR reaction was used to detect transcripts of TJ-associated genes in the *in vitro* model preparations. Transcripts of TJ-associated genes detected included MARVEL-domain containing TJ proteins occludin a (*ocln a*) and tricellulin (*tric*) as well as various claudin (*cldn*) family TJ proteins including *cldn-3b*, *cldn-18*, and *cldn-18* (**Figure 6-4A**). TJ-associated genes that were investigated but were not detected in the model preparation included *ocln*, *cldn-10* and *cldn-14*. Western blot analysis of

cultured epithelium total protein isolate resolved a band corresponding to sea lamprey Ocln-a, but no antibody reactivity against Ocln was observed (**Figure 6-4B**).

Preparations on cell culture insert were used to examine the effects of 11-deoxycortisol on TER. Physiologically relevant concentrations of 11-deoxycortisol at 10 ng/mL transiently altered TER of cultured sea lamprey gill cells in this study, but no significant difference was observed after this time period (**Figure 6-5**).

6.6. Discussion

6.6.1. Overview

The current study reports that explants from larval sea lamprey gill can be used to generate a primary cultured model gill epithelium for the study of larval lamprey gill function. The model can be prepared on both solid substrate and cell culture inserts. While explant outgrowth is finite on solid substrate, the use of inserts with a growth area of 0.3 cm^2 allowed the gills cells to develop into a confluent layer, or epithelium, that exhibited an appreciable TER of ~ 600 Ω cm^2 after ~ 2 weeks in culture. Furthermore, the cultured larval lamprey gill epithelium model that develops on cell culture inserts exhibits a TJ protein gene expression profile that mirrors the intact gill and the electrophysiological properties are close to, but slightly lower, than those described for FW teleost fishes. When the model epithelium is treated with the corticosteroid 11-deoxycortisol, a significant (albeit transient at ~ 13 days) reduction in TER is seen in preparations treated with a higher dose of 10 ng/mL. Taken together, observations indicate that the primary cultured larval sea lamprey gill models derived from explants will provide a useful tool to further understand the branchial physiology of this basal vertebrate.

6.6.2. Notes on Establishment of Sea Lamprey Gill Explants

To examine the physiology of the sea lamprey gill, a variety of techniques to maintain viable cultures of larval sea lamprey gill cells were explored. Initially, I focused on culture systems with isolated gill cells that mirrored the techniques used for the primary culture of teleost gill cells (Pärt et al, 1993; Kelly et al. 2000). While I had initial success in culturing isolated lamprey gill cells that adhered and aggregated on culture substratum, the size of the ammocoete gill greatly limited the number of cells that could be isolated by enzymatic digest (i.e. approximately 2 million cells from all gill arches of a single lamprey versus over 250 million cells from a rainbow trout). Therefore, it became apparent that each experiment with isolated larval lamprey gill cells would require a large number of animals to generate sufficient experimental samples, and this does not align with the Canadian Council on Animal Care three Rs of humane animal experimentation – replacement, reduction and refinement (https://ccac.ca/en/three-rs-and-ethics/). By taking advantages of the adherent growth properties of epithelial cells, I was able to use explant cultures to generate an outgrowth of gill cells on substratum that, over time, provided a model epithelium. Depending on the surface area for growth, this allowed gill material from one fish to generate between 6 - 8 model epithelia. Not only does this approach provide an increased number of biological replicates for the study of model gill epithelia derived from the larval sea lamprey gill, but it also aligns with CCAC three Rs philosophy.

The migration of gill cells onto culture substrata was directly observable by light microscopy approximately three days following explant placement. Unattached gill explants would disintegrate and were removed from culture. Daily examination of the preparation was conducted and while bacterial contamination was rare, there exist potential for fungal

contamination as yeast is part of sea lamprey diet. For this reason, it was critical to pay close attention to the initial wash step and the experiments were never conducted on the day of feeding.

In utilizing the gill tissue as an explant, the current technique allows the original gill tissue to effectively seed the culture substratum with lamprey gill cells. The idea of removing the original explant tissue, so as to leave a uniform layer of gill cells on the culture substrate, was explored. However, in the culture of explants on permeable supports, it was found to be difficult to ensure that the PET membrane of the culture inserts remain intact after manipulation. Nevertheless, the explant-derived lamprey culture was largely composed of gill epithelium (over 90% of culture surface) and demonstrates development of electrical resistance upon confluence, and this technique has been applied frequently in mammalian derived explant models. The lamprey preparations exhibit a plateau in TER that is ~ 600 Ω cm^2 after ~ 15 days in culture. This TER value is close to the 800 – 1000 Ω cm^2 reported for primary cultured gill epithelium models derived from select species of FW teleost fish (Wood et al. 1998; Kelly and Wood 2002; Chasiotis and Kelly 2011). Typically, an epithelium that falls within this TER range would be considered electrically tight because the TER is an order of magnitude higher than that measured across epithelia that are classically considered to be "leaky", such as the rat jejunum (67 Ω cm^2 , Fromm et al, 1985) or flounder kidney (23 Ω cm^2 , Dickman and Renfro 1986). It is also higher than the TER measured across surrogate models of the SW teleost fish gill which are ~ 200 – 250 Ω cm^2 and contain numerous shallow "leaky" TJs (for review see Wood et al 2002). Nevertheless, it is lower than the typical FW teleost fish, but it is worth noting that the osmolality of larval lamprey blood, at ~ 225 mOsmol kg^{-1}, is considerably lower than that of a FW teleost fish 300 mOsmol kg^{-1}) as well as a lamprey residing in FW following metamorphosis (~ 260 mOsmol kg^{-1}). So, the slightly lower TER of a cultured larval lamprey gill epithelium may reflect a slightly leakier gill

epithelium versus other FW fish and this could be functionally meaningful in these animals. Finally, while the current preparation of cultured gill cells exhibits canonical epithelial cell morphology, future work using scanning and transmission electron microscopy should be conducted to identify the surface topography of the epithelium, including how many cell-layers the epithelium possesses, and more details on cellular composition as well as TJ architecture.

6.6.3. TJ Proteins in the Culture Sea Lamprey Gill Explants

The vertebrate TJ complex is multiprotein junctional structure located on the apical-lateral side of epithelial cells (Günzel and Fromm, 2012)). The TJ complex mediates paracellular permeability of an epithelial layer (González-Mariscal et al. 2003; Günzel and Yu 2013; Zihni et al. 2016), and recently it has been a focal point in piscine osmoregulation (reviewed by Chasiotis et al. 2012). TJ-associated MARVEL proteins and the claudin family of TJ proteins have not only been identified in the sea lamprey but have also been reported to respond to alterations in environmental salt content (Kolosov et al. 2017; Kolosov et al. 2020). Furthermore, sea lamprey development and metamorphosis has been shown to coincide with altered TJ mRNA abundance during specific developmental stages (see Chapter 5). Because the TJ complex is a hallmark that plays a central role in the barrier function of epithelial tissue, it is important to identify the molecular and biochemical components of the TJ complex in a model that would be used to investigate the physiological properties of an organ where epithelial barrier properties are crucial.

Examining the molecular physiology of primary cultured larval lamprey gill epithelium TJ-associated genes revealed that the molecular composition of the model epithelium TJ complex mirrored that of the intact larval lamprey gill. In particular, data on the transcript abundance of genes encoding Cldn TJ proteins indicated that *cldn-3b*, *-19*, and *-18* in the model exhibited an identical pattern of abundance when compared to the whole gill, with *cldn-3b* > *cldn-19* > *cldn-18*

(Kolosov et al. 2020; see Chapter 5). In addition, *cldn-14* was not detected in the gill model, and this gene was also found to be absent in the intact gill (Kolosov et al. 2020; see Chapter 5). However, *cldn-10* was also undetectable in the primary cultured larval lamprey gill epithelium, and this gene is found in the intact gill (Kolosov et al. 2020; see Chapter 5). In teleost fish gill epithelia, recent evidence supports the idea that Cldn-10 TJ proteins play a central role in Na^+ secretion when fish reside in SW. This is because Cldn-10 proteins in the teleost fish gill (1) possess ion-selective pore forming properties (Marshall et al 2018), (2) are found exclusively in ionocytes that are responsible for salt secretion (Bui et al. 2014; Chen et al. 2020), and (3) increase in abundance in SW (or hypersaline) conditions versus FW (Bui et al. 2014; Chen et al. 2020). In line with some of this evidence, it has also been found that in primary cultured teleost fish gill epithelium models that are composed of gill pavement cells only (i.e. models that lack ionocytes), genes encoding *cldn-10* proteins are missing (Bui and Kelly 2011; Kolosov et al. 2014). So, this could mean that in larval sea lamprey gill, *cldn-10* is associated with gill ionocytes and that these ionocytes may be missing from this model. In this regard, further morphological characterization will reveal whether the cultured preparation contains ionocytes or not. However, it is also worth noting that recent studies have shown that acclimation of larval lamprey to ion-deficient water resulted in an increase in gill *cldn-10* mRNA abundance, whereas acclimation to seawater decreased gill *cldn-10* mRNA abundance (Kolosov et al. 2020). This is the opposite to what we might expect based on evidence emerging from teleost fish studies. Furthermore, the distribution of *cldn-10* in lamprey is broad, whereas in teleost fishes, Cldn-10 proteins are typically restricted to organs where epithelia interface directly with the surrounding environment (i.e. the gill and skin). Because of this, as well as observed alterations in *cldn-10* abundance in other organs

following salinity change, Kolosov et al (2020) have suggested that Cldn-10 may exhibit organ-specific function/s in lamprey and that it may be a barrier-forming protein in these animals.

In addition to genes encoding Cldn TJ proteins, analysis of TJ-associated MARVEL proteins provided further evidence that TJ architecture in the model lamprey gill epithelium strongly resembles the intact gill. More specifically, transcript encoding Tric and Ocln-a were present in the model preparation, but *ocln* was absent. For the Ocln proteins, observations at the transcriptional level were supported by Western blot analysis using species-specific, custom synthesized antibodies, which also showed the presence of Ocln-a and absence of Ocln in the model. In the intact larval lamprey gill, Tric, Ocln and Ocln-a are all present (Kolosov et al. 2017), but Ocln primarily localizes to gill vasculature. This would indicate that the model lamprey preparation is composed of gill epithelium cells only.

6.6.4. Effects of 11-Deoxycortisol on TER of Culture Lamprey Explants

The steroid hormone 11-deoxycortisol is currently proposed to be a functional corticosteroid hormone in the sea lamprey (Close et al. 2010; Shaughnessy et al. 2020). In this regard, CYP11B1 (and CYP11B2), which are critical in cortisol synthesis, are not present in the sea lamprey genome (Close et al. 2010; Shaughnessy et al. 2020). Study using injection of sea lamprey with corticotropin releasing hormone caused an elevation in plasma 11-deoxycortisol, while 11-deoxycortisol injection resulted in an increase in gill Na^+-K^+-ATPases activity (Close et al. 2010). This latter change in gill enzyme activity is broadly considered to reflect a change in osmoregulatory status because in the gill of fishes, Na^+-K^+-ATPase is abundant in ionocytes, where it plays a key role in regulating transcellular solute movement across the gill epithelium (Zadunaisky 1984). However, there are no studies on the direct effect of this hormone on endpoints of paracellular solute movement or paracellular permeability in lamprey. TER, which is a measure

of both transcellular and paracellular resistance of an epithelium, is primarily influenced by changes in paracellular permeability because epithelial TJs control the parallel elements of the paracellular pathway (for review see Anderson and Van Itallie 2009). Therefore TER is a reliable, overall measure of epithelium permeability as dictated by changes in TJ properties. The TER of primary cultured gill epithelia derived from the gill of various teleost fish species have proved to be sensitive to the main corticosteroid found in this group of animals, cortisol (Kelly and Wood 2001; Kelly and Wood 2002; Chasiotis and Kelly 2011). However, only a transient effect of 11-deoxycortisol was observed on day 13 of treatment. This may suggest that these preparations and, by proxy, larval lamprey gill epithelium permeability, has limited response to corticosteroids. However, there are several factors to consider in this regard. The first is that the larval lamprey is a stenohaline FW fish, and there is evidence to suggest that the permeability properties of cultured stenohaline fish gill models may be far less sensitive to corticosteroid treatment than euryhaline species (Kelly and Wood 2001; Kelly and Wood 2002; Chasiotis and Kelly 2011). In addition, while teleost fish models respond to physiologically-relevant doses of hormone, a clear and robust response is typically associated with high doses of hormone (Kelly and Wood 2001; Kelly and Wood 2002; Chasiotis and Kelly 2011). Indeed, a lower dose and lack of sensitivity by the ammocoetes may have both contributed to the current results. While Close and colleagues (2010) conducted their studies using adult sea lampreys, a recent study by Shaughnessy (2020) has further demonstrated *ex vivo* larval lamprey gills do not respond to direct 11-deoxycortisol treatment. Therefore, potential development of lamprey gill epithelium using cells derived from metamorphosing sea lampreys and adults may require elucidating the role of corticosteroids in this basal vertebrate.

6.7. Conclusions and Perspectives

The current study investigated larval lamprey gill epithelium derived from explants as a surrogate model of the sea lamprey ammocoete gill. We demonstrated that sea lamprey gill epithelium can be maintained on culture substrata including permeable inserts. The cultured gill epithelium exhibit canonical epithelial cell morphology and molecular profiling demonstrates transcripts of TJ-associated proteins, as well as the presence of OCLN-a immunoreactivity. The current sea lamprey gill culture technique opens potential avenues for future physiological and toxicological study of the lamprey tissue with an emphasis on cellular regulation. While only a transient effect of 11-deoxycortisol was observed in the current study, future experiments may address the effect of this corticosteroid in the sea lamprey by altering the experimental parameters. Finally, the sea lamprey life cycle consists of a complex developmental cycle that includes remodeling of the gill organ during metamorphosis. Future studies may potentially expand the epithelium culture technique to the various stages of the sea lamprey life cycle.

6.8. References

Bartels H and Potter I (1991) Structural changes in the zonulae occludentes of the chloride cells of young adult lampreys following acclimation to seawater. Cell Tissue Res 265: 447–457.

Bartels H and Potter IC (1993). Intercellular junctions in the water-blood barrier of the gill lamella in the adult lamprey (*Geotria australis*, *Lampetra fluviatilis*). Cell Tissue Res 274: 521–532.

Bartels H and Potter IC (2004). Cellular composition and ultrastructure of the gill epithelium of larval and adult lampreys: Implications for osmoregulation in fresh and seawater. J Exp Biol 207: 3447–3462.

Bui P, Bagherie-Lachidan M and Kelly SP (2010) Cortisol differentially alters claudin isoforms in cultured puffer fish gill epithelia. Mol Cell Endocr 317: 120-126.

Bui P and Kelly SP (2011) Claudins in a primary cultured puffer fish (*Tetraodon nigroviridis*) gill epithelium In Methods in Molecular Biology, Volume 762, Claudins: Methods and Protocols, pp. 179 –194. Ed. T. Kursad. Humana Press, Springer, New York.

Bui P and Kelly SP (2014) Claudin-6, -10d and -10e contribute to seawater acclimation in the euryhaline puffer fish *Tetraodon nigroviridis*. J Exp Biol 217: 1758–1767.

Bury NR, Schnell S and Hogstrand C (2014) Gill cell culture systems as models for aquatic environmental monitoring. J Exp Biol 217: 639 – 650.

Chasiotis H, Wood CM and Kelly SP (2010) Cortisol reduces paracellular permeability and increases occludin abundance in cultured trout gill epithelia. Mol Cell Endocr 323: 232-238.

Chasiotis H and Kelly SP (2011) Effect of cortisol on permeability and tight junction protein transcript abundance in primary cultured gill epithelia from stenohaline goldfish and euryhaline trout. Gen Comp Endocr 172: 494 – 504.

Chasiotis H, Kolosov D, Bui P and Kelly SP (2012) Tight junctions, tight junction proteins and paracellular permeability across the gill epithelium of fishes: a review. Resp Physiol Neurobiol 184: 269 – 281.

Chen CC, Marshall WS, Robertson GN, Cozzi RRF, Kelly SP (2020) Mummichog gill and operculum exhibit functionally consistent claudin-10 paralog profiles and Claudin-10c hypersaline response. Open Biol *Accepted*.

Close DA, Yun SS, McCormick SD, Wildbill AJ and Li W (2010) 11-Deoxycortisol is a corticosteroid hormone in the lamprey. PNAS 107(31): 13942 – 13947.

Dickman KG and Renfro JL (1986) Primary culture of flounder renal tubule cells: Transepithelial transport. Am J Physiol - Ren Fluid Electrolyte Physiol 251: f424 – 432.

Fletcher M, Kelly SP, Pärt P, O'Donnell MJ and Wood CM (2000). Transport properties of cultured branchial epithelia from freshwater rainbow trout: a novel preparation with mitochondria-rich cells. J Exp Biol 203: 1523-1537.

Foskett K, Scheffey C (1982) The Chloride Cell : Definitive Identification as the Salt-Secretory Cell in Teleosts. Science 215 (4529): 164–166.

Freshney RI (2010) Culture of animal cells: a manual of basic technique and specialized applications, 6th ed. John Wiley & Sons, Inc. Hoboken, USA.

Fromm M, Schulzke JD, and Hegel U (1985) Epithelial and subepithelial contributions to transmural electrical resistance of intact rat jejunum, in vitro. Pflügers Arch Eur J Physiol 405: 400–402.

González-Mariscal L, Betanzos A, Nava P and Jaramillo BE (2003) Tight junction proteins. Prog Biophys Mol Bio 81: 1 – 44.

Gess RW, Coates MI and Rubidge BS (2006) A lamprey from the Devonian period of South Africa. Nature 443: 981 – 984.

Gilmour KM, Pärt P, Prunet P, Pisam M, McDonald DG and Wood CM (1998) Permeability and morphology of a cultured branchial epithelium from rainbow trout during prolonged exposure to freshwater. J Exp Zool 281: 531 – 545.

Günzel D and Yu ASL (2013) Claudins and the Modulation of Tight Junction Permeability. Physiol Rev 93: 525 – 569.

Günzel D and Fromm M (2012) Claudins and other tight junction proteins. Compr Physiol 2: 1819–1852. doi.org/10.1002/cphy.c110045

Karnaky KJ, Degnan KJ and Zadunaisky JA (1977) Chloride transport across isolated opercular epithelium of killifish: a membrane rich in chloride cells. Science 195 (4274): 203 – 205.

Karnaky KG Jr and Kinter WB (1977) Killifish opercular skin: a flat epithelium with a high density of chloride cells. J Exp Zool 99(3):355-364.

Kelly SP and Wood CM (2001) Effect of cortisol on the physiology of cultured pavement cell epithelia from freshwater trout gills. Am J Physiol-Reg I 281: R811 – R820.

Kelly SP and Wood CM (2001) The physiological effects of 3,5',3'-triiodo-L-thyronine alone or combined with cortisol on cultured pavement cell epithelia from freshwater rainbow trout gills. Gen Comp Endocr 123: 280 – 294.

Kelly SP and Wood CM (2002) Prolactin effects on cultured pavement cell epithelia and pavement cell plus mitochondria-rich cell epithelia from freshwater rainbow trout gills. General and Gen Comp Endocr 128: 44 – 56.

Kelly SP and Wood CM (2002) Cultured gill epithelia from freshwater tilapia (Oreochromis niloticus): Effect of cortisol and homologous serum supplements from stressed and unstressed fish. Journal of Membrane Biology: 190 (1): 29-42.

Kelly SP, Fletcher M, Pärt P and Wood CM (2000) Procedures for the preparation and culture of "reconstructed" rainbow trout branchial epithelia. Methods in Cell Science 22: 153 – 163.

Kolosov D and Kelly SP (2013) A role for tricellulin in the regulation of gill epithelium permeability. Am J Physiol – Reg Int Comp Physiol 304: R1139-R1148

Kolosov D, Bui P, Chasiotis H and Kelly SP (2013) Claudins in teleost fishes. Tissue Barriers 1:3 e25391.

Kolosov D, Chasiotis H and Kelly SP (2014) Tight junction protein gene expression patterns and changes in transcript abundance during development of model fish gill epithelia. J Exp Biol 217: 1667 – 1681.

Kolosov D, Bui P, Donini A, Wilkie MP and Kelly SP (2017) A role for tight junction-associated MARVEL proteins in larval sea lamprey (*Petromyzon marinus*) osmoregulation. J Exp Biol 220: 3657 – 3670.

Kolosov D, Bui P, Wilkie MP and Kelly SP (2020) Claudins of sea lamprey (*Petromyzon marinus*) – organ-specific expression and transcriptional responses to water of varying ion content. J Fish Biol 96: 768 – 781.

Loh YH, Christoffels A, Brenner S, Hunziker W and Venkatesh B (2004) Extensive Expansion of the Claudin Gene Family in the Teleost Fish, *Fugu rubripes*. Genome Res 14(7): 1248 – 1257.

Marshall WS (1977) Transepithelial potential and short-circuit current across the isolated skin of Gillichthys mirabilis (Teleostei: Gobiidae), acclimated to 5% and 100% seawater. J Comp Physiol 114: 157–165.

Nogueira LS, Chen CC, Wood CM and Kelly SP (2020) Effects of copper on a reconstructed freshwater rainbow trout gill epithelium: Paracellular and intracellular aspects. Comp Biochem Phys C. doi:10.1016/j.cbpc.2020.108705

Nelson JS (2006) *Fishes of the World*. 4th ed. John Wiley and Sons, Inc. New Jersey, USA.

Pärt P, Norrgren L, Bergstrom E and Sjoberg P (1993) Primary Cultures of Epithelial Cells from Rainbow Trout Gills. J Exp Biol 175: 219 – 232.

Shaughnessy CA, Barany A and McCormick SD (2020) 11-Deoxycortisol controls hydromineral balance in the most basal osmoregulating vertebrate, sea lamprey (*Petromyzon marinus*). Sci Rep 10: 1–13.

Smith JJ, Kuraku S, Holt C, et al. (2013) Sequencing of the sea lamprey (*Petromyzon marinus*) genome provides insights into vertebrate evolution. Nat Genet 45: 415 – 421.

Wood CM and Pärt P (1997). Cultured branchial epithelia from freshwater fish gills. J Exp Biol 200: 1047-1059.

Wood CM, Gilmour KM, and Pärt P (1998) Passive and active transport properties of a gill model, the cultured branchial epithelium of the freshwater rainbow trout (*Oncorhynchus mykiss*). Comp Biochem Physiol - A Mol Integr Physiol 119: 87–96.

Zadunaisky J (1984) The chloride cell: the active transport of chloride and the paracellular pathways. In *Fish Physiology*. Hoar WS and Randall DJ ed. Academic Press, New York, NY. P. 129 – 176.

Zihni C, Mills C, Matter K and Balda MS (2016) Tight junctions: from simple barriers to multifunctional molecular gates. Nat Rev Mol Cell Bio 17: 564 – 580.

Chapter 7. Integration and Future Directions

The fish gill is a multi-functional organ that contributes significantly to the extra-renal ionoregulation in fishes (Evans et al., 2005). In my thesis, I examined how the branchial epithelium contributes to the overall hydromineral balance by examining the molecular physiology of the tight junction (TJ) complex, and I developed a new tool to study branchial physiology in a basal vertebrate. In order to dissect the barrier properties of the gill organ, I utilized a primary cultured gill epithelium model derived from rainbow trout (*Oncorhynchus mykiss*) to examine factors that regulate the molecular physiology and biochemistry of the gill TJ assembly. In this respect, I examined the use of native serum (NS) to augment the authenticity of primary cultured trout gill epithelium preparations (Chapter 2) and explored the effects of thyroid hormone (TH) 3,5',3'-triiodo-L-thyronine (T_3) on cultured trout epithelia (Chapter 3). Using the seawater-adapted killifish (*Fundulus heteroclitus*), I examined how Claudin-10 isoforms contribute to teleost hypoosmoregulation and the role of Claudin-10c as a putative ion-channel (Chapter 4). Moreover, I examined the molecular physiology of TJs in the gills of metamorphosing sea lampreys (*Petromyzon marinus*) and the effects of full seawater acclimation in young lamprey adults (Chapter 5). Finally, I have developed the first reported primary cultured epithelium model derived from the sea lamprey gill organ (Chapter 6).

The fish gill epithelium is a physical barrier that separates the extracellular fluid from the aquatic medium. Under physiological circumstances, the fish gill epithelium separates two significantly different environments (i.e. blood and the aquatic environment) that results in high osmotic gradient. Consequently, the freshwater fish gill epithelium is considered a "tight" barrier with significant resistance to paracellular solute movements. In contrast to the gill epithelia of freshwater fishes, gill epithelia of seawater fishes are often described as "leaky" as they allow

selective unidirectional ion movement while maintaining the overall barrier properties. My thesis focused on understanding how TJ proteins selectively mediate the resistive properties of the gill epithelia and gill epithelium models. Ultimately, my thesis also led to the development of a primary cultured sea lamprey gill epithelium, a model that can provide potential insights on TJ physiology and diversification of more derived vertebrates.

The successful use of NS supplement in primary cultured trout epithelium model has generated cultured preparations with robust barrier properties, defeating previous assumptions that trout serum and plasma can be deleterious to cultured gill cells. Current findings expand on the knowledge that endocrine factors not only alter the permselective properties of the gill epithelium, but TH may also modulate the direction of ion-transport. This hypothesis is supported by observations in altered transcript abundance of Na^+,K^+-ATPase α1b isoform and Claudin-10c in cultured gill epithelia derived from freshwater acclimated rainbow trout in direct response to T_3 treatment. This can provide insight on how elevated TH level prepares anadromous salmonids for seawater migration. However, altered directional transport may require a coordinated effort in conjunction with other osmoregulatory hormones and not TH alone. This idea may be difficult to examine using the current culture preparation as cultured gill models derived from freshwater fishes do not exhibit robust transport characteristics of the native gill organ.

The role of Claudin-10c as a selective cation channel was further highlighted in the current thesis in hypersaline acclimated killifish, where an increase in Claudin-10c was closely coupled to the localization of apical anion channels that drives Na^+ extrusion in seawater acclimated fishes. A significant observation from this study was that while glycosylation of claudins has been suggested previously using bioinformatics, the current experiments provides empirical evidence of glycosylation in the killifish gill and opercular epithelia. Moreover, the current experiment

demonstrated a functional shift in glycosylated Claudin-10c in direct response to salinity acclimation. The exact function of glycosylation in killifish Claudin-10c is not known and requires further investigation. The complexity and the extend of post-translational modifications in Claudin-10c cannot be determined using the methods utilized in my thesis. Nevertheless, post-translational modification mechanisms may explain the difference in previous studies where the predicted and observed molecular weights of Claudins that also did not agree (Katoh and Katoh 2003; Kolosov and Kelly 2017). In contrast to mammalian and teleost Claudin-10 proteins that are thought to be conductive ion-channels, sea lamprey Claudin-10 appears to have important roles in barrier formation. The sea lamprey developmental study demonstrated that while changes in TJ transcript occurred in metamorphosing sea lampreys that may partly be associated to tissue and organ reorganization, salinity acclimation outweighs the changes that occurred during metamorphosis as it is critical to maintain the overall hydromineral balance during salinity acclimation.

With respect to further expanding on the current findings, the NS experiment demonstrated that the anti-coagulating agent heparin can be deleterious to cultured trout epithelia. This current finding may underscore the reason that high plasma concentration, which require the use of anti-coagulating agent during preparation, can be detrimental to primary cultured trout epithelia (Wood et al., 2002). However, future experiments are needed to explore the possibility of using heparin as a pharmacological agent to selectively disrupt cultured membranes. In the NS study, while there was a significant increase in the transepithelial electrical resistance in cells supplemented with NS, only a select number of TJ transcripts were altered by the NS treatment. Therefore, the experiment raises important future directions on determining the endogenous factors in NS (which may not be present in commercially available sera, or do not have the same affinity to the receptors in the fish

gill cells) that can selectively target these TJ encoding genes. This is especially important as there may exist potential native endocrine and mitogenic factors augmenting the barrier properties of the gill organ that have yet to be identified. The current study has demonstrated that cultured trout epithelium remains a viable tool for studying the physiology of the gill organ, and NS supplement can be used in place of mammalian sera when required.

The T_3 study has generated data that suggests its significance in seawater acclimation. Primary cultured epithelium has a significant advantage over *in vivo* and *ex vivo* studies. Salmonid metamorphosis is orchestrated by a number of endocrine factors, and primary culture is an isolated system that allows targeted effects to be examined. Primary cultured epithelium is especially advantageous in dissecting T_3's mechanism of action. Limited literature exists on the physiological role of T_3 in vertebrate epithelium. Future studies should address how T_3 targets cell signaling pathways to determine how the hormone regulates the barrier properties of the gill epithelium. Notably, future studies should address the changes in Claudin-10c and Claudin-28b transcript that are in close association with ionocytes. Experiments should also address whether T_3 signaling is regulated by T_3 permeability through the plasma membrane via T_3 transporters, by peripheral deiodination mechanisms, or by activation/deactivation of T_3 receptors. Finally, future studies are required to address whether T_3 in cultured epithelium (that consists of pavement cells and ionocytes) alters transport properties in response to asymmetrical conditions.

The sea lamprey is an emerging model for fish physiology. The sea lamprey has an indirect developmental life cycle and complex cellular composition of the gill epithelium that varies throughout development (Bartels and Potter, 2004; Peek and Youson, 1979). Because of this prolonged indirect development, the sea lamprey is a stenohaline model during the larval phase and euryhaline as adults. Endocrine regulation of the sea lamprey gill epithelium is currently

focused on 11-deoxycortisol as it is the presumptive glucocorticoid in this basal vertebrate. The current study successfully generated a cultured gill epithelium model derived from explants of larval lamprey gill. The current experiment also demonstrated cultured sea lamprey epithelia may only respond to 11-deoxycortisol in a transient manner. While the current model overcomes the architectural complexity of the gill organ, future studies should examine whether the cell heterogeneity of the native gill organ is maintained in the current culture model. Future cultured lamprey gill epithelium models can also be developed from other sea lamprey life cycle stages to understand whether the life cycle stage will increase the gill epithelium sensitivity to 11-deoxycortisol in adult lampreys as suggested in previous studies (Close et al., 2010; Rai et al., 2015; Shaughnessy et al., 2020). Furthermore, primary culture gill epithelium model derived from lamprey developmental and adult stages can encompass the unique cellular composition that is unique to each life cycle stages. Studies focusing on the receptor response to 11-deoxycortisol are also warranted to determine their association with changes in the physiology of the sea lamprey TJ assembly. Future studies may elucidate whether the presence of 11-deoxycortisol is associated with euryhalinity as well as address potentially unknown osmoregulatory factors in the larval life cycle stages if it exists.

The current cultured lamprey gill epithelium model exhibits transepithelial electrical resistance of a polarized epithelium. The current sea lamprey model gill epithelium can potentially be expanded to include permeability and asymmetrical studies (*i.e.* Freshwater apical and culture medium on basolateral sides of inserts) to understand how osmotic stress and increased gradient mediate the TJ physiology of the cultured gill cells. Furthermore, mechanisms that regulate the barrier properties of the sea lamprey gill model can be examined using the current technique. Despite genes encoding for TJ-associated genes were detected in this model with a positive

detection of OCLN-a protein, further experiments should demonstrate the localization of TJ proteins in cultured sea lamprey gill epithelium model using microscopy techniques. The overall morphology of the sea lamprey gill model should also be examined. A critical question with the current model is whether ionocytes were present in the current model. The presence and absence of ionocytes in the model will be critical in addressing the difference in the function of the sea lamprey gill at various life cycles stages. Finally, similar to the primary cultured gill epithelium developed for bony fishes, the current model will allow the lab to further elucidate the barrier properties and ion-transport characteristics that may mimic the *in vivo* lamprey gill organ.

7.1. References

Bartels, H., Potter, I.C. (2004) Cellular composition and ultrastructure of the gill epithelium of larval and adult lampreys: Implications for osmoregulation in fresh and seawater. J Exp Biol 207: 3447-3462.

Close, D.A., Yun, S.S., McCormick, S.D., Wildbill, A.J., Li, W. (2010) 11-Deoxycortisol is a corticosteroid hormone in the lamprey. Proc Natl Acad Sci 107: 13942-13947.

Evans, D.H., Piermarini, P.M., Choe, K.P. (2005) The multifunctional fish gill: Dominant site of gas exchange, osmoregulation, acid-base regulation, and excretion of nitrogenous waste. Physiol Rev 85: 97-177.

Katoh, M., Katoh, M. (2003) CLDN23 gene, frequently downregulated in intestinal – type gastric cancer, is a novel member of the CLAUDIN gene family. Int J Mol Med 11: 683-689.

Kolosov, D., Kelly, S.P. (2017) Claudin-8d is a cortisol-responsive barrier protein in the gill epithelium of trout. J Mol Endocrinol 59: 299-310.

Peek, W.D., Youson, J.H. (1979) Transformation of the interlamellar epithelium of the gills of the anadromous sea lamprey, *Petromyzon marinus L.,* during metamorphosis. Can J Zool 57: 1318-1332.

Rai, S., Szeitz, A., Roberts, B.W., Christie, Q., Didier, W., Eom, J., Yun, S.S., Close, D.A. (2015) A putative corticosteroid hormone in Pacific lamprey, *Entosphenus tridentatus*. Gen Comp Endocrinol 212: 178-184.

Shaughnessy, C.A., Barany, A., McCormick, S.D. (2020) 11-Deoxycortisol controls hydromineral balance in the most basal osmoregulating vertebrate, sea lamprey (*Petromyzon marinus*). Sci Rep 10: 1–13.

Wood, C.M., Eletti, B., Pärt, P. (2002) New methods for the primary culture of gill epithelia from freshwater rainbow trout. Fish Physiol Biochem 26: 329-344.